# OFFSHORE ENERGY HUBS

FEASIBILITY ASSESSMENT OF HUB TOPOLOGIES

## AUTHORS:

Daniel Müller, Postdoc, Technical University of Denmark (DTU)

Mirza Nuhic, Postdoc, Technical University of Denmark (DTU)

Domagoj Hart, Project Manager and R&D Engineer, SuperGrid Institute

Gustavo Figueiredo Gontijo, Power System Engineer, Ørsted A/S

Syed Hamza Hasan Kazmi, Project Manager, Ørsted A/S

## REVIEWERS:

Jesper Hjerrild, Senior Lead Power System Specialist, Ørsted A/S

Troels Stybe Sørensen, Senior Chief Specialist, Ørsted A/S

Kim Høj Jensen, Senior Key Expert, Siemens Gamesa Renewable Energy

## OTHER CONTRIBUTORS:

Alberto Bertinato, DC Grid Control and Protection Group Leader, SuperGrid Institute

Hjörtur Jóhannsson, Professor, Technical University of Denmark (DTU)

Nicolaos Cutululis, Professor, Technical University of Denmark (DTU)

Frede Blaabjerg, Professor, Aalborg University (AAU)

Xiongfei Wang, Professor, Aalborg University (AAU)

Liang Huang, Postdoc, Aalborg University (AAU)

Pukar Mahat, Senior Grid Expert, Siemens Gamesa Renewable Energy

Daniela Pagnani, Power System Engineer, Ørsted A/S

Aivaras Celna, Industrial PhD, Ørsted A/S

# TABLE OF CONTENTS

# 1. EXECUTIVE SUMMARY

This report evaluates various offshore energy hub (OEH) topologies — alternating current (AC), direct current (DC) and hybrid — drawing inspiration from prior studies, notably the North Sea Wind Power Hub (NSWPH) consortium's assessment. Emphasizing cost-effectiveness and grid security, the analysis from the referenced study focuses on minimizing investment and operational costs while ensuring reliability. In the previous investigations, AC and DC internal interconnectors (IIs) were extensively compared, which revealed higher initial costs for DC IIs due to expensive components, but lower operational expenditures attributed to reduced power transmission losses. From a control perspective, advanced techniques were needed for AC hubs versus conventional control in DC models, whereas AC hubs' advantage in redistributing wind energy during faults, compared to DC hubs potential shutdowns in affected zones necessitates further research for asymmetric AC fault handling in AC OEHs.

This report is focused on bridging gaps from prior reports and extending research, utilizing three feasibility criteria, i.e., expandability, economics, and functionalities & controllability. Expandability analysis defined base configurations for AC, DC, and hybrid hubs, proposing modular approaches for expansion cases involving additional offshore wind farms (OWFs), shore connections, and connections to other OEHs. Economic assessment calculated capital expenditure (CAPEX) and operational expenditure (OPEX) for each hub topology and expansion case, including losses based on nominal OWF power operation. Notably, this work addressed the disregarded fast blocking/unblocking functionality of the high-voltage direct-current (HVDC) converters in DC protection design from a prior study. Functionalities & controllability assessed hub availability, comparing topologies under different fault conditions, as well as in terms of control and stability issues. It identified control challenges for AC and DC hubs, indicating future studies for the project's Task 2.2.

# 2. INTRODUCTION

## 2.1. BACKGROUND

The study carried out in this report is a feasibility assessment comparing different topologies of OEHs, i.e., AC, DC, and hybrid, aiming at identifying advantages and drawbacks of each of these topologies. Feasibility assessments of OEHs have been presented in recent projects whose reports [1], [ [2] served as an inspiration and starting point for the analysis performed in this work. One of the most complete and detailed studies, which was the main reference for this report, is the feasibility assessment performed by the SuperGrid Institute for the NSWPH consortium [1].

In [1], a techno-economic analysis was performed comparing the different OEH topologies in terms of CAPEX and OPEX, protection strategies and design, and system constraints. Essentially, the approach of the study presented in [1] was to find the optimal hub solution by limiting the electrical infrastructure, i.e., minimizing investment costs, minimizing electrical losses, while respecting the security of electricity supply to the onshore AC grids according to pre-defined constraints and criteria.

In [1], a complex study case corresponding to a meshed HVDC grid composed of several modular hub blocks was considered and analysed. Based on this study case, a reliability assessment was performed, which reflected the trade-off between reduced power curtailment and increased CAPEX by considering circuit redundancy for a list of different load flow conditions. This study could also account for contingency cases. Besides the reliability analysis, the protection design of the study case was carried out in [1]. The main considered constraint for the protection design was the onshore AC system criteria, which allows for a certain loss of power infeed depending on the probability of a given failure. Based on these criteria, considering different busbar configurations for the different block types, as well as considering different fault types applied to different elements of the system, the number of necessary DC circuit breakers (DCCBs) and the size of DC reactors (DCRs) were designed. It is important to mention that allowing for the functionality of fast blocking/unblocking of certain HVDC converters can allow for the reduction of the size of the DCRs and lead to other benefits. However, this functionality was not considered in the DC protection design carried out in [1].

Another important study performed in [1], that served as a starting point for the work presented in this report, was the comparison between the AC and DC IIs that define the AC and DC hub topologies. This comparative analysis was performed for a specific section of the base study case corresponding to two busbars located relatively close to each other. The CAPEX comparative analysis included the cost of converters, cables, AC and DC circuit breakers, transformers, as well as the footprint cost for the components of each hub topology considering the area cost of offshore platforms. The CAPEX results showed that DC IIs are still considerably more expensive than their AC counterpart, which can be mainly attributed to the presently still high cost of DCCBs as well as the considerable space requirement of DCCBs and DCRs combined with the high cost of space offshore. The report emphasized that the outcome of the comparative analysis could change considerably when an increasing maturity of DCCBs in the industry results in reduced prices. The CAPEX results were also highly influenced by the area cost offshore and an optimized solution for OEHs in terms of platform versus artificial island solution could change the results in favour of the DC II solution.

The OPEX analysis comparing the AC and DC IIs was divided into transmitted power and electrical losses. The transmitted power assessment reflected the economic losses related to loss of opportunities of transferring power due to cable transfer capability limitations and converter power limitations. The main conclusion was that the AC hub presented reduced power transfer capability due to converter power limitations. Moreover, the study highlighted that the inter-zone power transfer capability is compromised in an AC hub in case of a converter fault. Regarding the electrical losses, the main conclusion was that the AC hub presented increased overall losses due to converter (and associated transformer) losses and increased cable losses. Thus, even though the DC hub (considering the DC II) presented a considerably increased CAPEX in comparison to the AC hub (considering the AC II) for the given study case, the DC hub presented a reduced total expenditure (TOTEX) due to the reduced OPEX in relation to the AC hub (considering that TOTEX = CAPEX + OPEX).

Some functionalities and control challenges were also analyzed in the comparative assessment between the AC and DC hub topologies. For example, it was identified that an AC hub would have to rely on advanced control techniques for the offshore HVDC stations to share the grid-forming functionality of the offshore grid since these converters would be connected together through the AC II while the DC hub, on the other hand, would result in independent and decoupled offshore AC grids that could be formed by a conventional V/f control (with fixed voltage and frequency) applied to each individual converter station. Simulation studies were carried out to compare the AC and DC hub topologies in case of the offshore HVDC converter blocking due to an internal fault and in case of a fault in the II. The simulations highlighted the fact that an AC hub presented higher availability of wind energy due to the possibility of rerouting the power of an OWF whose HVDC converter had been blocked. The wind energy would be redistributed through the offshore AC coupler and through other HVDC stations that remained online. In the DC hub case, the OWF would have to shut down in case of a fault in its HVDC station. The study also highlighted the fact that, even though the wind power could be redistributed in the AC hub case, some power curtailment could eventually be required to avoid exceeding the power ratings of the remaining HVDC converters. The simulation studies related to faults in the IIs identified the need of more research in case of an asymmetrical AC fault in the II of an AC OEH due to the challenges of handling this type of fault by the HVDC converters operating in shared grid-forming mode.

## 2.2. METHODOLOGY AND FEASIBILITY CRITERIA

The approach adopted in this work was to identify gaps in the previous reports (those used as references to this one) and to identify extended studies to be carried out as a continuation of the work performed in those reports. The feasibility criteria adopted in this work to compare the different hub topologies were divided into three topics, i.e., expandability, economic and functionalities & controllability (see Figure 1).


*Figure 1: Feasibility criteria topics adopted in this work.*

In the expandability topic, one base case configuration was defined for each hub topology (AC, DC, and hybrid). A modular approach was proposed to analyse different expansion cases, i.e., when a new OWF is to be added to the hub, when a new shore connection (based on the spoke concept) is to be added to the hub and when a new connection to another OEH is to be added to the hub. The expandability assessment essentially lists down the needed components and the number of these components required for each expansion case applied to each of the hub topologies.

In the economic assessment, calculations of CAPEX are carried out for each hub topology, considering each different expansion case, using as an input the component count performed in the expandability analysis. In terms of OPEX, losses are calculated for the AC and DC hub cases analysing two different situations: when wind power transfer to shore is prioritized, considering nominal power operation of the OWFs, and when inter-area power transfer is prioritized.

In the functionality and controllability topic, availability, protection, and control and stability are assessed. When it comes to availability, the different hub topologies are compared in terms of hub capacity (external) and generation capacity (internal). The availability of the hubs is assessed considering different fault conditions in different elements of the system, i.e., converter fault, spoke fault and II fault. Finally, in the control and stability item, different control and stability challenges are identified for the AC and DC hub topologies emphasizing the advantages and drawbacks of these hub configurations. These challenges will be used as an inspiration for the studies to be addressed in Task 2.2 of this project.

As previously mentioned in subsection 2.1, the DC protection design study performed in [1] disregarded the functionality of the fast blocking/unblocking of the HVDC converters, which can allow for a reduction of the size of the DC reactors along with other benefits. Thus, this study is performed as part of this report. Since this is a study exclusively related to the DC OEH topology and its protection design (not applicable to the AC topology), then it was not considered as being part of the feasibility assessment comparing the different hub configurations. The results of the DC protection design considering the blocking functionality of the HVDC converters are presented in Section 6 of this report.

# 3. HUB DESIGN

## 3.1. BASE TOPOLOGIES

The scope of this study is to assess the feasibility of different topology solutions for a generic OEH. For this purpose, the base scenario of the hub is chosen such that it reflects the smallest possible configuration that allows operation as an OEH – a system consisting of two HVDC converters and two OWFs. The hub topology – AC, DC or Hybrid – refers to the nature of the interconnection between these elements. The AC hub solution relies on a high-voltage offshore AC system to interconnect OWFs along with their corresponding offshore HVDC stations, which are connected to shore in a point-to-point configuration. The DC solution, on the other hand, splits the HVDC system into offshore converters that independently supply islanded AC systems, where the OWFs are integrated, and interconnect the HVDC converters on their DC sides, forming an HVDC grid. The hybrid solution combines the AC and DC topologies by providing an interconnected AC system as well as a multi-terminal DC (MTDC) system, which enables the option to operate the hub in either AC- or DC-coupled mode.

The layout and rating of the HVDC system is based on the 2-GW standard solution adopted by TenneT [3] – a bipole system with dedicated metallic return (DMR) and a DC voltage level of ± 525 kV. Considering a potential MTDC system it is important to note that the voltage rating of the first implementation also sets the standard for future expansions as it determines the voltage level of the entire interconnected DC system – at least while high-voltage, high-power DC-DC converters are not mature enough in the industry.

The sizing of the individual components and the decisions in terms of the protection design depend on the requirements of the onshore AC systems to which the hub is connected. These requirements define the maximum amount of power that can be lost following a particular fault type and are usually determined based on the available generation reserves within a specific region and across the whole synchronous area. Even though OEHs could theoretically be connected to different onshore AC systems, and thereby access reserves from multiple onshore systems, it has been decided to consider in this work only the AC system criteria defined within NSWPH [1] which is summarized in Table 1.

*Table 1: Considered onshore AC system criteria.*

| **Fault category** | **High probability** | **Low probability** | **Very low probability** |
|---|---|---|---|
| **Probability** | ~$10^2$ occ/100y | ~$10^0$-$10^1$ occ/100y | ~$10^{-3}$-$10^{-4}$ occ/100y |
| **Example** | Converter pole fault | Line fault, busbar fault | Line fault or busbar fault + breaker failure |
| **Allowable permanent power loss** | 1 GW | 2 GW | 3 GW |
| **Allowable temporary power loss (<150ms)** | 1 GW | 3 GW | 3 GW |

Conceptually, the system of an OEH can be split into three main components as indicated in Figure 2.

1. The wind power generation and potential local loads, such as power-to-X (PtX) or storage systems, which are locally connected to the hub and therefore could be considered as hub internal elements.
2. The external connections that interface the hub with different external systems. The external connections could be either spokes connecting the hub to onshore systems or hub interconnectors connecting the hub to other hubs.
3. The electrical system of the hub itself. The main purpose of this system is to provide the connections between both internal and external systems, allowing for energy exchange between different external and internal elements. The hub electrical system includes, transformers, offshore HVDC stations, AC and DC IIs, etc.

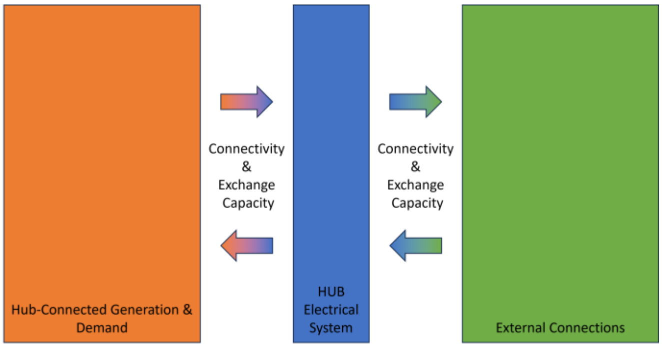


*Figure 2: Active power exchange capacities of the OEH.*

Each of these interfaces has its own maximum power exchange capacity. For larger hubs, the internal flow restrictions of the hub system might also become a relevant factor as these could impose a limit on the power exchange between different zones. For the systems assessed in this study, and the expansion cases considered, these limits are not relevant but for larger systems it could make sense to break down the hub into individual hub nodes. One of the outcomes of the study assessing the feasibility of the hub-and-spoke concept by NSWPH [1] was the optimal sizing of the II capacities. It was determined that, for the given study case (an interconnected system of five OEHs and fourteen spokes), the optimal size of the IIs was 2 GW. It has been decided that this capacity would be used within the scope of the present study as a reference design. The design of the different OEH topologies considered in this report was based on various reference elements that are summarized in Table 2. The details about the reference designs for the AC, DC, and Hybrid OEH solutions are described in the following sections.

*Table 2: Reference designs used as input for the OEH topology solutions.*

| **Element** | **Value/Design** | **Reference design** |
|---|---|---|
| DC system converter voltage and power rating. | ±525 kV, 2 GW bipole with DMR. | TenneT - 2 GW program [3] and 'Ijmuiden Ver' OWF [4]. |
| 400-kV AC busbar system. | Double busbar double breaker (DBSB). | Energinet – Energy Island Bornholm [5]. |
| 66-kV AC OWF busbar system. | Double busbar single breaker (DBSB). | TenneT - 'Ijmuiden Ver' OWF [6] & [7]. |
| DC busbar system. | Double busbar single breaker (DBSB). | NSWPH [1]. |
| II capacity. | 2 GW between nodes (1 GW per DC pole). | NSWPH [1]. |

### 3.1.1. AC Hub Design

The base solution of the AC hub is shown in Figure 3, and it features two point-to-point HVDC systems that are interconnected through two parallel AC IIs linking the offshore AC busbars, which represent the nodes of the AC hub. Each interconnector has a capacity of 1 GW. The two OWFs (OWF1 and OWF2) have a rated capacity of 2 GW each and are further split into 1 GW sections, "a" and "b".

The maximum exchange capacities between the different systems, in normal operation, are indicated in Figure 4. The internal capacity of the hub, which is here the combined capacity of the OWFs, is equal to 4 GW. For this base solution, the external capacity determined by the two 2 GW HVDC systems is equal to the internal capacity. The capacity of the IIs restricts the maximum exchange between the AC busbars to 2 GW, which in this baseline design does not impose any limitations since 2 GW is anyway the maximum power that can be exported to shore through one of the bipoles.

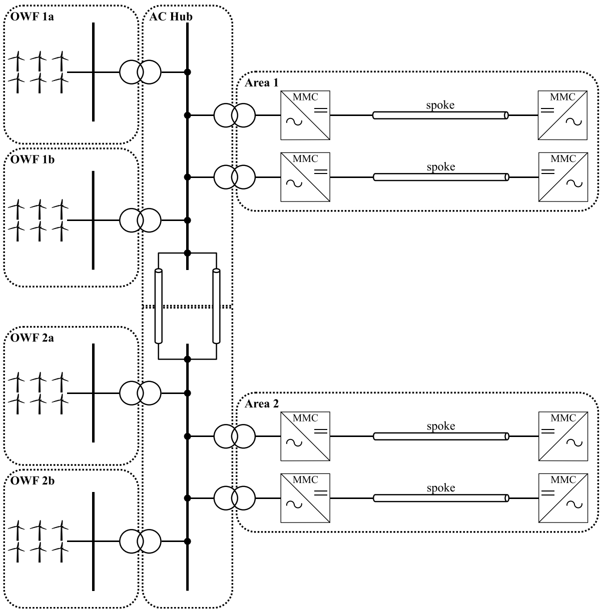


*Figure 3: AC Hub.*

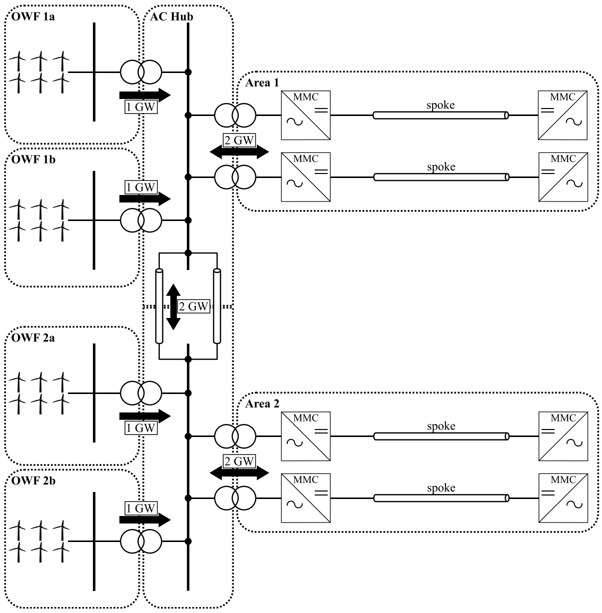


*Figure 4: AC hub exchange capacities. Numbers and arrows indicate the maximum exchange capacities across the different interfaces.*

Two main modes of operation can be identified for an OEH – export of wind power and operation in interconnector mode where the OEH serves as a link between two different areas allowing to exchange power between them. For the AC hub, these two modes are shown in Figure 5 and Figure 6, respectively.

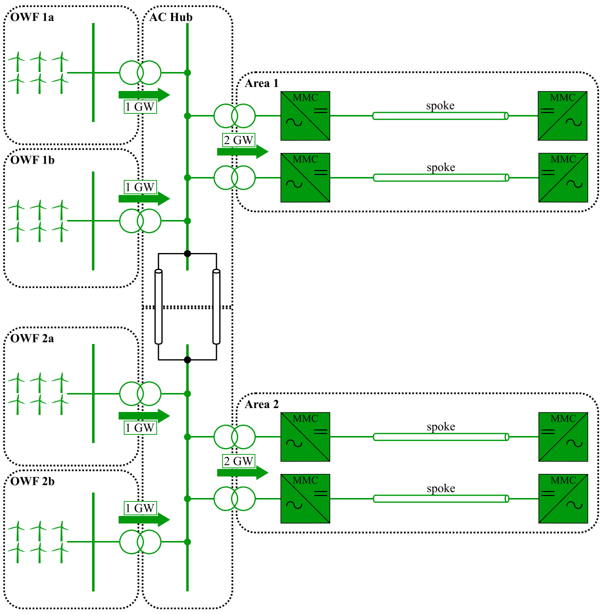


*Figure 5: AC Hub in wind export mode. Green indicates elements with active power flow and the respective power exchange across the interfaces of the OEH.*

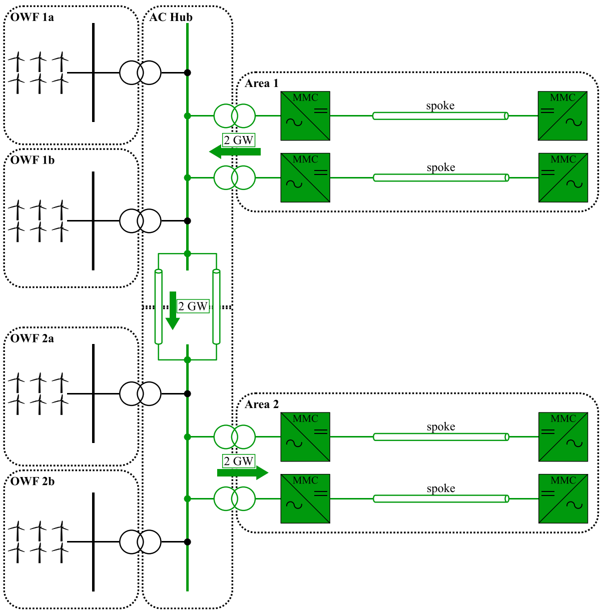


*Figure 6: AC Hub in interconnector mode. Green indicates elements with active power flow and the respective power exchange across the interfaces of the OEH.*

In the case of the AC hub operating in interconnector mode (shown in Figure 6), it is worth noting that the active power flows through the interconnected AC path and therefore requires two conversion stages, DC-AC-DC, at the OEH. Wind power export from the hub does not substantially differentiate from the current concept of point-to-point HVDC except that multiple AC areas can be directly accessed by the OWFs. This is particularly relevant in situations where a given OWF operates at low wind speeds while others produce larger wind energy quantities. In this case, the OWF producing higher wind energy could help to feed different AC synchronous areas. Besides, in case the OEH has higher spoke capacity compared to the combined capacity of offshore wind, then wind power can be exported to the areas which offer the highest electricity price, therefore optimizing the utilization of the produced wind power.

Based on the reference design data indicated in Table 2, a detailed AC hub solution including specific component ratings and detailed descriptions of the AC busbar configuration and their protection is developed. An illustration of this reference solution for the AC hub, which also serves as an input to the CAPEX estimation, is provided in Figure 7.

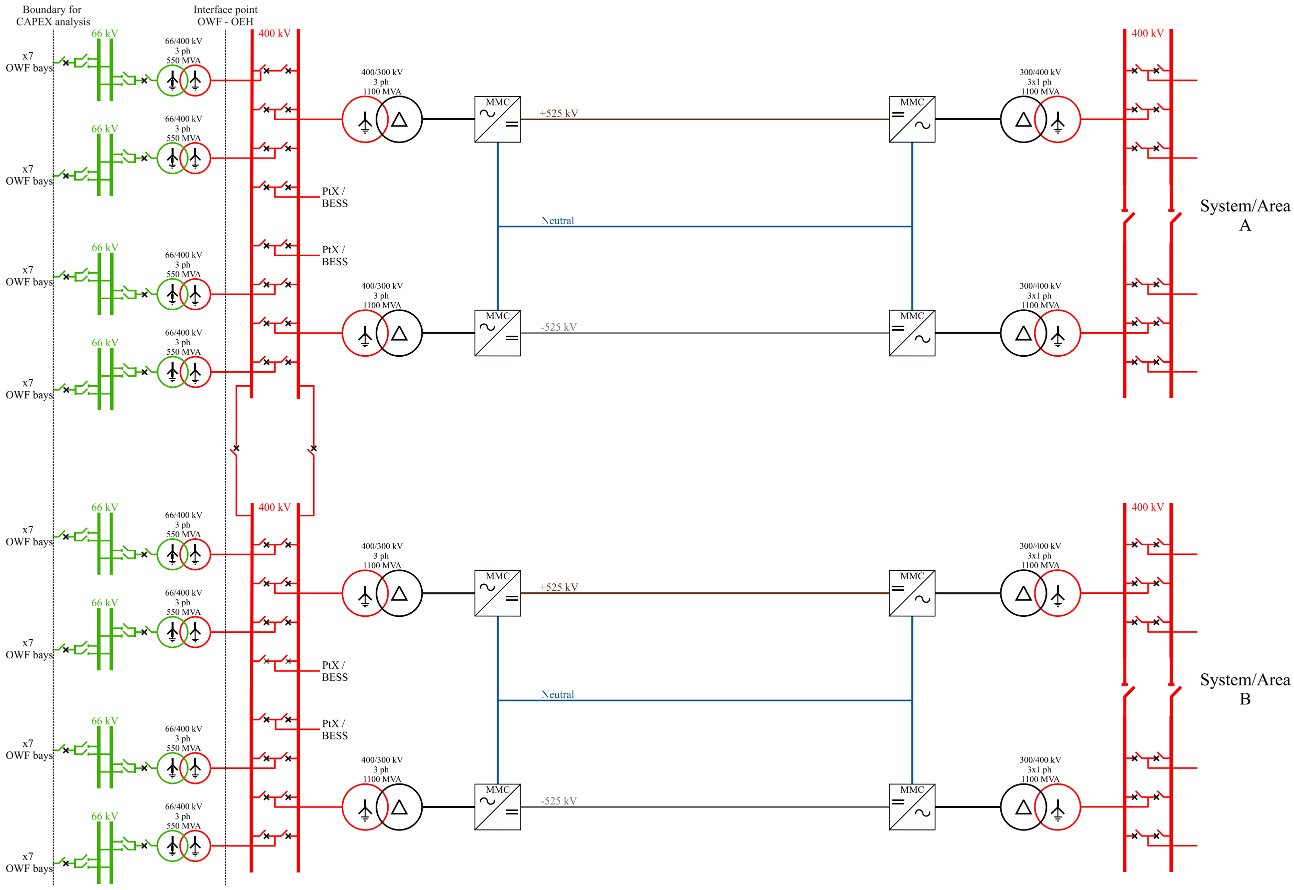


*Figure 7: Generic AC hub solution used for CAPEX analysis.*

### 3.1.2. DC Hub Design

A simplified illustration of the DC hub concept based on the initial OEH scenario is shown in Figure 8. The main difference to the AC solution is the location of the interface point to the interconnected electrical system of the hub. While the AC solution directly integrates all elements through an offshore interconnected AC system, the DC solution splits the point-to-point HVDC systems into multiple sections associated with individual HVDC converters. The offshore converters are, in this solution, associated with individual AC subsystems, which in its simplest form are small islanded systems with a maximum exchange capacity equal to the power rating of the modular multilevel converter (MMC), which is equal to 1 GW. The different offshore MMCs are then linked on the DC side of the converters, which also serves as the interface point for the spokes, connecting the DC hub to the onshore systems.

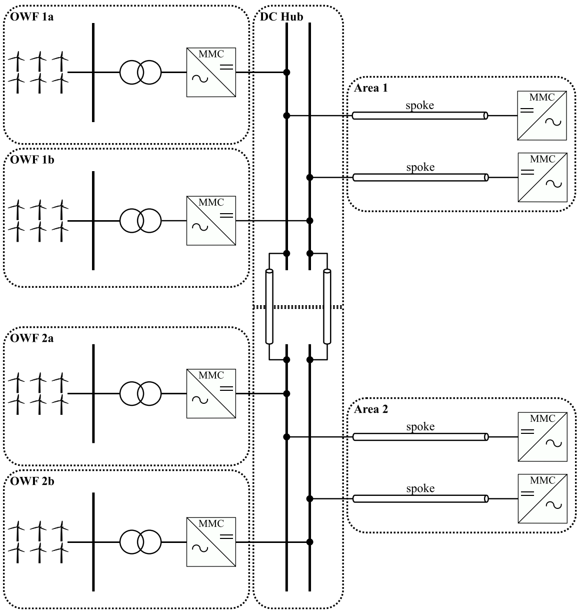


*Figure 8: DC Hub.*

A DC hub operating in power export mode, as indicated in Figure 9, in principle acts as multiple point-to-point HVDC systems and therefore no significant difference can be observed compared to the power exchange of the AC hub in Figure 5. In the interconnector mode, illustrated in Figure 10, the DC interface point has the advantage that the active power exchanged between areas 1 and 2 does not need to flow through the offshore converters, and associated converter transformers, which significantly reduces the losses in this operating mode.

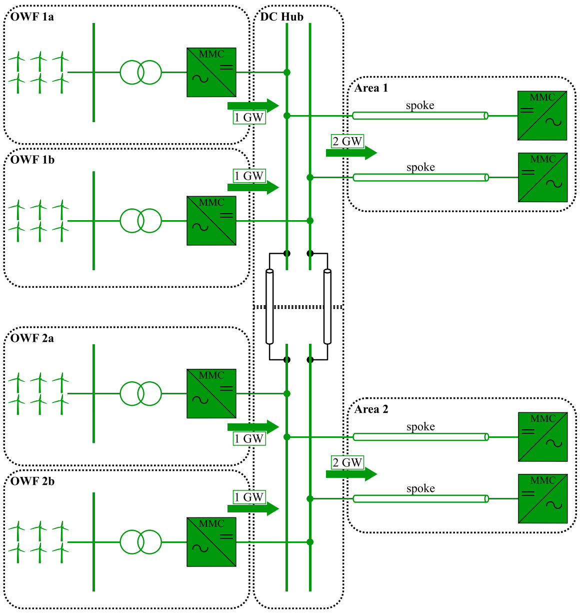


*Figure 9: DC Hub in wind export mode. Green indicates elements with active power flow and the respective power exchange across the interfaces of the OEH.*

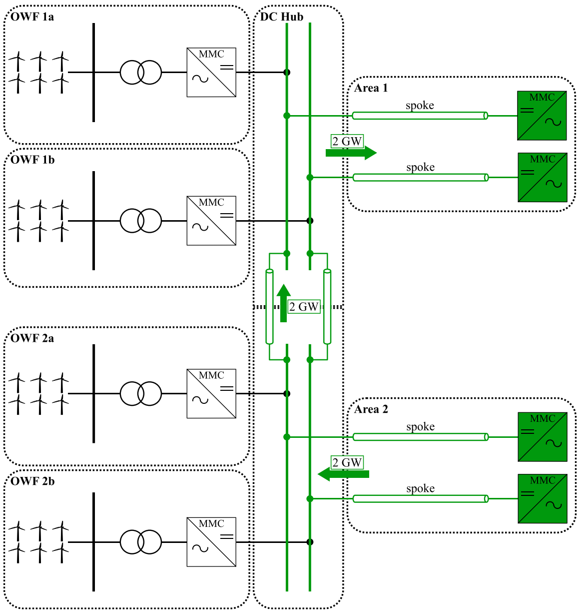


*Figure 10: DC Hub in interconnector mode. Green indicates elements with active power flow and the respective power exchange across the interfaces of the OEH.*

In line with the AC hub topology, a detailed solution for the DC OEH has been developed. The solution indicated in Figure 11 features a detailed representation of the DC busbar design, which is based on the outcome of [1], where a DBSB scheme with no DCCB at the offshore MMCs has been identified as the optimal solution considering the given onshore AC system criteria.

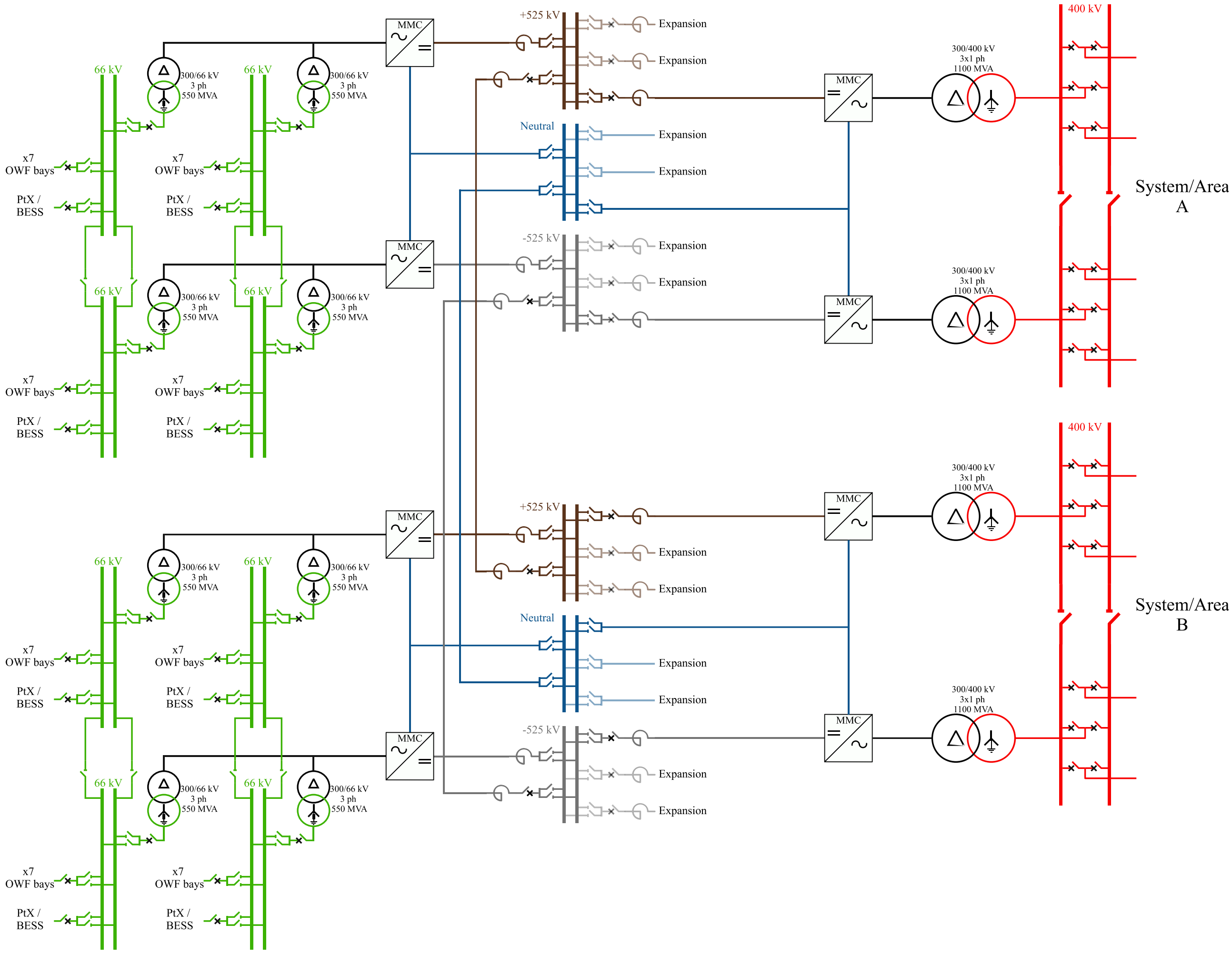


*Figure 11: Generic DC hub solution used for CAPEX analysis. This topology includes a coupling option of the HVDC bipoles on the 66-kV side of the transformers. The benefits of this solution are discussed in more detail in section 5.1.*

### *DC Busbar specification and protection:*

To comply with the onshore AC system criteria, the maximum capacity of each DC node (busbar system) is 2 GW, which allows for a total of five potential feeders (five connection points in each busbar), each with a capacity of 1 GW. This design choice is the outcome of an optimization process performed in [1], where the optimal busbar configuration including its protection has been determined based on the investment cost, expected energy curtailment and compliance with the AC system criteria. A 2-GW busbar is the minimum requirement for expanding the hub by another DC busbar system as indicated in Figure 12, while allowing the flexibility to connect an additional spoke to an existing busbar system as shown in Figure 13.

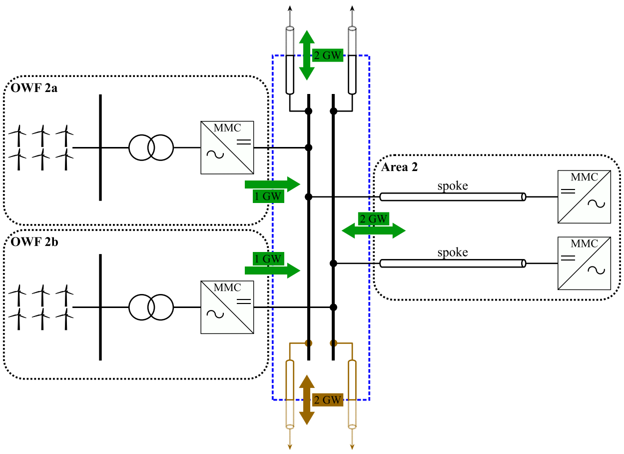

*Figure 12: 4-GW DC hub node (2 GW per pole) with 4 feeders per pole here indicated by the introduction of an additional II. Green illustrates the original exchange capacities, while brown shows the added II and the additional capacity due to the expansion.*

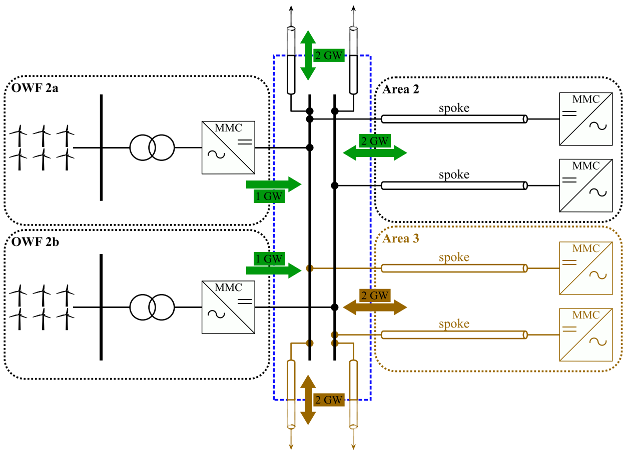

*Figure 13: 4-GW Hub node (2 GW per pole) with 5 feeders per pole. Illustrated on the example of a spoke and II. Green illustrates the original exchange capacities, while brown shows the new elements and the additional capacity due to the expansion.*

### 3.1.3. Hybrid Hub Design

The hybrid hub solution, indicated in Figure 14, is a combination of the AC and the DC solutions. The main reasoning for the hybrid hub topology from a transmission system operator (TSO) point of view, considering the maturity of the key technologies that are needed to implement each of the solutions, is described in the publicly available document from Energinet [8].

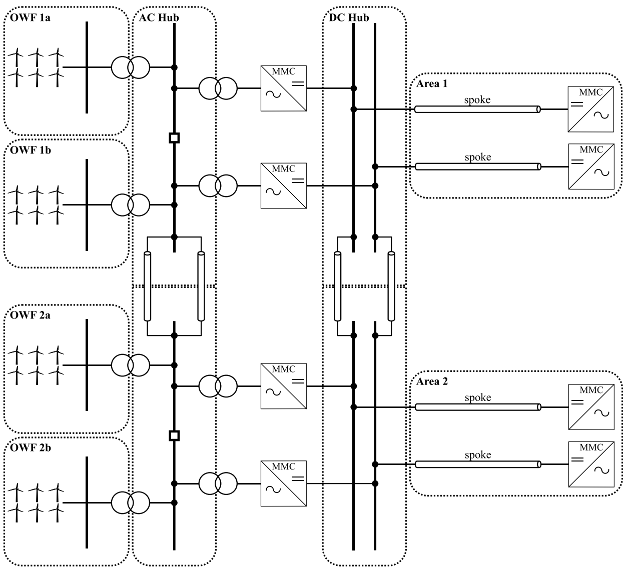

*Figure 14: Hybrid hub solution. Only one of the coupling options (AC or DC) is active at a time. The AC busbars can further be sectionalized into individual pole sections. The different operating modes are shown in Figure 15, Figure 16 and Figure 17.*

The key point of the concept is the opportunity to operate the hub either in AC coupled mode, as shown in Figure 15, or in DC coupled mode, as in Figure 16, where the green and red colors represent the normally-closed and normally-open elements, respectively. This provides redundancy, which helps to mitigate the control and stability risks associated with the specific solutions. Mainly, the limited operational experience of a multi-terminal DC system and DC protection systems imposes an increased risk where the AC coupling option can provide a backup solution.

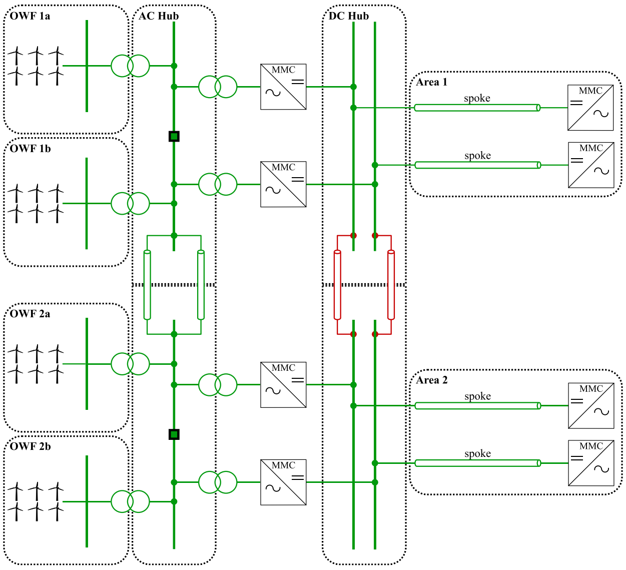


*Figure 15: Hybrid Hub in AC coupled mode. Green elements are in service (or breaker closed) while red elements are disconnected (or breakers open).*

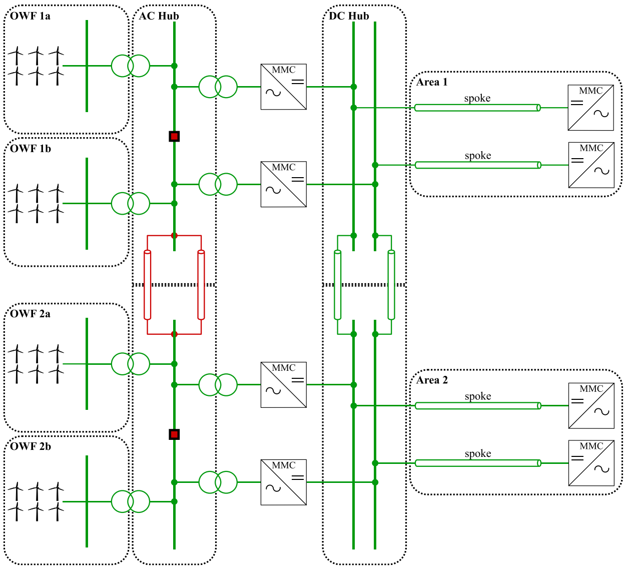


*Figure 16: Hybrid Hub in DC coupled mode – decoupled poles. Green elements are in service (or breaker closed) while red elements are disconnected (or breakers open).*

Compared to the AC OEH topology, the AC system of the hybrid hub requires additional options that allow to sectionalize the interconnected AC system into smaller subsystems. Two main modes of operation are considered for a hybrid hub operating in DC coupled mode. The AC system can either be split into subsystems associated with individual converter poles, where the number of islanded AC systems is equal to the number of offshore MMC converters, or operate in bipole coupled mode, where two converters of the HVDC bipoles operate in parallel grid-forming mode (see Figure 17). This operating mode is facilitated by the fact that the converter poles are electrically decoupled on the DC side.

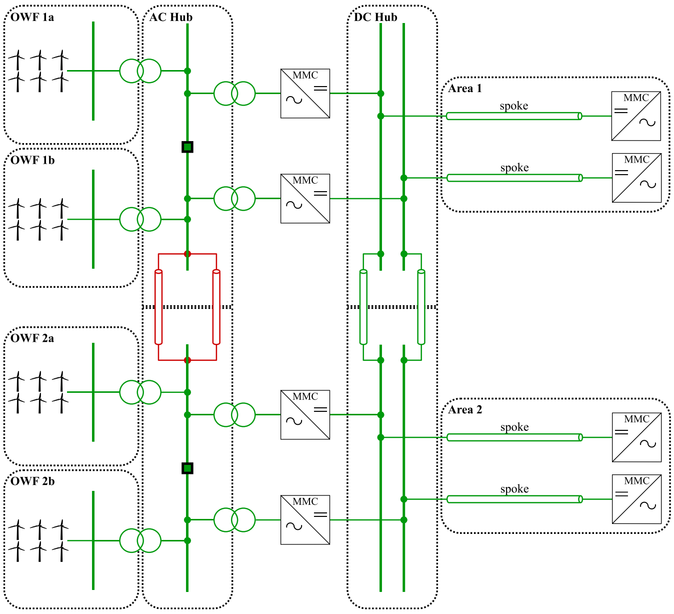


*Figure 17: Hybrid Hub in DC coupled mode – coupled poles. Green elements are in service (or breaker closed) while red elements are disconnected (or breakers open).*

The detailed solution for the hybrid hub for the use in the CAPEX analysis and further work in the project is shown in Figure 18. The main considerations are the same as for the AC and DC hub solutions previously discussed. The design of the AC system is the same as for the AC hub solution shown in Figure 7 with the difference that the bipole systems can be further split into individual poles. The DC busbar design is the exact same than that of the DC hub solution shown in Figure 11.

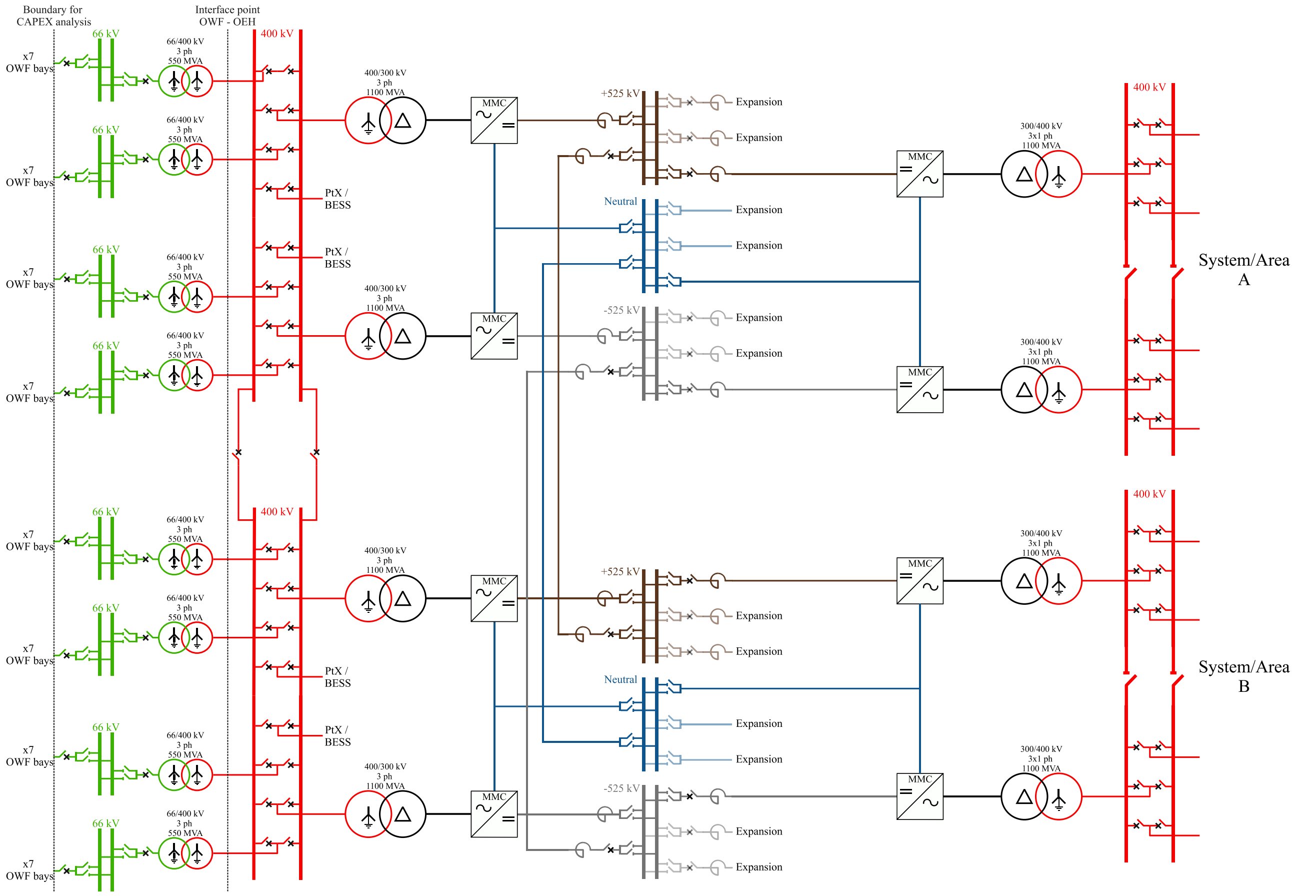


*Figure 18: Generic hybrid hub solution used for CAPEX analysis.*

### 3.1.4. INTERFACES AND INTERNAL LAYOUT OF THE OWF

The AC and Hybrid hub solutions, feature an interconnected AC system with an assumed voltage of 400 kV and the interface point between the OWFs and the OEH is located at the 400 kV busbar systems. The DC hub solution does not contain an additional AC bus and the OWFs are expected to directly interface with the OEH a voltage level suitable for connection of the offshore collector system of the OWF (in this report assumed as 66 kV). Since the focus of this study is to provide a comparative cost-analysis of the different hub solutions, the CAPEX analysis of the AC and Hybrid hub is stretched further to include a simplified representation of the 66 KV system as indicated in Figure 11 and Figure 18. The purpose of this solution is to consider the additional cost of the 66 kV system, that is otherwise shifted from the OEH to the OWF.

It should be noted that the chosen hub solution can impose different restrictions in terms of the layout and design of the collector system of the OWF. The AC hub solution allows to flexibly adjust the internal topology of the OWF according to the optimal design solution if the intended design complies with the requirements at the interface point of the OEH. The options for designing the internal layout of the OWF in case of the hybrid hub are restricted by the fact that the internal connections need to reflect the operating mode of the OEH. That is, the OWF always needs to be sectionalized into the same subsystems as the current operational configuration of the AC system of the OEH. The DC hub solution further limits the design choices for the electrical layout of the OWF since the interface point with the hub is provided at the 66 kV busbars and the transformer configuration and AC interconnection scheme are considered part of the hub design.

The optimal design of the 66 kV system is out of scope for the CAPEX analysis of the hub solutions and only a very simplified representation consisting of transformers and busbar systems is considered. The busbar layout and transformer rating are adopted from one of TenneT's HVDC-connected OWF [6], [7]. While the specific transformer winding layout is not considered as a specific cost input to the CAPEX analysis, it should be noted that a neutral earthing through a resistance is recommended for the star point on the 66-kV side of the transformers. The reason for this choice is to limit zero-sequence fault currents that could otherwise require larger cross-section of the array-cable shield wire, significantly increasing the cost of the array cables. Furthermore, an AC coupling option for the DC hub has been adopted to improve, to some extent, the limited availability of wind power in case of converter pole faults compared to the hybrid and AC solution. This is discussed in more detail in section 5.1.

It is recommended to perform further studies with the scope to optimize the overall system by considering the impact of the decisions regarding the hub topology on the cost and performance of the OWFs.

## 3.2. EXPANDABILITY

In the context of this report, expandability refers mainly to the conceptual integration of new elements into an existing hub solution. OEHs should allow the flexibility to modularly expand any kind of existing hub solution by either adding new offshore wind capacity or adding spokes that either expand the capacity of an existing connection or connect to an entirely new area. Furthermore, it should be possible to interconnect different OEHs that together form an interconnected offshore power system. An illustration of such a complex hub solution is provided in Figure 19.

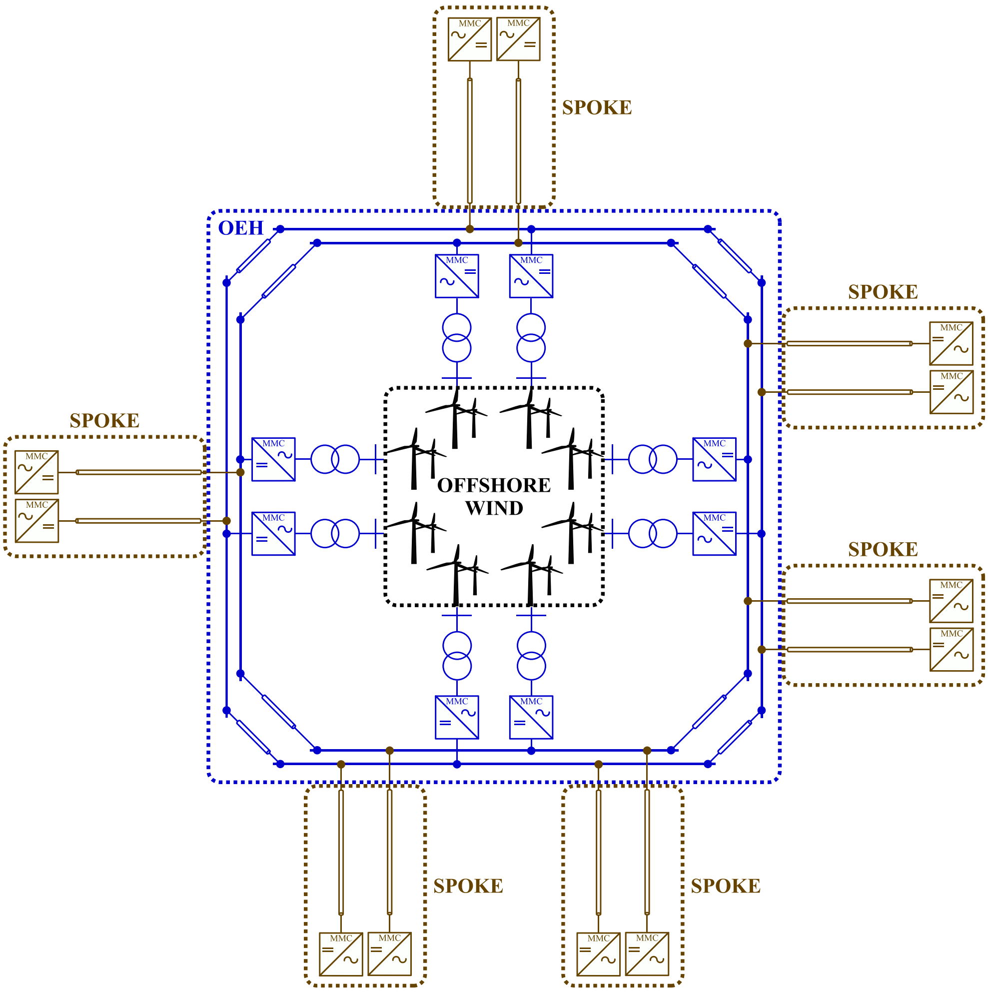


*Figure 19: Illustration of a potential hub expansion based on DC topology – This solution features a total of 8 GW wind capacity and 12 GW combined capacity of the connected spokes. The coloring indicates the classification of the elements: Blue – OEH, Brown – spokes & Black – OWF.*

To assess the CAPEX of different modular expansions of the base solutions, various relevant expansion cases are identified. The main expansions considered are related to increasing the installed capacity of offshore wind, by adding new OWFs, and increasing the external capacity, either for the purpose of power exchange or wind power export, by adding new spokes to the hub. Depending on the topology, these expansions can be achieved in different ways. It is assumed that busbar systems (both AC and

DC) are associated with HVDC converter stations. That is, a new busbar system is added whenever a hub expansion requires an additional offshore converter. Furthermore, it is assumed that the external capacity, that is the power that can be evacuated from the hub, is always equal or larger than the connected wind capacity. The main reason for this choice is the fact that, at this stage, the presence of significant amounts of local (internal) loads is disregarded.

### 3.2.1. AC Hub

The AC hub solution consists of an interconnected AC system that links the different OWFs and spokes which, in this solution, are essentially regular point-to-point HVDC systems. Increasing the exchange capacity of the hub with external systems, by adding an additional spoke, requires installation of a full HVDC system as indicated in Figure 20. Additionally, the AC system needs to be expanded by a new AC busbar and IIs, with a capacity of 2 GW, that connect the new busbar to the existing hub.

In an AC hub, an OWF expansion requires either a new or a previous spoke expansion to be able to evacuate the added wind power generation. In case of a previous spoke expansion, an additional OWF only requires the equipment specifically associated with the OWF, which are essentially the 66/400-kV transformers and busbars (as indicated in Figure 21).

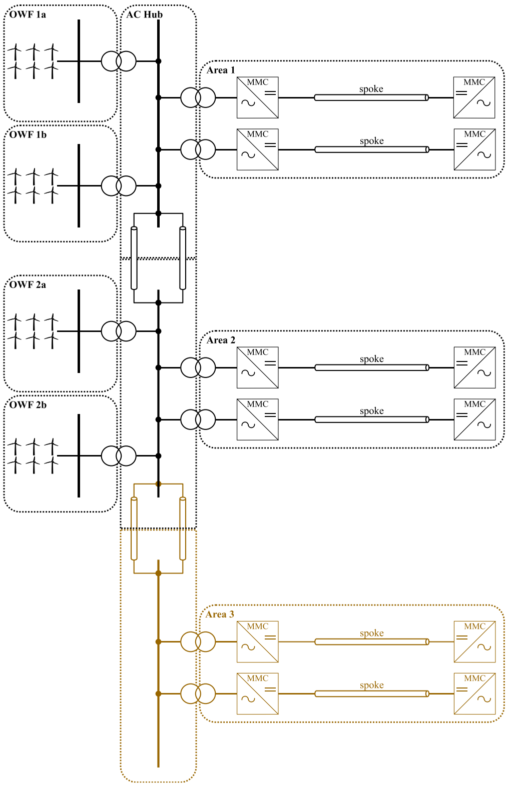


*Figure 20: Spoke expansion of the AC hub. New elements and interfaces due to the expansion are highlighted in brown.*

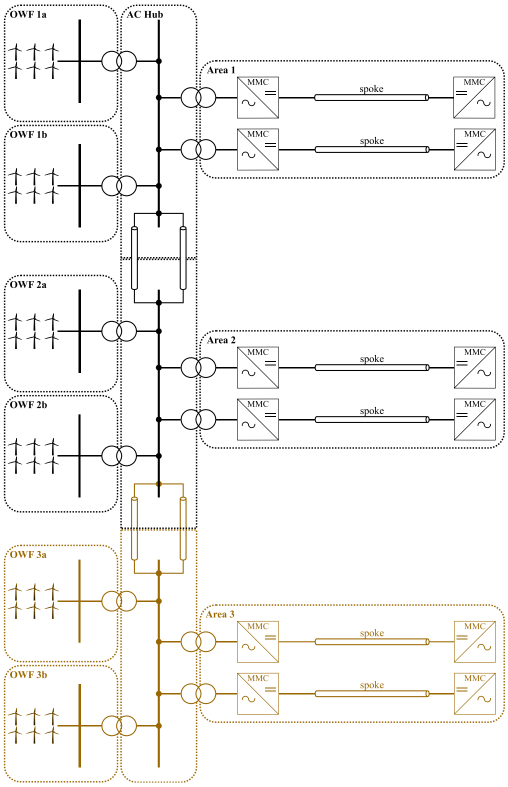


*Figure 21: OWF expansion of the AC hub. New elements and interfaces due to the expansion are highlighted in brown.*

Interfacing one AC OEH with another essentially requires the same equipment as a spoke expansion since, for an AC realization of the hubs, the connection requires a regular point-to-point HVDC system. The AC-hub-to-AC- hub interconnection expansion is indicated in Figure 22, while the other hub-to-hub interconnection options are addressed in section 3.2.2.

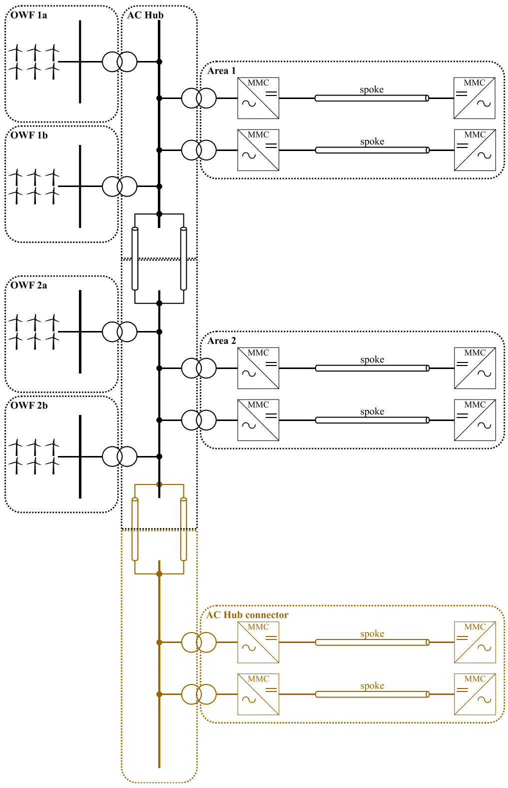


*Figure 22: AC OEH - AC OEH interconnector. New elements and interfaces due to the expansion are highlighted in brown.*

### 3.2.2. DC Hub

In constrast to an AC hub expansion, the DC solution allows to expand the hub with new spokes on the existing busbars if the node capacity is not yet exceeded. The maximum capacity of a DC node is illustrated in Figure 13. Expansion by a single spoke, as indicated in Figure 23, does not require an additional busbar system due to availabity of feeders (space for 5 feeders per busbar).

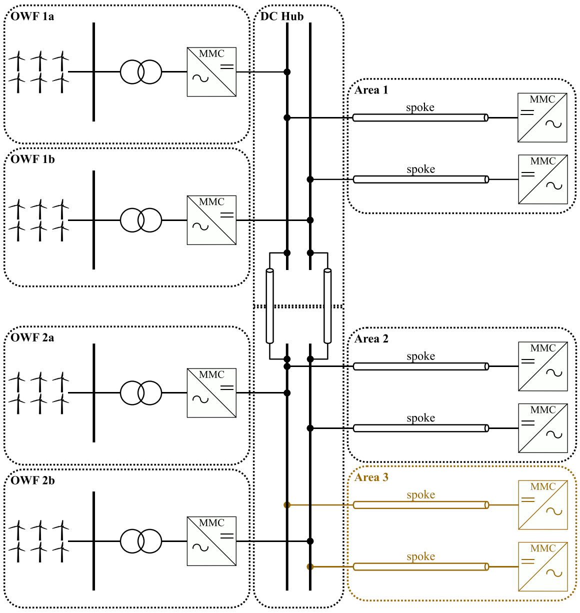


*Figure 23: DC Hub spoke expansion on an existing DC busbar. New elements and interfaces due to the expansion are highlighted in brown.*

Since DC busbars in the DC hub topology are mainly associated with the offshore converters, and these can be conceptually considered as part of the OWF, an expansion aiming at increasing the wind power capacity of the hub always introduces a new DC node. Two potential options for this kind of expansion can be considered. The OWF expansion can occur after a previous spoke expansion at an existing DC bus, shown in Figure 24, which illustrates the DC hub's potential for modular, stepwise expansion. The new DC node can then later be used for further spoke expansions. The alternative option, shown in Figure 25, is a parallel expansion by an OWF and a spoke, where they are both connected to the same, new, DC busbar.

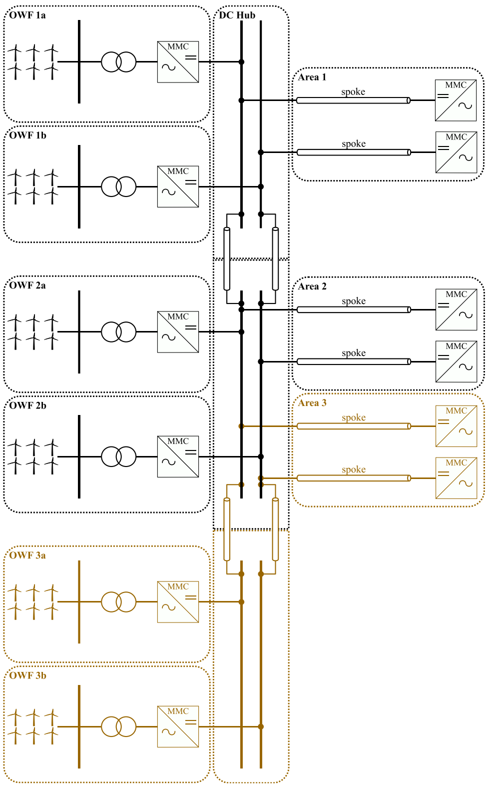


*Figure 24: OWF expansion after a previous spoke expansion. New elements and interfaces due to the expansion are highlighted in brown.*

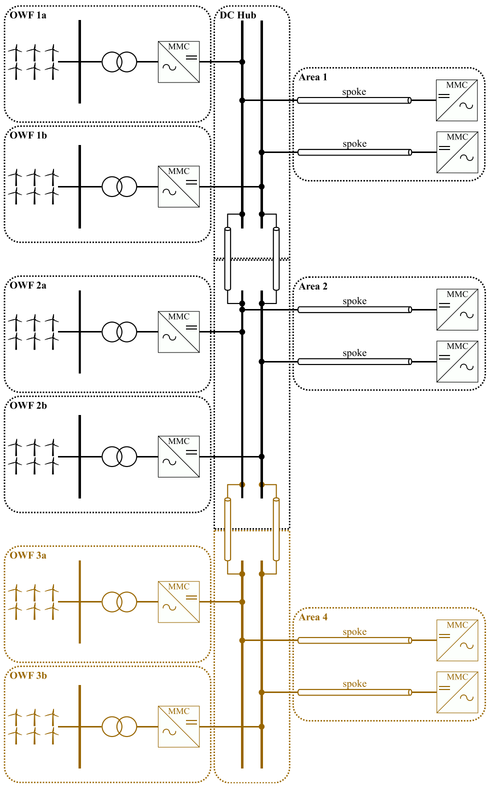


*Figure 25: Combined OWF and spoke expansion. New elements and interfaces due to the expansion are highlighted in brown.*

Expanding the hub via a hub-to-hub connection depends on the configuration of the hub at the receiving end. Facilitating a connection to a hub with an AC topology requires additional converters at the AC hub, while an interconnection to another DC hub only requires a cable connection and DC protection system at both ends. These two options are illustrated in Figure 26 and Figure 27, respectively.

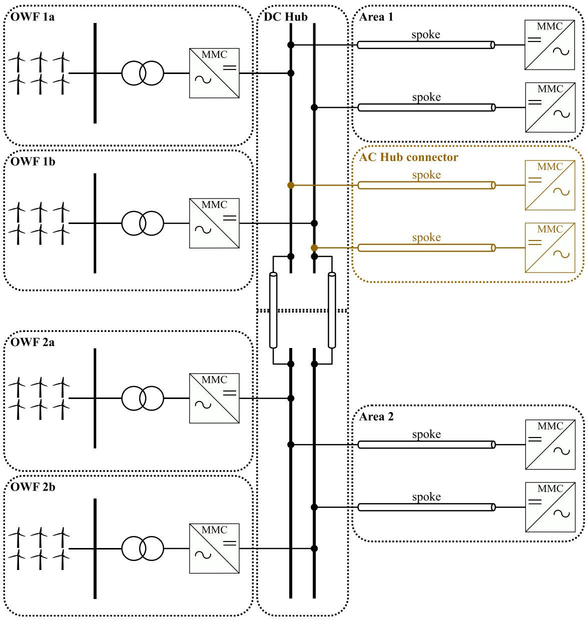


*Figure 26: DC OEH - AC OEH interconnector. New elements and interfaces due to the expansion are highlighted in brown.*

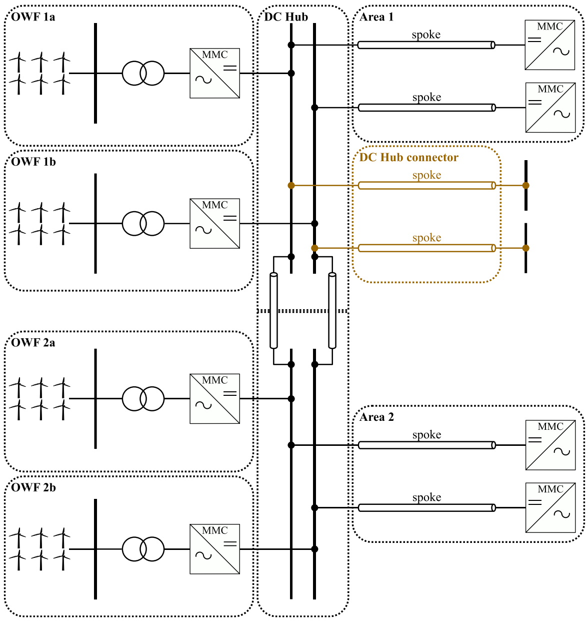


*Figure 27: DC OEH - DC OEH interconnector. New elements and interfaces due to the expansion are highlighted in brown.*

### 3.2.3. HYBRID HUB

The hybrid hub by design contains a full AC as well as DC infrastructure and can therefore be expanded on both sides. These two expansion options are conceptually illustrated in Figure 28, which shows an expansion on the AC side of the hybrid hub, and Figure 29, which illustrates the expansion on the DC side.

Apart from expanding on a single side of the hub, a hybrid expansion could also be achieved. One option for a hybrid expansion is illustrated in Figure 30, where the OEH following the AC expansion of Figure 28 is further extended by a single spoke on the DC side. The problem with this kind of configuration, however, is that the exchange capacity between the AC and DC hub is still the same as in the base case. This can impose a limitation in terms of the active power exchange capacity between the systems connected to the AC hub and these interfaced with the DC hub. When the scope of the expansion is to preserve the hybrid hub topology rather than expanding an individual configuration, both hub sides can be expanded as illustrated in Figure 31.

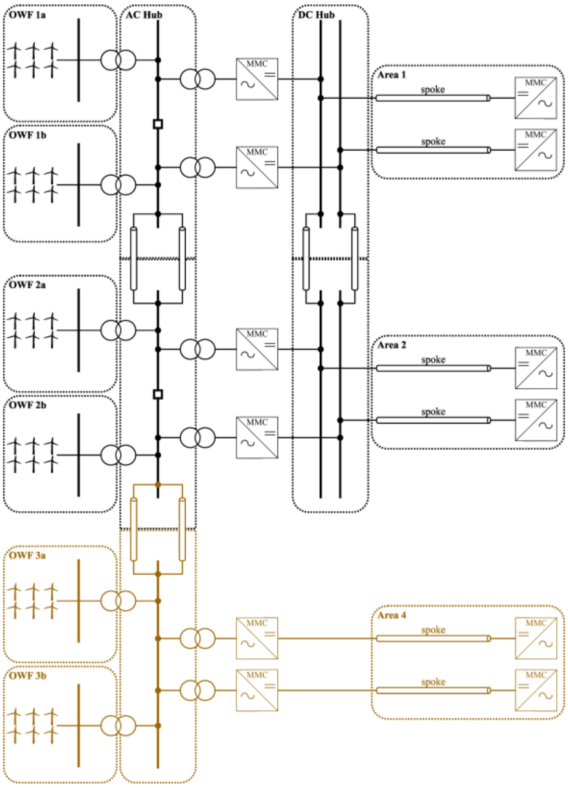


*Figure 28: Example of an AC side expansion of the Hybrid hub. New elements and interfaces due to the expansion are highlighted in brown.*

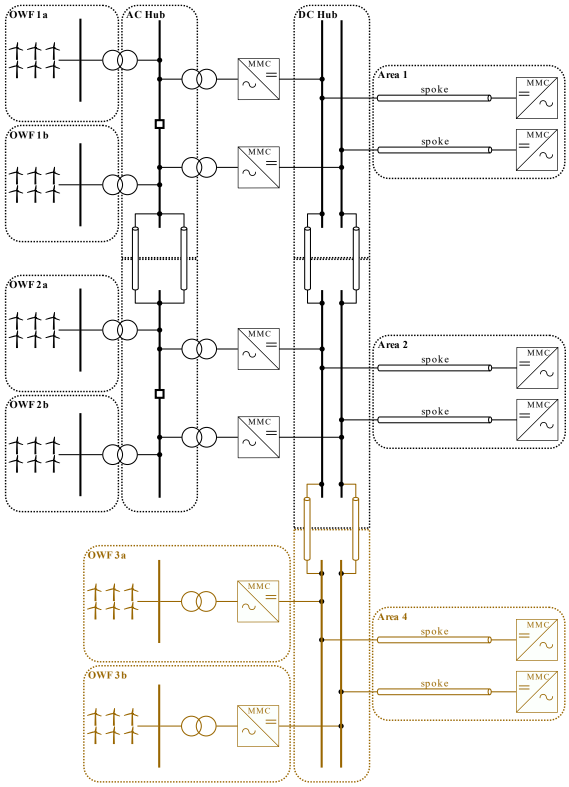


*Figure 29: Example of a DC side expansion of a Hybrid hub. New elements and interfaces due to the expansion are highlighted in brown.*

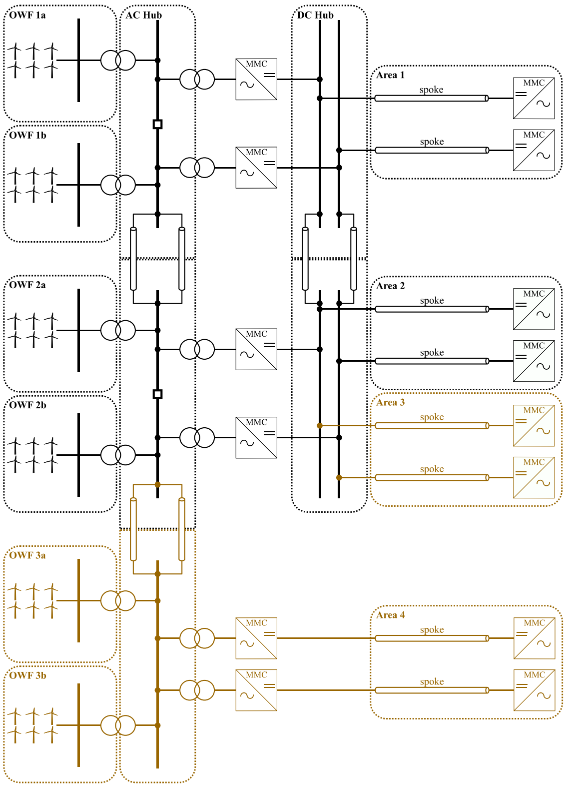


*Figure 30: Example of a Hybrid hub expansion on the AC and DC side. New elements and interfaces due to the expansion are highlighted in brown.*

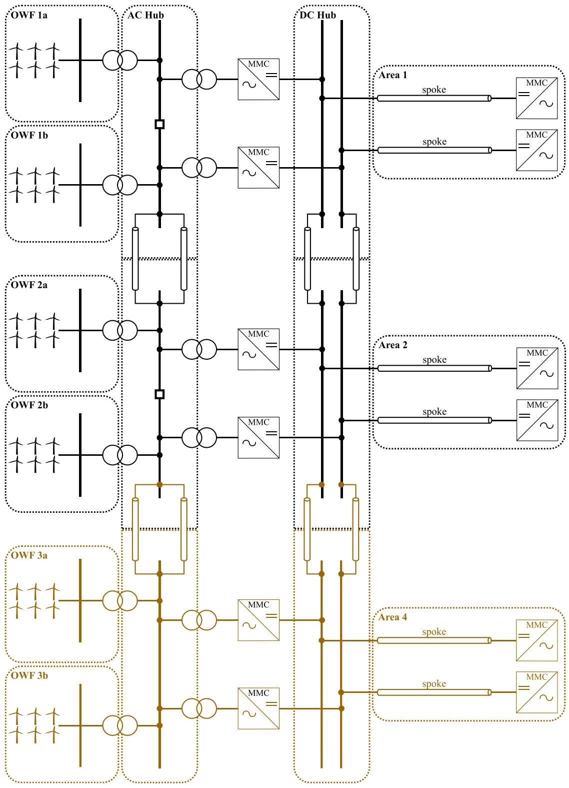


*Figure 31: Expanding the hybrid hub while preserving the full hybrid solution. New elements and interfaces due to the expansion are highlighted in brown.*

## 3.3. COMPONENT LIST

In this section, a comprehensive list of all relevant components for all hub topologies and the expansion options is provided, including the basic ratings. The base case is the initial, basic topology as described in section 3.1. The four expansion options include the additional components for expanding the hub.

- AC hub and DC hub (Table 3 and Table 4, respectively):
    - Expansion option 1: expanding the hub with an additional windfarm and a spoke (onshore area connection).
    - Expansion option 2: expanding the hub with an additional spoke.
    - Expansion option 3: expanding the hub with an additional windfarm.
    - Expansion option 4: expanding the hub towards another hub. This option includes two scenarios, basically a scenario where the topologies of the two hubs are mirrored and when they are different.
        - Scenario 1 – mirrored topologies: AC hub expanded to an AC hub, and DC hub expanded to a DC hub.
        - Scenario 2 – differing topologies: AC hub expanded to a DC hub, and DC hub expanded to an AC hub.
- Hybrid hub (Table 5, Table 6, and Table 7):
    - Expansion option 1: expanding the hub with an additional windfarm and a spoke. Includes three possible scenarios.
        - Scenario 1: hybrid expansion – that considers an expansion on the AC & DC side and thereby preserving the hybrid topology across the expansion.
        - Scenario 2: expansion on the AC side – expansion only connects to the AC system of the original hub.
        - Scenario 3: expansion on the DC side – expansion only connects to the DC system of the original hub.
    - Expansion option 2: expanding the hub with an additional spoke. Includes three possible scenarios, which are the same as in the first expansion option.
    - Expansion option 3: expanding the hub with an additional windfarm. Includes three possible scenarios, which are the same as in the first expansion option.
    - Expansion option 4: expanding the hub towards another hub.
        - Scenario 1: mirrored expansion: full-scale to full-scale, AC to AC and DC to DC.
        - Scenario 2: differing expansion, full-scale to AC, full scale to DC, AC to DC, and DC to AC.

*Table 3: List of components for the AC Hub.*

| Components | Ratings | Base case | Expansion option 1 (Area + OWF) | Expansion option 2 (Area) | Expansion option 3 (OWF) | Expansion option 4 (Hub-to-Hub) AC-AC | Expansion option 4 (Hub-to-Hub) AC-DC |
|---|---|---|---|---|---|---|---|
| | | # of Components | Additional | Additional | Additional | Additional | Additional |
| Converters | MMC Converter<br>200 modules per arm (3kV per module)<br>DC Side Rated voltage: 525kV<br>AC Side Rated Voltage: 300kV | 8 | 4 | 4 | 0 | 4 | 2 |
| Transformers | Offshore three phase two winding transformer<br>66kV/400kV<br>550MVA Yg/Yg, uk: 15% | 8 | 4 | 0 | 4 | 0 | 0 |
| | Offshore three phase two winding transformer<br>300kV/400kV<br>1050 MVA D/Yg, uk: 15% | 4 | 2 | 2 | 0 | 4 | 2 |
| | Offshore three phase two winding transformer<br>66kV/300kV<br>550MVA Yg/D, uk: 15% | 0 | 0 | 0 | 0 | 0 | 0 |
| | Onshore three single phase two winding transformer<br>300kV/400kV<br>3 x 350MVA Y/Yg, uk: 15% | 4 | 2 | 2 | 0 | 0 | 0 |
| Busbars and Circuit Breakers | Double busbar double breaker Offshore 400kV | 2 | 1 | 1 | 1 | 2 | 1 |
| | Circuit breaker<br>400kV, >800A | 16 | 8 | 0 | 8 | 0 | 0 |
| | Circuit breaker<br>400kV, >1600A | 10 | 6 | 6 | 2 | 12 | 6 |
| | Double busbar double breaker Onshore 400kV | 2 | 1 | 1 | 0 | 0 | 0 |
| | Circuit breaker<br>400kV, >1600A | 24 | 12 | 12 | 0 | 0 | 0 |
| | Double busbar Single breaker Offshore 66kV | 8 | 4 | 0 | 4 | 0 | 0 |
| | Circuit breaker<br>66kV, 1250A | 56 | 28 | 0 | 28 | 0 | 0 |
| | Circuit breaker<br>66kV, >4800A | 8 | 4 | 0 | 4 | 0 | 0 |
| | Double busbar Single breaker Offshore 525kV | 0 | 0 | 0 | 0 | 0 | 0 |
| | Circuit breaker<br>525kV, 1905A | 0 | 0 | 0 | 0 | 0 | 2 |
| | DC reactor<br>525kV, >1905A, 180mH | 0 | 0 | 0 | 0 | 0 | 2 |
| Cables<br>OHL Couplers<br>GIS couplers | OHL or Cable or Busbar Coupler<br>400kV, >1600A | 2 | 2 | 2 | 2 | 4 | 2 |
| | Overhead line, GIS coupler or Cable<br>525kV, >1905A | 0 | 0 | 0 | 0 | 0 | 0 |
| | Undersea spoke cable<br>525kV, 1905A | 6 | 3 | 3 | 0 | 3 | 3 |

*Table 4: List of components for the DC Hub.*

| Components | Ratings | Base case | Expansion option 1 (Area + OWF) | Expansion option 2 (Area) | Expansion option 3 (OWF) | Expansion option 4 (Hub-to-Hub) DC-DC | Expansion option 4 (Hub-to-Hub) DC-AC |
|---|---|---|---|---|---|---|---|
| | | # of Components | Additional | Additional | Additional | Additional | Additional |
| Converters | MMC Converter<br>200 modules per arm (3kV per module)<br>DC Side Rated voltage: 525kV<br>AC Side Rated Voltage: 300kV | 8 | 4 | 2 | 2 | 0 | 2 |
| Transformers | Offshore three phase two winding transformer<br>66kV/400kV<br>550MVA Yg/Yg, uk: 15% | 0 | 0 | 0 | 0 | 0 | 0 |
| | Offshore three phase two winding transformer 300kV/400kV<br>1050 MVA D/Yg<br>uk: 15% | 0 | 0 | 0 | 0 | 0 | 2 |
| | Offshore three phase two winding transformer<br>66kV/300kV<br>550MVA Yg/D, uk: 15% | 8 | 4 | 0 | 4 | 0 | 0 |
| | Onshore three single phase two winding transformer<br>300kV/400kV<br>3 x 350MVA Y/Yg, uk: 15% | 4 | 2 | 2 | 0 | 0 | 0 |
| Busbars and Circuit Breakers | Double busbar double breaker Offshore<br>400kV | 0 | 0 | 0 | 0 | 0 | 1 |
| | Circuit breaker<br>400kV, 800A | 0 | 0 | 0 | 0 | 0 | 0 |
| | Circuit breaker<br>400kV, 1600A | 0 | 0 | 0 | 0 | 0 | 6 |
| | Double busbar double breaker Onshore<br>400kV | 2 | 1 | 1 | 0 | 0 | 0 |
| | Circuit breaker<br>400kV, >1600A | 24 | 12 | 12 | 0 | 0 | 0 |
| | Double busbar Single breaker<br>66kV | 8 | 4 | 0 | 4 | 0 | 0 |
| | Circuit breaker<br>66kV, 1250A | 56 | 28 | 0 | 28 | 0 | 0 |
| | Circuit breaker<br>66kV, 4800A | 8 | 4 | 0 | 4 | 0 | 0 |
| | Double busbar Single breaker<br>525kV | 6 | 3 | 0 | 3 | 0 | 0 |
| | Circuit breaker<br>525kV, 1905A | 8 | 6 | 2 | 4 | 4 | 2 |
| | DC reactor<br>525kV, 1905A. 180mH | 12 | 8 | 2 | 6 | 4 | 2 |
| Cables<br>OHL Couplers<br>GIS couplers | OHL or Cable or Busbar Coupler<br>400kV, 1600A | 0 | 0 | 0 | 0 | 0 | 2 |
| | Overhead line, GIS coupler or Cable<br>525kV, 1905A | 3 | 3 | 0 | 3 | 0 | 0 |
| | Undersea spoke cable<br>525kV, 1905A | 6 | 3 | 3 | 0 | 3 | 3 |

Table 5: List of components of the Hybrid Hub for the full-scale expansion.

| Components | Ratings | Base case | Expansion option 1 (Area + OWF) Full | Expansion option 2 (Area) Full | Expansion option 3 (OWF) Full | Expansion option 4 (Hub-to-Hub) Full-Full | Expansion option 4 (Hub-to-Hub) Full-AC | Expansion option 4 (Hub-to-Hub) Full-DC |
|---|---|---|---|---|---|---|---|---|
| | | # of Components | Additional | Additional | Additional | Additional | Additional | Additional |
| Converters | MMC Converter<br>200 modules per arm (3kV per module)<br>DC Side Rated voltage: 525kV<br>AC Side Rated Voltage: 300kV | 8 | 4 | 4 | 2 | 4 | 4 | 2 |
| Transformers | Offshore three phase two winding transformer<br>66kV/400kV<br>550MVA Yg/Yg, uk: 15% | 8 | 4 | 0 | 4 | 0 | 0 | 0 |
| | Offshore three phase two winding transformer<br>300kV/400kV<br>1050 MVA D/Yg, uk: 15% | 4 | 2 | 2 | 2 | 4 | 4 | 2 |
| | Offshore three phase two winding transformer<br>66kV/300kV<br>550MVA Yg/D, uk: 15% | 0 | 0 | 0 | 0 | 0 | 0 | 0 |
| | Onshore three single phase two winding transformer<br>300kV/400kV<br>3 x 350MVA Y/Yg, uk: 15% | 4 | 2 | 2 | 0 | 0 | 0 | 0 |
| Busbars and Circuit Breakers | Double busbar double breaker Offshore<br>400kV | 4 | 2 | 2 | 2 | 4 | 4 | 2 |
| | Circuit breaker<br>400kV, >800A | 16 | 8 | 0 | 8 | 0 | 0 | 0 |
| | Circuit breaker<br>400kV, >1600A | 10 | 6 | 6 | 6 | 12 | 12 | 6 |
| | Double busbar double breaker Onshore<br>400kV | 2 | 1 | 1 | 0 | 0 | 0 | 0 |
| | Circuit breaker<br>400kV, >1600A | 24 | 12 | 12 | 0 | 0 | 0 | 0 |
| | Double busbar Single breaker<br>66kV, ?A | 8 | 4 | 0 | 4 | 0 | 0 | 0 |
| | Circuit breaker<br>66kV, 1250A | 56 | 28 | 0 | 28 | 0 | 0 | 0 |
| | Circuit breaker<br>66kV, >4800A | 8 | 4 | 0 | 4 | 0 | 0 | 0 |
| | Double busbar Single breaker<br>525kV | 6 | 3 | 3 | 3 | 6 | 3 | 3 |
| | Circuit breaker<br>525kV, 1905A | 8 | 6 | 6 | 4 | 12 | 6 | 8 |
| | DC reactor<br>525kV, >1905A | 12 | 8 | 8 | 6 | 16 | 8 | 10 |
| Cables OHL Couplers GIS couplers | OHL or Cable or Busbar Coupler<br>400kV, >1600A | 2 | 2 | 2 | 2 | 4 | 2 | 2 |
| | Overhead line, GIS coupler or Cable<br>525kV, >1905A | 3 | 3 | 3 | 3 | 6 | 3 | 3 |
| | Undersea spoke cable<br>525kV, 1905A | 6 | 3 | 3 | 0 | 3 | 3 | 3 |

*Table 6: List of components of the Hybrid Hub for the AC side expansion.*

| Components | Ratings | Base case | Expansion option 1 (Area + OWF) AC Side | Expansion option 2 (Area) AC Side | Expansion option 3 (OWF) AC Side | Expansion option 4 (Hub-to-Hub) AC-AC | Expansion option 4 (Hub-to-Hub) AC-DC |
|---|---|---|---|---|---|---|---|
| | | # of Components | Additional | Additional | Additional | Additional | Additional |
| Converters | MMC Converter<br>200 modules per arm (3kV per module)<br>DC Side Rated voltage: 525kV<br>AC Side Rated Voltage: 300kV | 8 | 4 | 4 | 0 | 4 | 2 |
| Transformers | Offshore three phase two winding transformer<br>66kV/400kV<br>550MVA Yg/Yg, uk: 15% | 8 | 4 | 0 | 4 | 0 | 0 |
| | Offshore three phase two winding transformer<br>300kV/400kV<br>1050 MVA D/Yg, uk: 15% | 4 | 2 | 2 | 0 | 4 | 2 |
| | Offshore three phase two winding transformer<br>66kV/300kV<br>550MVA Yg/D, uk: 15% | 0 | 0 | 0 | 0 | 0 | 0 |
| | Onshore three single phase two winding transformer<br>300kV/400kV<br>3 x 350MVA Y/Yg, uk: 15% | 4 | 2 | 2 | 0 | 0 | 0 |
| Busbars and Circuit Breakers | Double busbar double breaker Offshore<br>400kV | 4 | 2 | 2 | 2 | 4 | 2 |
| | Circuit breaker<br>400kV, >800A | 16 | 8 | 0 | 8 | 0 | 0 |
| | Circuit breaker<br>400kV, >1600A | 10 | 6 | 6 | 2 | 12 | 6 |
| | Double busbar double breaker Onshore<br>400kV | 2 | 1 | 1 | 0 | 0 | 0 |
| | Circuit breaker<br>400kV, >1600A | 24 | 12 | 12 | 0 | 0 | 0 |
| | Double busbar Single breaker<br>66kV, ?A | 8 | 4 | 0 | 4 | 0 | 0 |
| | Circuit breaker<br>66kV, 1250A | 56 | 28 | 0 | 28 | 0 | 0 |
| | Circuit breaker<br>66kV, >4800A | 8 | 4 | 0 | 4 | 0 | 0 |
| | Double busbar Single breaker<br>525kV | 6 | 0 | 0 | 0 | 0 | 0 |
| | Circuit breaker<br>525kV, 1905A | 8 | 0 | 0 | 0 | 0 | 2 |
| | DC reactor<br>525kV, >1905A | 12 | 0 | 0 | 0 | 0 | 2 |
| Cables<br>OHL Couplers<br>GIS couplers | OHL or Cable or Busbar Coupler<br>400kV, >1600A | 2 | 2 | 2 | 2 | 4 | 2 |
| | Overhead line, GIS coupler or Cable<br>525kV, >1905A | 3 | 0 | 0 | 0 | 0 | 0 |
| | Undersea spoke cable<br>525kV, 1905A | 6 | 3 | 3 | 0 | 3 | 3 |

*Table 7: List of components of the Hybrid Hub for the DC side expansion.*

| Components | Ratings | Base case | Expansion option 1 (Area + OWF) DC Side | Expansion option 2 (Area) DC Side | Expansion option 3 (OWF) DC Side | Expansion option 4 (Hub-to-Hub) DC-AC | Expansion option 4 (Hub-to-Hub) DC-DC |
|---|---|---|---|---|---|---|---|
| | | # of Components | Additional | Additional | Additional | Additional | Additional |
| Converters | MMC Converter<br>200 modules per arm (3kV per module)<br>DC Side Rated voltage: 525kV<br>AC Side Rated Voltage: 300kV | 8 | 4 | 2 | 2 | 2 | 0 |
| Transformers | Offshore three phase two winding transformer<br>66kV/400kV<br>550MVA Yg/Yg, uk: 15% | 8 | 0 | 0 | 0 | 0 | 0 |
| | Offshore three phase two winding transformer<br>300kV/400kV<br>1050 MVA D/Yg, uk: 15% | 4 | 0 | 0 | 0 | 2 | 0 |
| | Offshore three phase two winding transformer<br>66kV/300kV<br>550MVA Yg/D, uk: 15% | 0 | 4 | 0 | 4 | 0 | 0 |
| | Onshore three single phase two winding transformer<br>300kV/400kV<br>3 x 350MVA Y/Yg, uk: 15% | 4 | 2 | 2 | 0 | 0 | 0 |
| Busbars and Circuit Breakers | Double busbar double breaker Offshore<br>400kV | 4 | 0 | 0 | 0 | 2 | 0 |
| | Circuit breaker<br>400kV, >800A | 16 | 0 | 0 | 0 | 0 | 0 |
| | Circuit breaker<br>400kV, >1600A | 10 | 0 | 0 | 0 | 6 | 0 |
| | Double busbar double breaker Onshore<br>400kV | 2 | 1 | 1 | 0 | 0 | 0 |
| | Circuit breaker<br>400kV, >1600A | 24 | 12 | 12 | 0 | 0 | 0 |
| | Double busbar Single breaker<br>66kV, ?A | 8 | 4 | 0 | 4 | 0 | 0 |
| | Circuit breaker<br>66kV, 1250A | 56 | 28 | 0 | 28 | 0 | 0 |
| | Circuit breaker<br>66kV, >4800A | 8 | 4 | 0 | 4 | 0 | 0 |
| | Double busbar Single breaker<br>525kV | 6 | 3 | 0 | 3 | 0 | 0 |
| | Circuit breaker<br>525kV, 1905A | 8 | 6 | 2 | 4 | 2 | 4 |
| | DC reactor<br>525kV, >1905A | 12 | 8 | 2 | 6 | 2 | 4 |
| Cables<br>OHL Couplers<br>GIS couplers | OHL or Cable or Busbar Coupler<br>400kV, >1600A | 2 | 0 | 0 | 0 | 2 | 0 |
| | Overhead line, GIS coupler or Cable<br>525kV, >1905A | 3 | 3 | 0 | 3 | 0 | 0 |
| | Undersea spoke cable<br>525kV, 1905A | 6 | 3 | 3 | 0 | 3 | 3 |

# 4. ECONOMIC ANALYSIS

## 4.1. CAPEX ESTIMATION FOR HUB TOPOLOGIES

### 4.1.1. GENERAL METHODOLOGY AND APPROACH FOR CAPEX CALCULATIONS

In this section, a comparison of capital investment costs for the AC, DC, and Hybrid hub topology, including the expansion cases, will be provided. The base case is the reference for comparison, and it includes four wind farms with 1GW of installed capacity, two offshore HVDC bipoles rated at 2GW each, two onshore HVDC bipoles rated at 2GW each, two onshore DC connections (2GW spokes, 1GW per DC cable), and cables for offshore bipole interconnection.

There are four expansion cases considered in this study and they are based on the specifications given in section 3.2.

- Expansion option 1 includes adding two offshore windfarms of 1GW capacity and an additional spoke connecting the hub with an onshore system.
- Expansion option 2 is the addition of a spoke connecting the hub with an onshore system.
- Expansion option 3 is the expansion of the hub by adding two wind farms rated at 1GW each.
- Expansion option 4 is the hub-to-hub connection and we can differentiate between two possibilities in this case: the two connecting hubs have mirrored topologies, which means that they are both expanded either on the AC or the DC side or both, depending on the topology of the hubs; the second case considers a scenario where the target hub topology differs from the topology of the connecting hub. This means that the AC and DC hub expansion towards another hub has two possible configurations, while the hybrid hub has three.

Relevant data for the cost models is taken from the NSWPH report [1] with additional data provided by the SuperGrid institute. This includes cost for the AC and DC cables, DC protection and DC busbar systems, converters and transformers, and the platform cost. The footprint of the DC busbar system and DC breakers estimation are also taken from the NSWPH feasibility report [1]. Estimation of the converter station footprint was taken from the Energinet's market dialogue documentation for the Bornholm Energy Island project [5]. Offshore AC busbar system and protection cost models, as well as the footprint estimation requirements (including the transformer footprint estimations) were provided by Ørsted.

Components considered in this study are based on the detailed single line diagrams presented in Section 3.1 and they include:

- AC hub (single line diagram in Figure 7):
  - 66-kV DBSB system including the protection.
  - 400-kV DBDB offshore system including the protection.
  - 400-kV DBDB onshore system including the protection.
  - 66-kV/400-kV, 550-MVA transformers for the OWFs.
  - 300-kV/400-kV, 1050-MVA offshore and onshore converter transformers.
  - 300-kV AC/525-kV DC MMC offshore and onshore converters.

- 525-kV, 1.9-kA DC submarine spoke cables.
- 400-kV, 1.6k-A AC submarine interconnection cables.

- DC hub (single line diagram in Figure 11):
  - 66-kV DBSB system including the protection.
  - 400-kV DBDB onshore system including the protection.
  - 66-kV/300-kV, 550-MVA converter transformers for the OWFs.
  - 300-kV AC/525-kV DC MMC offshore and onshore converters.
  - 525-kV DBSB offshore DC system including the protection.
  - 525-kV, 1.9-kA DC submarine spoke and interconnection cables.
- Hybrid hub (single line diagram in Figure 18):
  - The components considered for the CAPEX estimation of the hybrid hub include the offshore AC system of the AC hub and the offshore DC system of the DC hub. The AC system of the hybrid hub differs from the AC system of the AC hub in the design of the 400-kV busbar system. When the hybrid hub is operated in the DC interconnected mode, the poles of each HVDC bipole can be decoupled on the AC side. The onshore system is the same as in the previous two topologies.

The full list of the required components for all topologies and expansion cases is given in the tables in section 3.3. Table 8 summarizes the costs of individual components including the surface area requirements per component.

*Table 8: Cost models and surface area requirements of individual components.*

| Components | Ratings | Surface Area requirements per unit (m^2)<br>Cable length [km] | Cost per unit / Cost per km |
|---|---|---|---|
| Converters | MMC Converter<br>200 modules per arm (3kV per module)<br>DC Side Rated voltage: 525kV<br>AC Side Rated Voltage: 300kV | 2.250,00 m^2 | 131,00 M€ |
| Transformers | Offshore three phase two winding transformer<br>66kV/400kV<br>550MVA Yg/Yg, uk: 15% | 128,00 m^2 | 7,00 M€ |
| | Offshore three phase two winding transformer<br>300kV/400kV<br>1050 MVA D/Yg, uk: 15% | 128,00 m^2 | 7,00 M€ |
| | Offshore three phase two winding transformer<br>66kV/300kV<br>550MVA Yg/D, uk: 15% | 128,00 m^2 | 7,00 M€ |
| | Onshore three single phase two winding transformer<br>300kV/400kV<br>3 x 350MVA Y/Yg, uk: 15% | 128,00 m^2 | 6,50 M€ |
| Busbars and Circuit Breakers | Double busbar double breaker Offshore<br>400kV | 583,00 m^2 | 0,80 M€ |
| | Circuit breaker<br>400kV, >800A | 4,00 m^2 | 0,12 M€ |
| | Circuit breaker<br>400kV, >1600A | 5,00 m^2 | 0,12 M€ |
| | Double busbar double breaker Onshore<br>400kV | 580,00 m^2 | 1,50 M€ |
| | Circuit breaker<br>400kV, >1600A | 5,00 m^2 | 0,12 M€ |
| | Double busbar Single breaker Offshore<br>66kV | 100,00 m^2 | 1,30 M€ |
| | Circuit breaker<br>66kV, 1250A | 3,00 m^2 | 0,03 M€ |
| | Circuit breaker<br>66kV, >4800A | 5,00 m^2 | 0,03 M€ |
| | Double busbar Single breaker Offshore<br>66kV | 150,00 m^2 | 1,30 M€ |
| | Circuit breaker<br>525kV, 1905A | 401,28 m^2 | 10,30 M€ |
| | DC reactor<br>525kV, >1905A | 17,78 m^2 | 1,33 M€ |
| Cables<br>OHL Couplers<br>GIS couplers | AC OHL or cable or busbar coupler<br>400kV, >1600A | 20,00 km | 1,02 M€ |
| | DC overhead line, GIS coupler or cable<br>525kV, >1905A | 20,00 km | 1,06 M€/km |
| | Submarine DC spoke cable<br>525kV, 1905A | 100,00 km | 1,06 M€/km |

### 4.1.2. Assumptions

As stated in the previous section, the CAPEX includes calculations for the cost of all components listed and the surface cost for all offshore equipment. The following assumptions apply to the CAPEX analysis:

- When it comes to the busbar systems of the base topologies, CAPEX calculations include the cost of the utilized components as well as the surface requirements for the connected feeders and associated protection components even if not utilized in the base case. The cost of extra components purposed for the expansions is not considered in the CAPEX analysis since they are only added when the expansion is implemented. When it comes to the footprint analysis, similarly to the CAPEX surface requirement analysis, the complete busbar system and the associated protection are considered (connected feeders and extra feeders for the expansion), i.e., it is assumed that the initial design of the busbar already accounts for the space required for future expansions even though the components are not there yet. As an example, if a given expansion requires adding an extra feeder DCCB, the cost of this device would not be considered in the CAPEX analysis of the base case, but the surface cost and space needed for it would already be considered in the CAPEX and footprint analysis of the base topology, respectively.
- The lengths of the spoke cables are assumed to be 100km. This is taken as an arbitrary length as the proposed hub design is generic and it does not represent a real case scenario. Furthermore, length of the spoke does not have any influence on the comparative CAPEX analysis of the different hub solutions, as all topologies include the same number of spokes with the same length and therefore scale equally with the considered spoke length.
- The length of the II cables is assumed to be 20km, which is approximately the breakeven length between the AC and DC interconnections, as per the CAPEX comparison in NSWPH report [1]. For shorter distances, AC has the edge over DC, while for longer distances, DC interconnection is the favorable solution.
- For the hub-to-hub expansion, it was considered the case where the expansion of both hubs is mirrored and the case where the expansion topology differs between the two hubs. For example, hub “A” is expanded on the AC side and connected with hub “B” which is expanded on the DC side, and vice versa.
- The cost of PtX installations and associated protection and surface area is not considered as the capacity, scale, and the location (centralized on the hub or distributed on wind turbines) has not been determined at this stage of the project.
- The cost and surface area of the supporting components such as synchronous condensers and STATCOMs are not considered as it is unknown, at this stage of the project, if they will be required and at which capacity.

### 4.1.3. CAPEX comparison of AC, DC, and Hybrid Hubs

For the CAPEX analysis, the base case topologies and five different expansion options are considered. The hybrid hub differs from the other topologies, as it provides the possibility for expansion on the AC side, DC side, or full hybrid expansion on both AC and DC sides. Figure 32 contains the results of the CAPEX analysis for all these cases. The total CAPEX includes the cost of the components and the associated surface area costs. The CAPEX of the base AC hub topology is taken as a reference for the comparison provided in Figure 32, which means that the cost of all other topologies and expansion options are normalized in relation to the cost of the AC hub base case.

The base case comparison shows that the AC hub is the favorable solution as the DC hub CAPEX is ~14% higher. The CAPEX for the hybrid hub is ~20% higher than the AC hub. The main driving factor being the cost and surface requirements of the DC protection system of the DC hub (large surface area required and high cost of the DCCBs).

When expanding the hub with additional OWFs, AC hub and hybrid hub expanded on the AC side are shown to be the favorable solutions because of the associated cost of the DC protection system of the DC hub and the fact that the new OWF can be coupled on the AC side without additional converters. This is further confirmed in Figure 33, where we can observe a significant difference in additional costs when expanding the DC hub with wind power capacity. The same can be observed for the hybrid hub when expanding it on the DC side. On the other hand, adding additional spokes (onshore connections) as well as establishing a connection from one hub to another shifts the advantage towards the DC solution. Figure 32 shows that the expansion of the hub towards additional areas shifts the CAPEX difference between the AC and DC hub in favor of the DC solution by ~7% in terms of CAPEX. This indicates that the cost savings of the spoke expansion (option 2) of the DC hub compared to the AC hub (see ΔCAPEX values for expansion option 2 in Figure 33) outweigh the significant cost advantage of the AC hub in the base solution. The DC hub advantage for a spoke expansion is mainly because the new spoke can be coupled on the DC side without additional converters. We can observe a similar pattern when expanding the hub towards another hub with mirrored topology. In this case, the DC solution is favorable in comparison to the AC solution. Similar results are observed for the hybrid solution when expanding on the DC side.

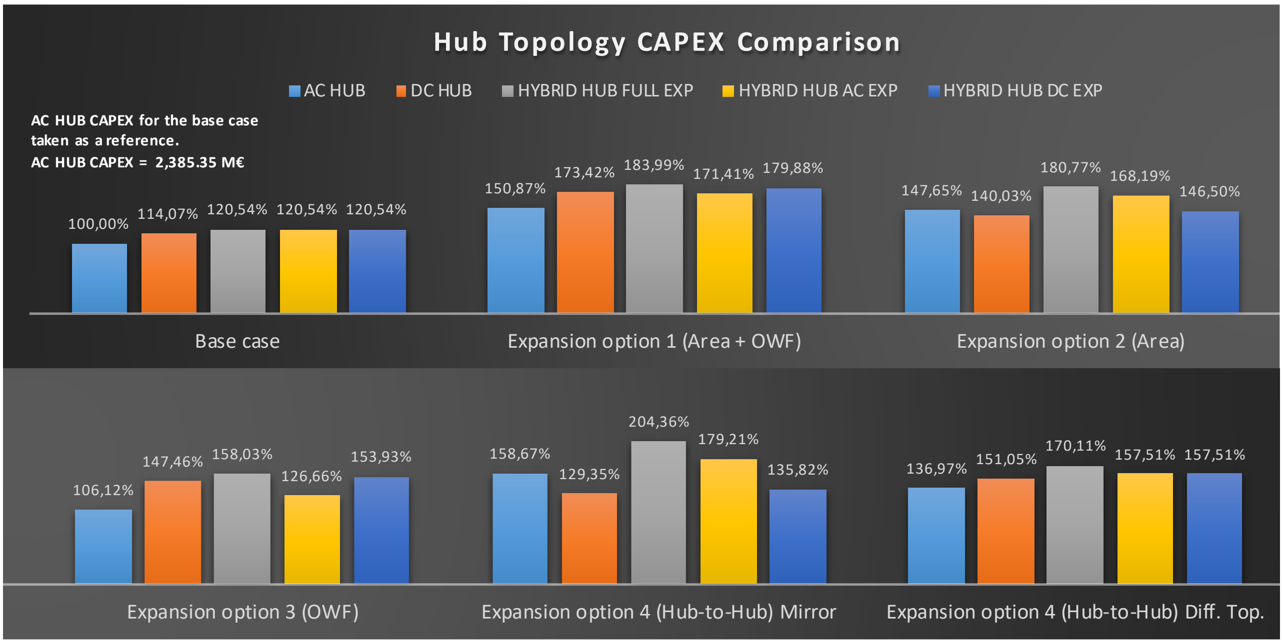


*Figure 32: CAPEX comparison for all topologies (includes the cost of all components and surface area cost).*

These results indicate that in terms of CAPEX, the preferred hub topology is strongly associated with the main purpose of the hub. If the main purpose of the hub is wind power export and the number of spokes is expected to be equal to the number of locally connected OWFs, then the AC solution has a clear advantage. The DC hub solution becomes favorable as soon as additional spokes are added to the hub and the connected spoke capacity outweighs the installed OWF capacity.

When expanding the hub towards another hub that has a different topology, the associated expansion costs are equal for the AC and DC hub cases (see Figure 33). This is because whether expanding the AC hub towards the DC hub or vice versa, the required components and surface area mirror each other. This is true for the hybrid hub as well when the expansion is either on the AC or the DC side of the hybrid hub, as is shown in Figure 33. The obvious exception is the case of the full-scale hybrid hub because of the cost associated with AC and DC side expansion on a single hub.

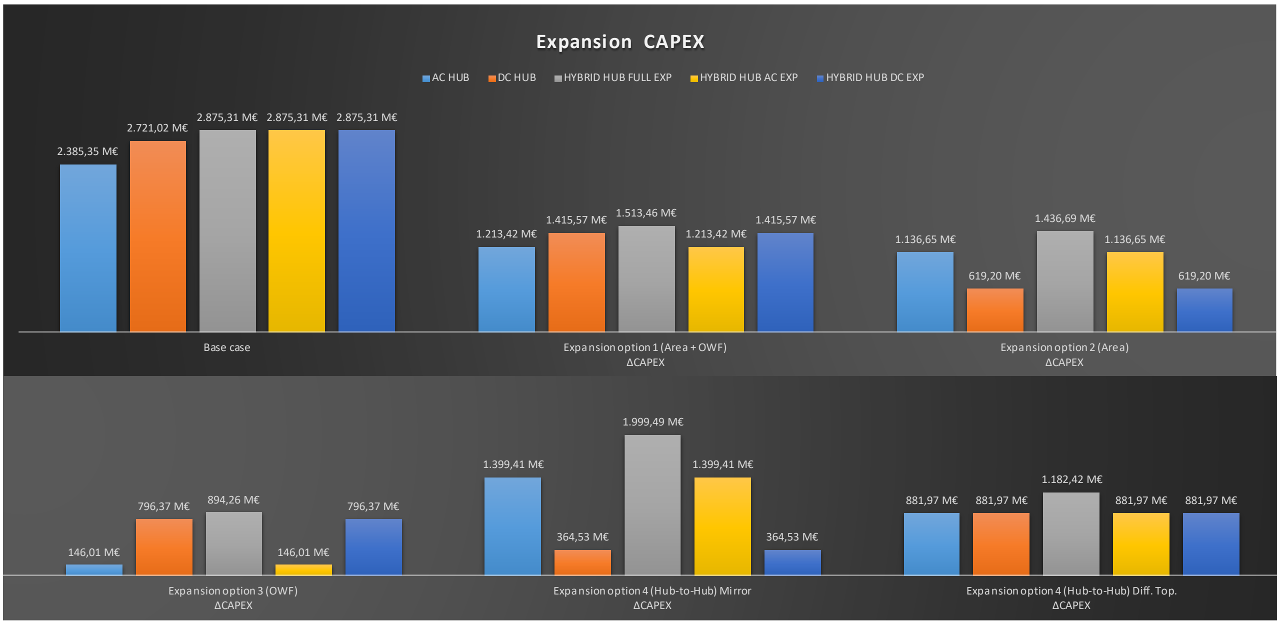


*Figure 33: Comparison of additional costs associated with expansion of different hub topologies.*

Figure 34 shows the cost breakdown per system for the base case of each hub topology. The AC offshore system includes transformers, busbar systems and protection. DC cables include spoke and II DC cables, while the DC offshore system includes the busbar systems and associated DC protection. The AC onshore system includes the converter transformers and the AC busbar system with associated protection.

The dominant factors across all three topologies are the DC cables and converters. This cost is mostly consistent for all three cases as they all have the same number of spokes with the same length, which indicates that the cost of the cables for establishing the internal interconnections contribute only with a small fraction of the total cost. This can be mainly attributed to their short length and the fact that only two hub nodes need to be connected. Converter-related costs (both offshore and onshore) are the main contributor to the overall system cost, as they account for over 50% of the cost. Transformers account for most of the cost of the AC offshore system for all hub topologies. The CAPEX of the offshore AC system of the DC hub is approximately half of the CAPEX of the AC system of the AC hub because the DC hub does not include the 400-kV intermediate busbar system and the associated set of transformers. Onshore AC system costs are the same for the different hub topologies.

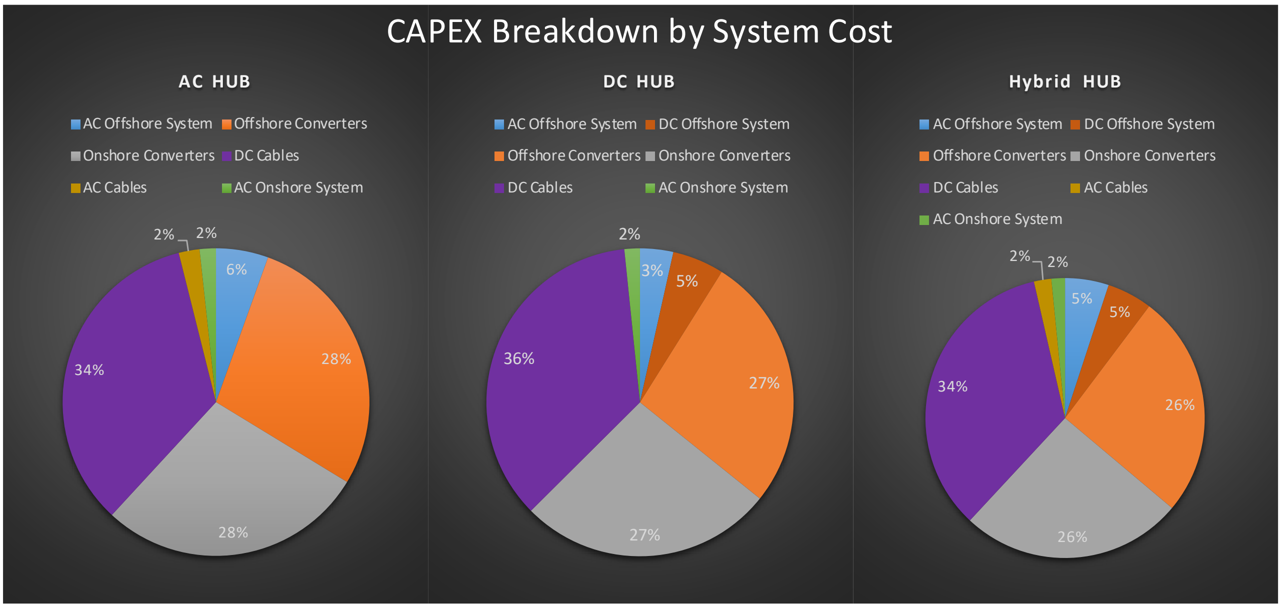


*Figure 34: Breakdown of CAPEX per system cost for the base case topologies.*

DC hub surface area requirements are ~46% higher than the AC hub as shown in Figure 35, and the reason for that fact is the significant size of the DC busbar system and the associated protection (DCCBs are the main factor). The hybrid hub requires ~61% more surface area in comparison to the AC hub. Expansion of wind power capacity gives an advantage to the AC hub and the hybrid hub when expanded on the AC side, again due to the significant area required for the DC protection system. When looking at the expansions towards additional areas or other hubs with mirrored topologies, the surface area of the DC hybrid hub (when expanded on the DC side) remains unchanged due to space being already allocated for the components required for the expansion, if there are enough available feeders for the expansion. The DC hub requires less space than the AC hub when expanding to another hub with mirrored topology, while for the expansion towards additional areas, there needs to be two additional onshore connections for the DC hub to require less surface area. When expanded on both the AC and DC side, the hybrid hub requires most surface area for all expansion cases as it needs to host both, additional AC and DC equipment.

Figure 36 shows the breakdown of surface area requirements for all systems of the base case topologies. For the AC hub, the dominant components in terms of surface area requirements are the converters, which account for 38% (and additional 38% for the onshore converters) of the total surface area. On the other hand, for the DC hub, the DC offshore system accounts for 27, the main driving factor being the DCCBs. Offshore converters account for ~30% of the total area requirements, and we can observe a similar pattern for the hybrid hub.

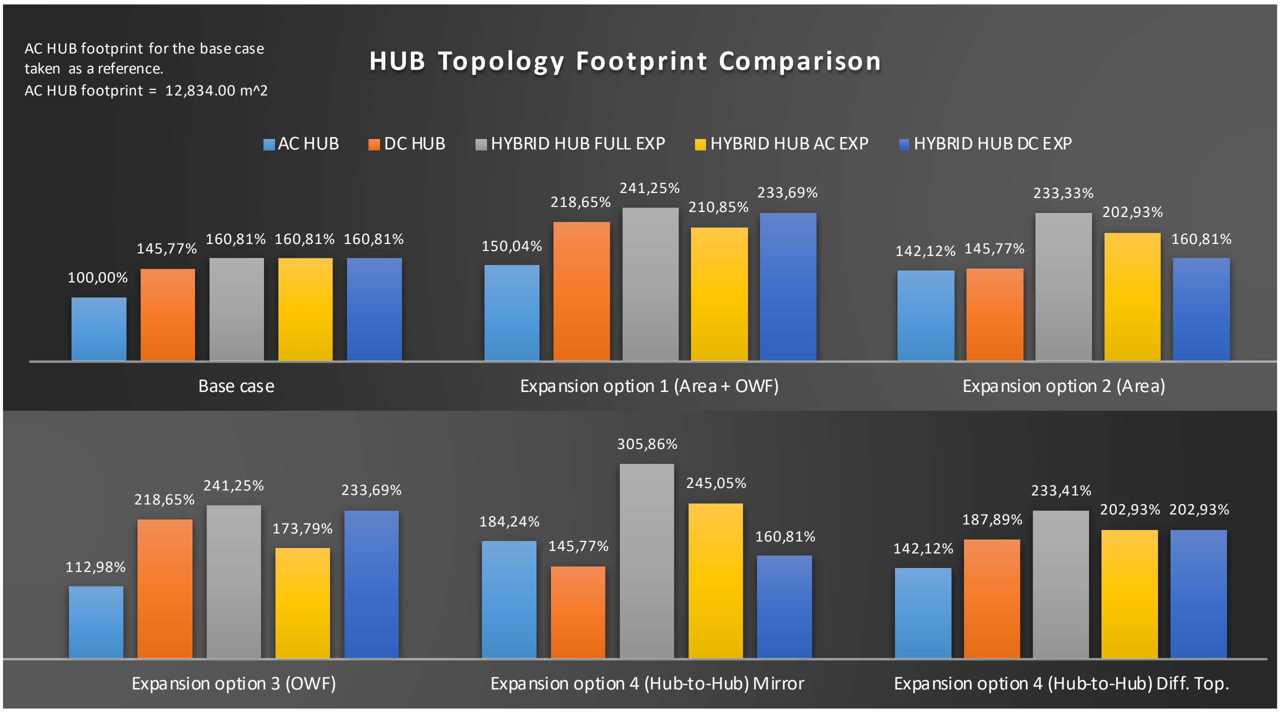


*Figure 35: Comparison of footprint requirements for all topologies (includes estimation for the offshore systems only).*

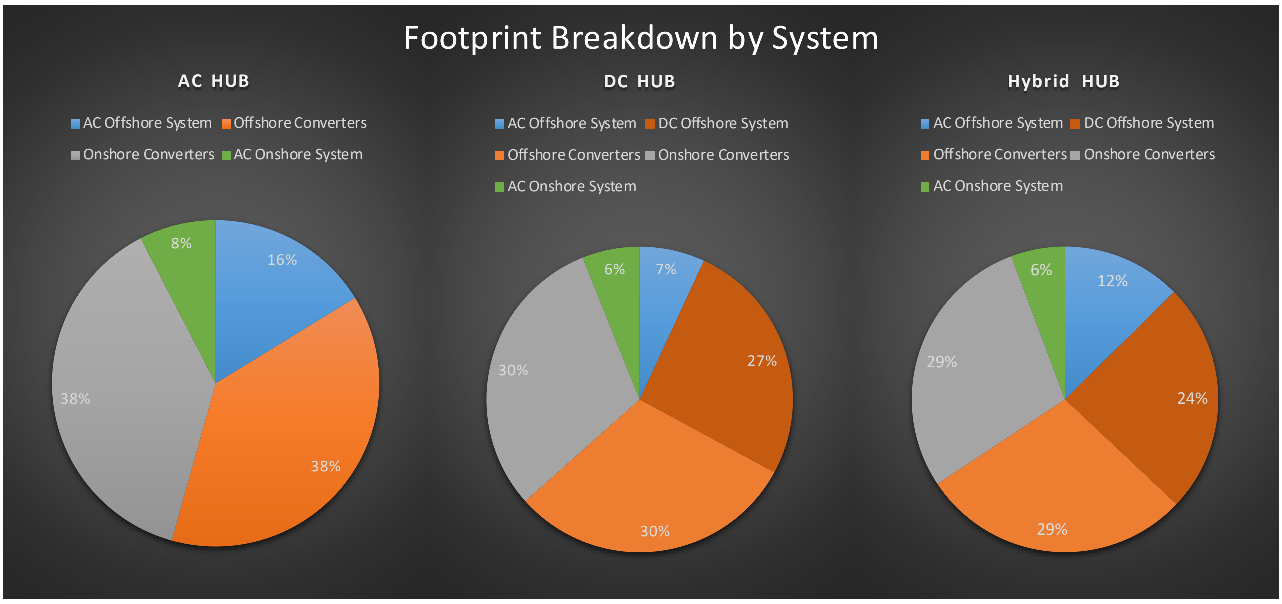


*Figure 36: Breakdown of footprint requirements per system (includes both offshore and onshore systems).*

Figure 37 shows the total CAPEX breakdown by system including the surface area cost. We can observe a similar pattern as in the component cost breakdown shown in Figure 34, with converter cost and the DC cable cost being the two dominant factors. However, for the DC and hybrid hubs, the cost contribution of the DC offshore system has increased substantially due to the area requirements of the DC breakers. The difference in cost of the offshore and onshore converters is caused by the fact that the cost of the onshore surface area has been neglected, as stated in Section 4.1.2.

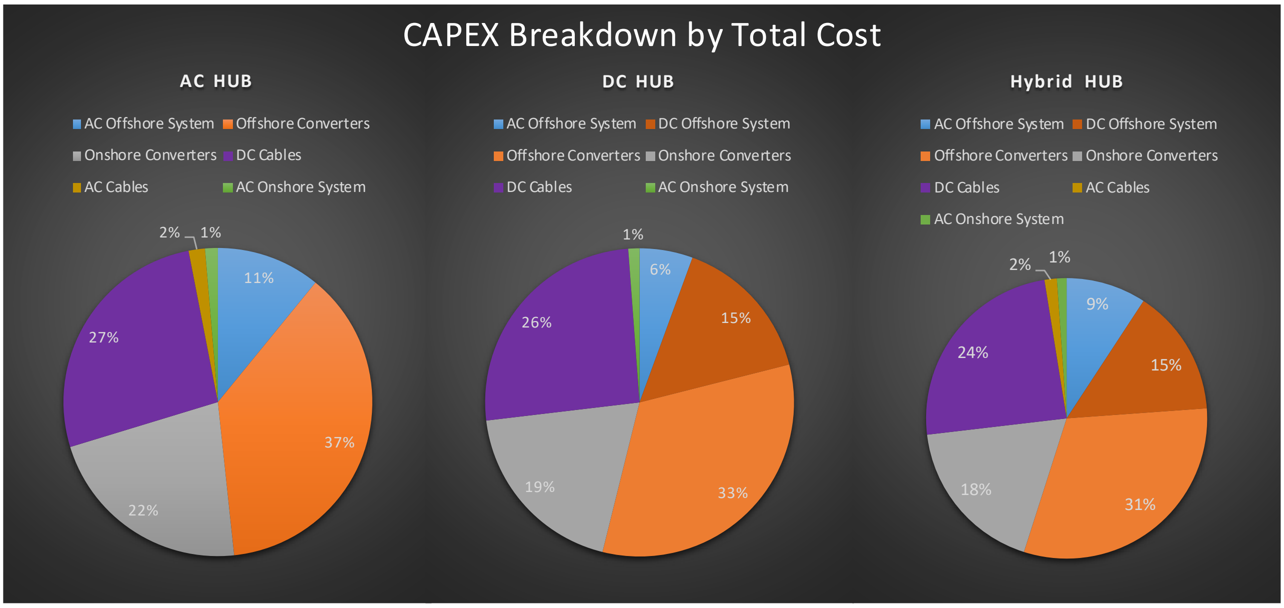


*Figure 37: Breakdown of total CAPEX (includes surface area costs) for the base case topologies.*

## 4.2. ESTIMATION OF LOSSES FOR BASE CASE TOPOLOGIES

The estimation of losses is typically associated with the optimal power flow solution. Since we are considering a generic hub without real power flow values, the losses were calculated for base cases of the AC and DC hub topologies and for rated capacities. Two scenarios were considered:

- Transferring wind power to the connected onshore areas for AC and DC hub topologies at rated capacities, which means transferring 4GW of wind power from OWFs to the connected onshore areas.
- Transferring power from one onshore area to another for AC and DC hub topologies at rated capacities, which means transferring 2GW of power, which is the rated capacity of the spokes connecting the onshore areas to the hub.

For the analysis of losses, the following were considered: converter related losses (switching losses conduction losses, and filter losses), converter transformer and OWF transformer losses (core/no-load losses and load losses, which include the winding and stray losses), AC cable losses and DC cable losses. The relevant loss data considered in the analysis is given in Table 9.

*Table 9: Data used for Loss Estimation of AC and DC hub topologies.*

| Component | Loss parameters | References |
|---|---|---|
| Converters | 1% at rated load | [9], [10] |
| Transformers | 0.15% at rated load | [11] |
| AC cables | 0.0152Ω per km | [12] |
| DC cables | 0.0072Ω per km | [1] |

Figure 38 and Figure 39 show the two mentioned scenarios for both the AC and DC hub topologies, respectively. The scenario for the wind power transfer is a straightforward case where all the power generated by the OWFs is transferred to the onshore systems via the two HVDC bipole links. However, when considering the case of power transfer between two onshore areas, we can observe that the AC hub requires two extra conversion stages on the offshore system, which makes it significantly different from the DC hub.

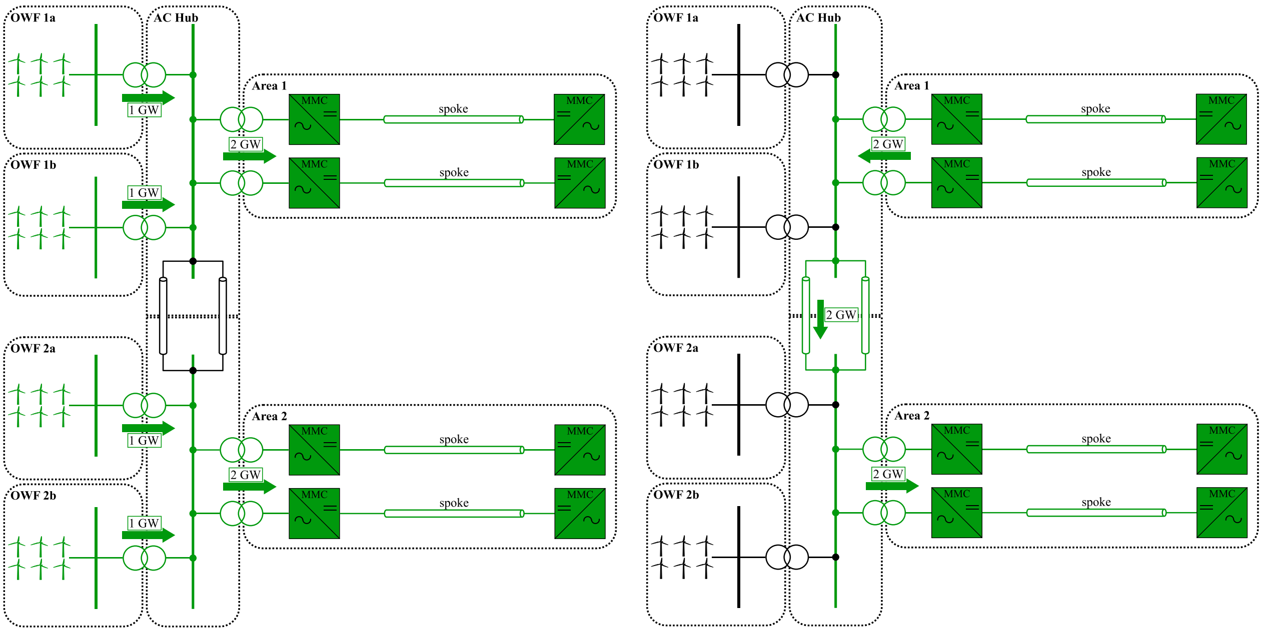


a) b)

*Figure 38: Illustration of power flows for AC hub loss estimation: a) wind power transfer; b) interarea power transfer. Green elements transfer active power while arrows and numbers indicate the exchange across the interfaces of the OEH.*

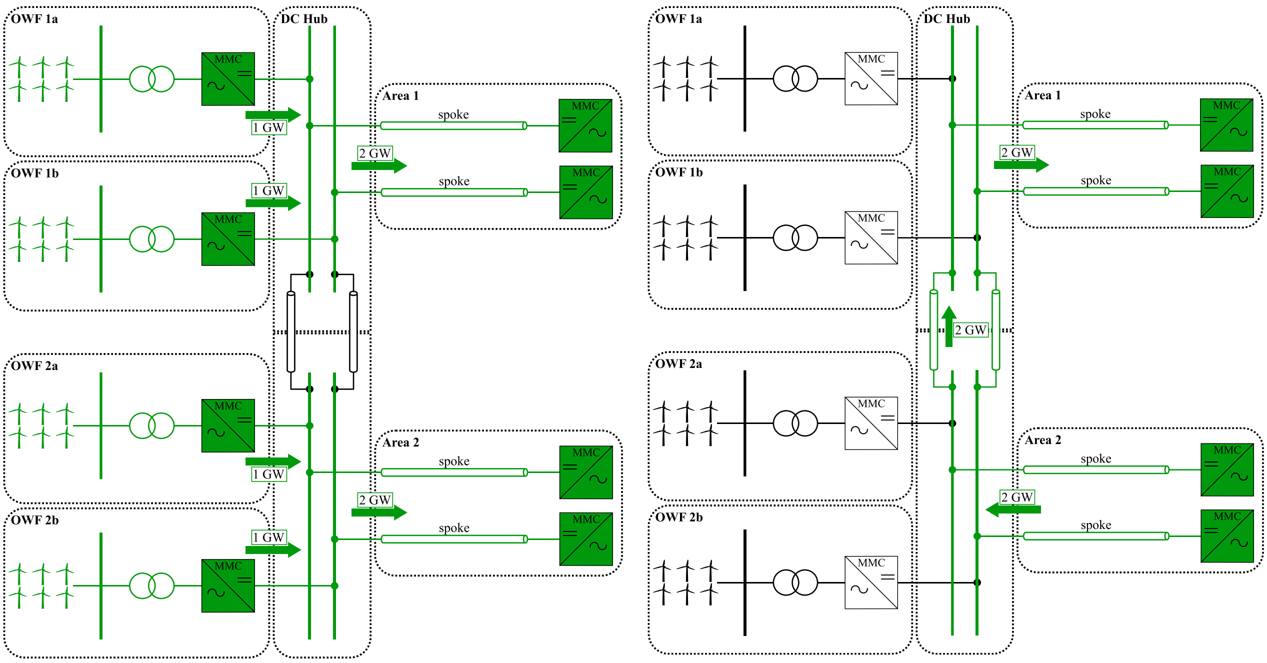


a) b)

*Figure 39: Illustration of power flows for DC hub loss estimation: a) wind power transfer; b) interarea power transfer. Green elements transfer active power while arrows and numbers indicate the exchange across the interfaces of the OEH.*

Figure 40 shows the summary of the loss analysis for the two scenarios. When transferring power from the OWFs to the onshore systems, the losses of the DC hub topology are slightly lower than the AC ones due to the intermediate 400kV busbar system in the AC hub, which includes an additional transformer in the offshore AC system. Power transfer between two onshore systems results in almost double the losses for the AC hub in comparison to the DC hub due to the two extra conversion stages for the transferred power on the offshore system.

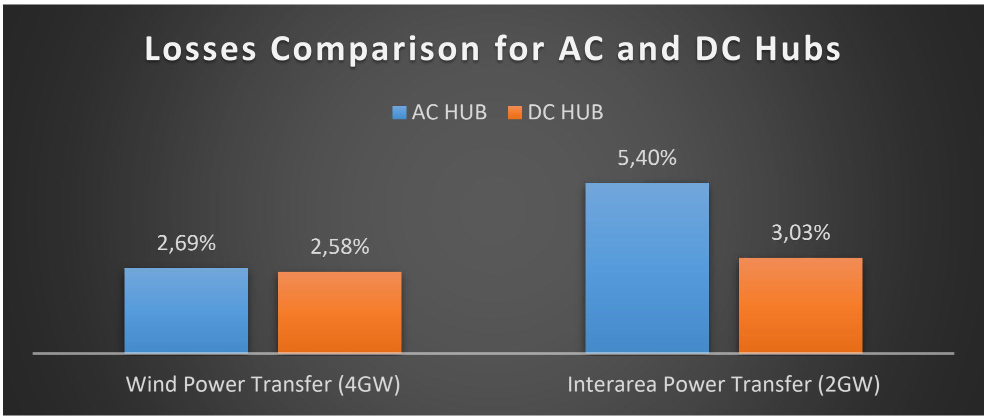


*Figure 40: Comparison of loss estimation between the AC and the DC hub for the two power flow scenarios.*

When analysing the loss breakdown per component shown in Figure 41, it can be observed that the dominant components are converters, with 76% for the AC hub and 80% for the DC hub. The difference between the two topologies in terms of losses are transformer losses, which is due to additional transformers on the AC hub, as previously explained. The DC cable losses are a function of the length and would change depending on the distance between the hub and the onshore system.

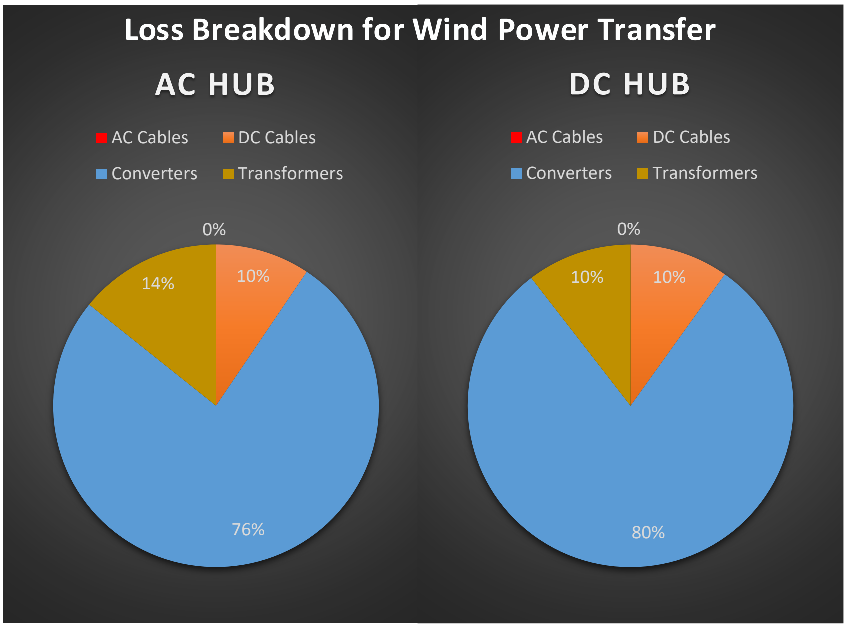


*Figure 41: Breakdown of losses per component for the AC and DC hub base topologies when transferring wind power to the onshore systems.*

For the second scenario, when the power is transferred from one onshore system to another, the loss distribution is still dominated by converters, similarly to the previous scenario, as shown in Figure 42. 75% of the total loss is the converter loss in the AC hub, while for the DC hub, the converter loss makes 69% of the total loss. In the AC case, it is possible to notice now the presence of losses in AC cables, which corresponds to the power being transferred through the AC IIs.

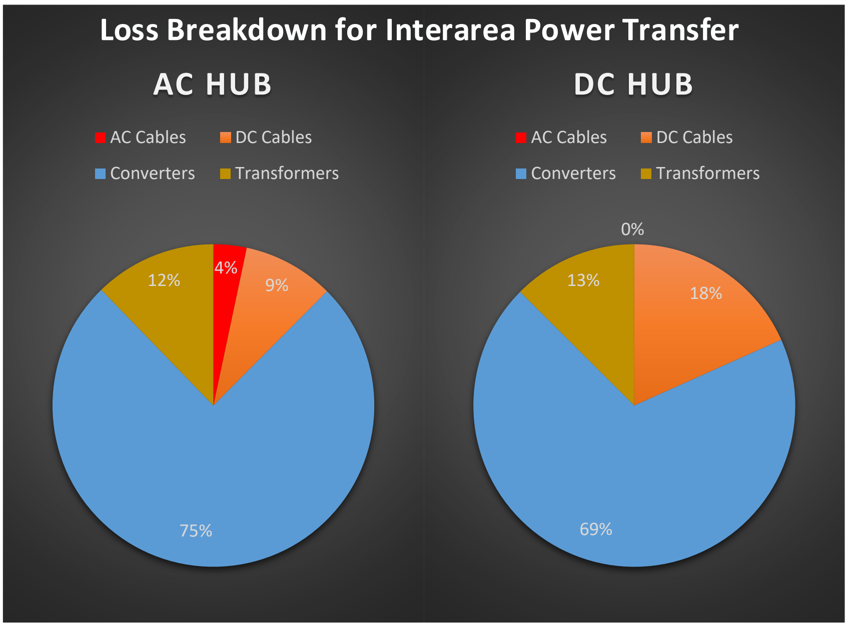


*Figure 42: Breakdown of losses per component for the AC and DC hub base topologies when transferring power between two onshore systems.*

# 5. FUNCTIONALITIES AND CONTROLLABILITY

## 5.1. AVAILABILITY

The purpose of this section is to assess the impact of unavailability of different transmission system elements on the transfer capacity of the OEH. The scenarios considered are the outage of a converter pole (scenario I), outage of a single pole HVDC cable associated with a spoke (scenario II) and the outage of an II that provides the internal connection of the different busbars within the hub (scenario III). To allow generalization of the study, no attempt is made to determine the expected energy not transmitted since this would require specific energy transfer scenarios, which further depend on the expected wind power production and the expected time the hub is operating in each mode - wind export and inter-area transfer.

To represent the likelihood and impact of a particular fault type, the probabilities and expected repair times of the different scenarios are converted to the percentage of total operating time where the individual elements are expected to be unavailable. The input data required for this calculation – mean time to failure (MTTF) and mean time to repair (MTTR) – are obtained from the feasibility study of the NSWPH programme [1]. The unavailability is calculated as follows:

$$unavailabity\ \% = \frac{MTTR}{MTTR + MTTF} \cdot 100\%$$

Table 10 summarizes the unavailability data and results.

*Table 10: Unavailability data [1].*

| Element affected | | MTTF [h] | MTTR [h] | % of time unavailable |
|---|---|---|---|---|
| **Converter pole** | **Forced** | 2920 | 24 | 0.815 % |
| | **Scheduled** | 17520 | 72 | 0.409 % |
| **Spoke (100 km)** | | 250285 | 1680 | 0.667 % |
| **II (20 km)** | | 1251429 | 1680 | 0.134 % |

To assess the impact of the unavailability scenarios on the different elements of an OEH the concept of exchange capacities introduced in section 3.1 is applied. Elements that remain fully operational following a fault are highlighted in green, elements that are out of service are shown in red, while elements that allow constrained operation, such as an HVDC converter operating in STATCOM mode, are indicated in yellow. The impact of the different fault scenarios on the maximum power exchange capacities follows a similar colouring scheme, where full capacity is indicated in green, reduced capacity is shown in yellow and red indicates the interfaces where no active power exchange can be achieved. The effect of the different fault scenarios is assessed in terms of their impact on the exchange capacities across the different hub interfaces:

- The external capacity, which refers to the capacity of the hub to exchange power with external systems through either spokes or hub-connectors.
- The internal capacity, which reflects the maximum exchange capacity between the hub and locally connected generation and demand. These are mainly considered to be OWFs and PtX. Since OWFs operate most of the hours below their maximum power capability, it is important to consider not only the maximum power capacity but also how the capacity is distributed across the different OWFs. This is reflected in the analysis as “connected OWF capacity”.
- The hub capacity, which represents the ability of the hub to transfer power between the internal nodes of the hub system through the IIs.

### 5.1.1. Converter Pole Fault (I)

The impact of a converter pole fault on an AC and DC hub are fundamentally different, which is mainly due to the location of the converter in respect to the interconnected hub system. A converter outage in the AC solution, shown in Figure 43, leads to the unavailability of an external connection, since no power can be transferred through the spoke of the affected converter. In this case, the onshore converter could still stay connected and operate in STATCOM mode to support the onshore grid, but no active power could be fed into the onshore system.

A pole outage at the DC hub impacts the internal system of the hub. In the initial solution, indicated in Figure 44, each converter is associated with a single islanded AC system and an outage therefore leaves the associated AC system disconnected to the hub leading to a loss of the entire wind power capacity within this system. The external capacity of the hub, that is, the ability to exchange power through the hub with the onshore systems, is unaffected by the unavailability of the converter pole.

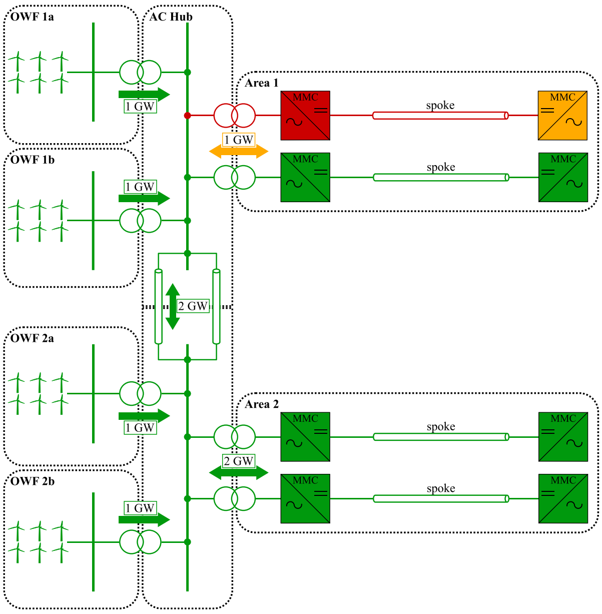

Figure 43: AC hub availability during converter pole faults.

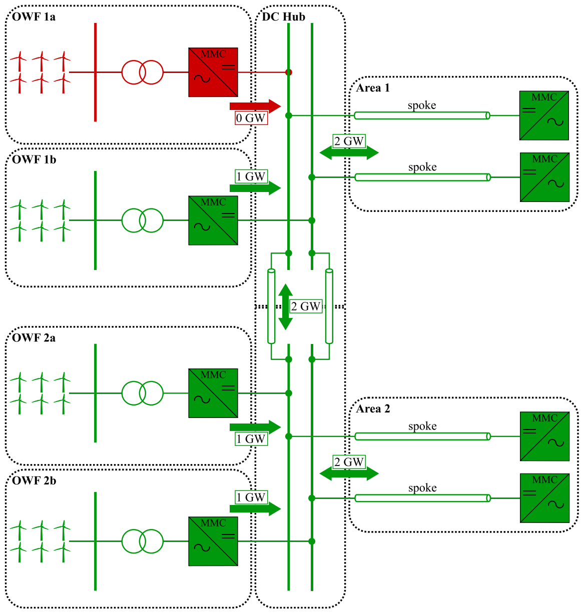

Figure 44: DC hub availability during converter pole faults without additional coupling of the AC systems.

The impact of the different outages on the hybrid hub generally depends on the operating mode and the hub operation can be optimized depending on the fault type. Similarly to a DC hub, the hybrid hub in DC operating mode allows to mitigate the impact of a pole fault on the external capacity at the cost of a loss of a wind farm. However, the hybrid hub allows for the interconnection of different offshore AC systems, i.e., the wind power availability can be increased by coupling the two poles of the same bipole. This allows all wind farms to stay connected to the hub, although with limited access to the remaining exchange capacity as indicated in Figure 45. Similar behaviour can be achieved in the DC hub topology by providing an optional coupling between the 66-kV busbars of the two poles of a bipole, as indicated in Figure 46. Since there is no significant distance between the two busbars, then the additional cost related to cables and AC protection is negligible in respect to the overall cost of OEH. Hence this option is considered and represented in the detailed single line diagram of the DC hub shown in Figure 11.

While the availability of wind power can be increased through these additional measures there is still a significant difference compared to the AC coupled hub solution. In the DC coupled case with additional connectors on the AC side, two OWFs (1a and 1b) share a total capacity of 1 GW, whereas the other two OWFs (2a and 2b) operate with their nominal capacity of 1 GW each. For the OWFs operating under reduced capacity this implies that a maximum average power of 500 MW can be exchanged for each OWF. In the case of the AC coupled hub, all four OWFs have access to a capacity of 3 GW, which can be evacuated from the hub. This significantly increases the available average power of the OWFs to 750 MW.

For the hybrid hub, the wind power exchange capacity could be optimized by coupling the different bipoles through the AC II and thereby switching to AC coupled mode. Particularly in case of scheduled outages this kind of redundancy allows to minimize, if not completely avoid, wind power curtailment during the entire downtime of the converter if converter pole maintenance is scheduled to coincide with low wind speed forecasts. This action, however, comes at the cost of restricting the external capacity, that is the capacity that is available for the exchange of power between different spokes. Due to the flexibility of the hybrid hub the decision, which operating mode is preferrable, can be optimized depending on the scheduled operation of the hub.

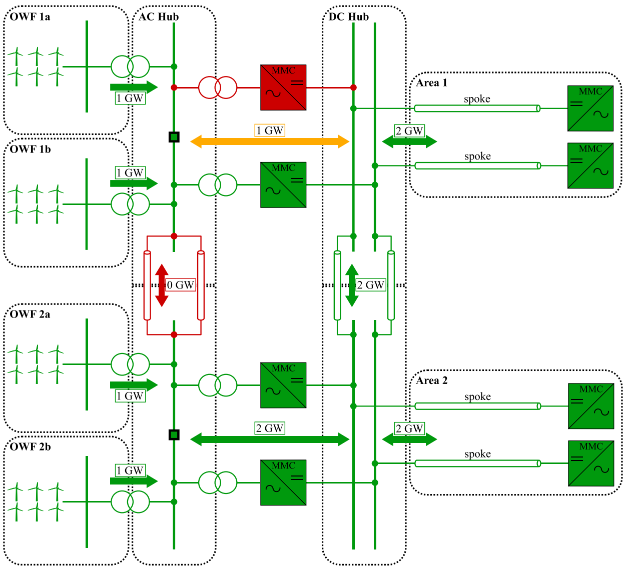


Figure 45: Hybrid hub availability during converter pole faults in DC coupled mode.

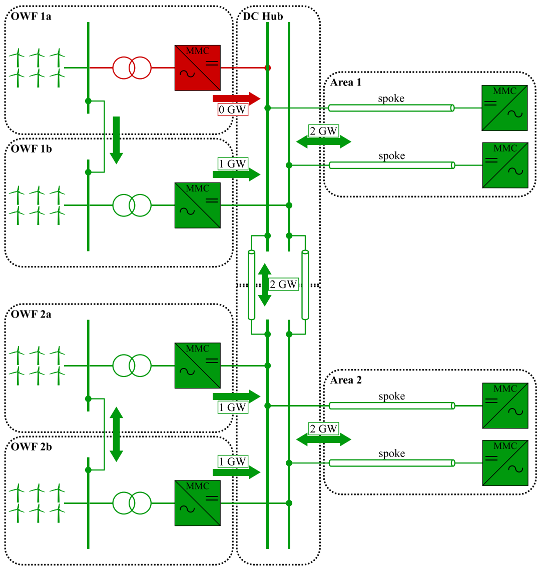


Figure 46: DC hub availability during converter pole faults with AC coupling of the HVDC bipoles.

For the DC hub and the hybrid hub operating in DC coupled mode, there are some additional aspects to consider as the optional AC connection can either be operated in ‘normally open’ or ‘normally closed’ state. Operation in ‘normally open’ mode has the benefit of not requiring any parallel grid-forming control as each of the converters would form an independent AC system and the connection would only be closed in case of an outage of one of the converter poles. This is, however, expected to lead to a temporary shutdown of the wind turbines connected to the faulty pole.

Operation in ‘normally closed’ mode requires both converters of a bipole to operate in parallel grid forming mode, which could impose control and stability challenges. Since it is expected that both converters are from the same manufacturer, compatibility risks can to some extend be avoided. If operation in bipole coupled mode is feasible, the temporary shutdown of the wind farm could potentially be avoided if the wind turbines, or at least part of the total capacity, are able to ride through the fault without tripping. Operation in bipole coupled mode further allows to balance the power flow within the DC system (between positive and negative poles) and thereby reduces the currents in the neutral circuit.

A hybrid hub operating in AC coupled mode exhibits the same behaviour as the AC hub. For the sake of completeness, this operating mode is indicated in Figure 47. The effect of the unavailability of a single converter pole on the different topology solutions is summarized in Table 11.

Table 11: Capacity reduction due to a converter pole fault.

| Topology | | External capacity reduction | Internal capacity reduction | | Hub capacity reduction |
|---|---|---|---|---|---|
| | | Exchange capacity | Connected OWF capacity | Exchange capacity | Exchange capacity |
| **AC** | | 1 GW | unaffected | unaffected | unaffected |
| **DC** | **No AC** | unaffected | 1 GW | 1 GW | unaffected |
| | **Optional AC** | unaffected | unaffected[1] | 1 GW | unaffected |
| **Hybrid** | **AC-coupled** | 1 GW | unaffected | unaffected | unaffected |
| | **DC-coupled** | unaffected | unaffected[1] | 1 GW | unaffected |

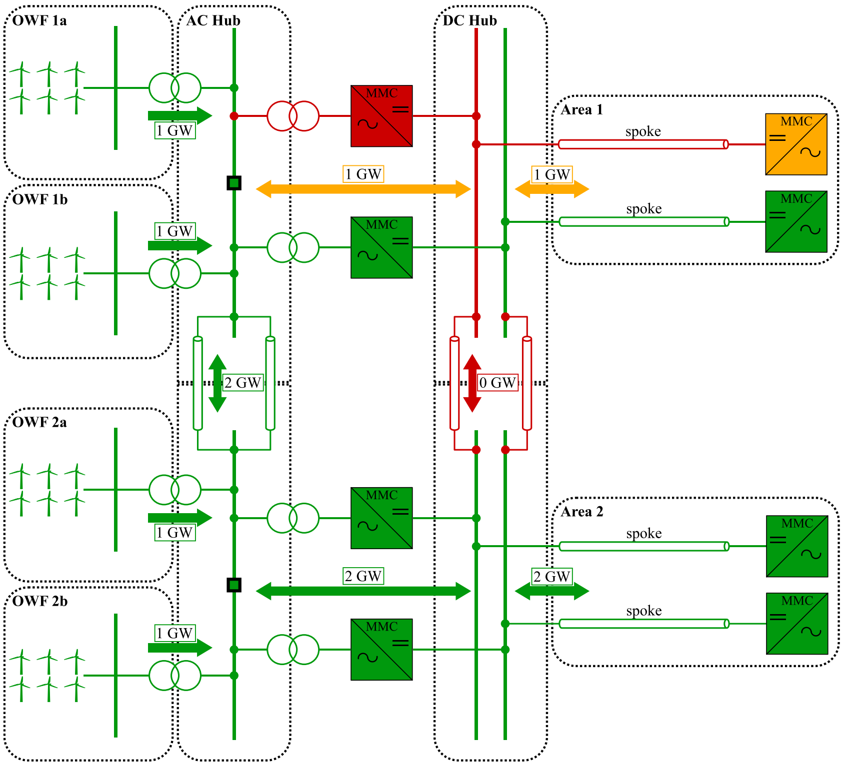


*Figure 47: Hybrid hub availability during converter pole fault in AC coupled mode.*

[1] Access to the available exchange capacity is limited as two OWFs are restricted by the combined flow through one MMC with 1 GW maximum capacity.

### 5.1.2. Spoke Fault (II)

A spoke fault in all cases restricts the maximum power exchange with the area the faulted pole connects to. This means that no matter the hub topology, as indicated in Figure 48 for the AC hub and Figure 49 for the DC hub, the external capacity of the hub, that is the ability to export wind power or exchange power through the hub is reduced. The main difference between the topologies is that, in the DC hub solution, all offshore converters remain operational while a spoke fault in the AC hub causes the loss of the converter interfaced with the faulted spoke.

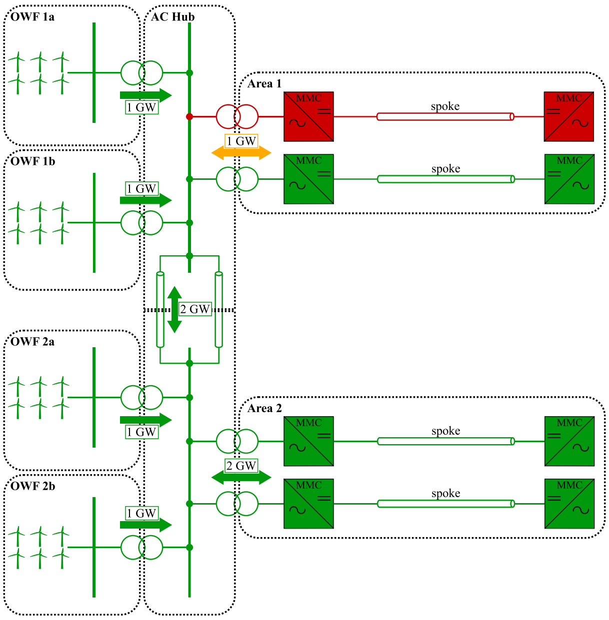


Figure 48: AC hub availability during spoke faults.

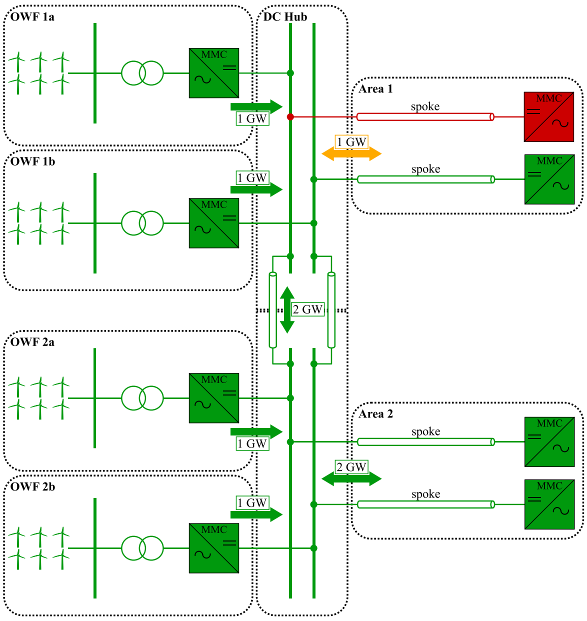


Figure 49: DC hub availability during spoke faults.

The effect on the hybrid hub is the same as for the dedicated hub solutions depending on the operating mode. The effect of the unavailability of a spoke on the different topology solutions is summarized in Table 12.

*Table 12: Capacity reduction due to a spoke fault.*

| **Topology** | | **External capacity** | **Internal capacity** | | **Hub** |
|---|---|---|---|---|---|
| | | **Exchange capacity** | **Connected OWF capacity** | **Exchange capacity** | **Exchange capacity** |
| **AC** | | 1 GW | unaffected | unaffected | unaffected |
| **DC** | **No AC** | 1 GW | unaffected | unaffected | unaffected |
| | **Optional AC** | 1 GW | unaffected | unaffected | unaffected |
| **Hybrid** | **AC-coupled** | 1 GW | unaffected | unaffected | unaffected |
| | **DC-coupled** | 1 GW | unaffected | unaffected | unaffected |

### 5.1.3. II Fault (III)

Faults on the IIs affect the ability of the hub to exchange power between the different hub nodes. They neither generally affect the ability to export wind power, nor do they affect the total capacity of the connected spokes. The limited capacity between the hub nodes will, however, in most cases lead to a reduction in the possible exchange of active power between different areas – if they are not connected to the same busbar – as it is the case in the base AC hub shown in Figure 50 and the DC solution shown in Figure 51. In both cases the capability of the hub to export the available wind power is unaffected while the trading capacity between areas 1 and 2 is halved to 1 GW.

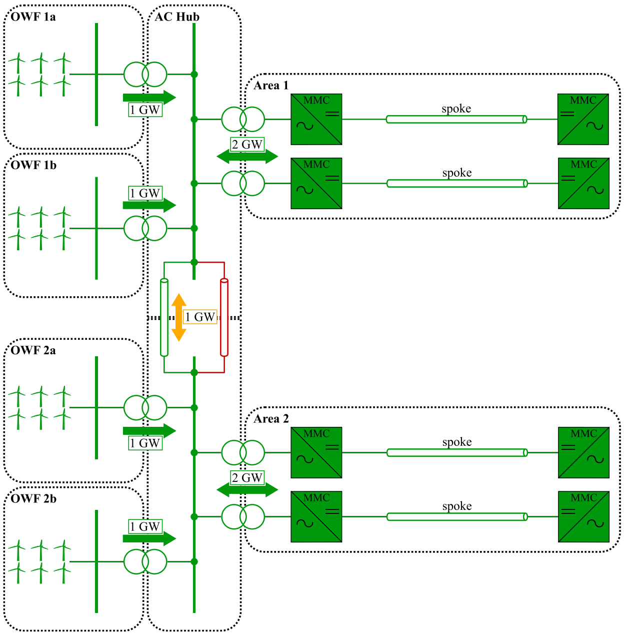


*Figure 50: AC hub availability during II faults.*

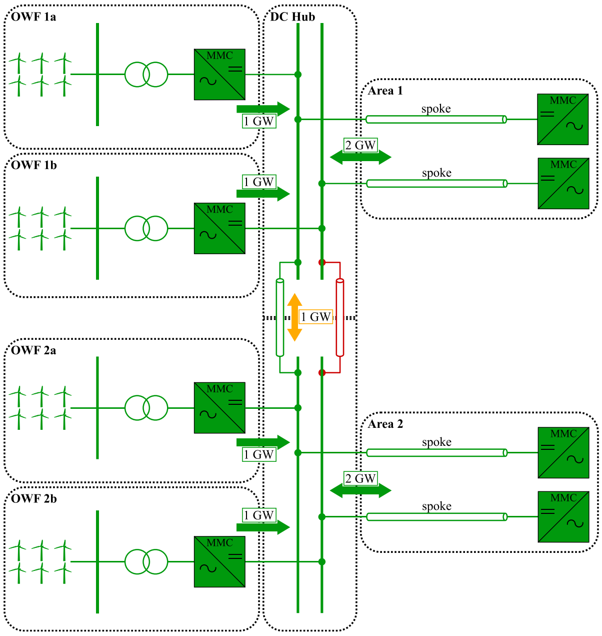


*Figure 51: DC hub availability during II faults.*

For the basic configuration of the hybrid hub, II faults can be mitigated by switching the pole coupling mode to the healthy system. That is, DC coupled mode in case of an AC II fault and AC coupled mode for a fault occurring at the DC II. Thereby the hub is unaffected by II faults. The effect of the unavailability of an II on the different topology solutions is summarized in Table 13.

Table 13: Capacity reduction due to an II fault.

| Topology | | External capacity | Internal capacity | | Hub |
|---|---|---|---|---|---|
| | | Exchange capacity | Connected OWF capacity | Exchange capacity | Exchange capacity |
| **AC** | | unaffected | unaffected | limited by hub exchange | 1 GW |
| **DC** | **No AC** | unaffected | unaffected | limited by hub exchange | 1 GW |
| | **Optional AC** | unaffected | unaffected | limited by hub exchange | 1 GW |
| **Hybrid** | **AC-coupled** | unaffected | unaffected | unaffected | unaffected, switch to DC |
| | **DC-coupled** | unaffected | unaffected | unaffected | unaffected, switch to AC |

## 5.2. CONTROL AND STABILITY

In this subsection, control and stability challenges of the AC and DC hub configurations are identified and discussed as summarized in Figure 52 below. These are initial discussions for the work to be carried out in Task 2.2 of the project.

| Control & Stability Challenges | |
|---|---|
| **AC Hub** | **DC Hub** |
| • AC-side small-signal interactions between offshore HVDC converters and between these converters and wind turbine converters.<br><br>• Liability issues and grid code updates to be investigated for the offshore wind farms from different developers with different wind turbine technologies sharing the offshore grid and connected nearby - voltage regulation responsibility in case of HVDC blocking.<br><br>• Challenges related to the operation of multiple HVDC stations connected nearby, sharing the responsibility of forming the offshore AC grid (advanced grid-forming techniques required with droop-based frequency control - more complex than traditional V/f mode).<br><br>• Challenges to handle asymmetrical faults in the offshore AC grid formed by multiple HVDC stations operating in shared grid forming mode.<br><br>• Coordinated control between offshore HVDC converters and wind turbine converters required to curtail wind power aiming at avoiding exceeding power limits of remaining HVDC stations in the event of blocking of one HVDC station. | • Shared DC-grid voltage regulation responsibility through droop-based control dealing with the fact that voltage is a local parameter differently from frequency in an AC system, which is global.<br><br>• DC-side small-signal interactions between HVDC stations regulating the HVDC grid voltages and power flow.<br><br>• Challenges related to the synchronization of the decoupled offshore AC grids in case of the blocking of one of the poles of the HVDC bipole in the presence of a backup AC coupler between the two poles.<br><br>• Control and stability challenges to be addressed depending on the size of the DC reactors defined in HVDC grid protection design.<br><br>• Eventual DC voltage regulation issues in weak nodes of the DC hub requiring coordinated control with offshore wind farms to adapt/curtail power injection, in some situations, to preserve the stability of the HVDC grid.<br><br>• Challenges to limit bipole neutral current in case of decoupled pole operation on the offshore AC side with different wind power generation in each pole of bipole. |

Figure 52: Control and stability challenges of AC and DC OEH topologies.

1. AC OEH: An AC OEH presents interesting advantages related to the availability of wind generation and other technical aspects, but it also presents non-negligible control and stability challenges, as presented below.

   - An AC OEH most likely will be a fully power-electronic-based AC network with several HVDC converters, wind turbine converters, electrolyzer converters, and others, connected with relatively small electrical distances among them. Several control interactions can occur leading to stability issues that could eventually result in the shutdown of the whole system. Moreover, the various power-electronic converters can be from different vendors with different control functionalities that can lead to more challenges for the operation of the AC hub, also because vendors usually deliver black-box models, to protect their intellectual property (IP) data, which will require clear processes and standards to define an approach to properly study the control and stability issues in a simulation environment.

   - In an AC OEH, different OWFs from different developers will be connected to this small AC grid formed by HVDC converter stations. There could be situations where the responsibility of maintaining the electrical quantities of the AC hub within tolerable limits will be pushed towards the OWFs (for example during an eventual failure or blocking of an HVDC converter) and then liability issues must be analysed to define clear guidelines and grid codes in such situations. For example, if overvoltages happen leading to the damaging of a given component, who would be responsible for that?

   - Another challenge of AC OEHs is the parallel operation of the HVDC stations in grid forming mode sharing the responsibility of creating the voltage amplitude and frequency in the offshore AC system. This is a more complex control than the traditional V/f control mode typically applied to OWFs connected through an HVDC transmission system. The shared grid-forming control of the offshore HVDC converters can be even more challenging if the stations are connected close to each other with a small electrical distance between them (low impedance), which can lead to stability issues.

   - Another challenge to the operation of parallel-connected HVDCs in shared grid-forming mode appears during asymmetrical faults at the offshore grid as mentioned in [1].

   - Finally, even though an AC hub can increase the wind energy availability in situations of failures in one of the HVDC stations offshore, the wind energy production might need to be reduced/curtailed to avoid exceeding the power ratings of the remaining HVDC converters. This situation could happen if one of the HVDC stations is blocked during high wind conditions. Some control coordination will be necessary between the HVDC stations and the OFWs to identify and act when wind generation curtailment is required, and this is another control challenge of an AC OEH.

2. DC OEH: A DC OEH essentially is an HVDC grid, which imposes many challenges especially because this is a completely new configuration of an electrical system that requires special technologies and that has different dynamics and control requirements in comparison to conventional AC grids. First, to properly operate an HVDC grid, many modern electrical devices

are required, such as DCCBs and eventually high-power high-voltage DC-DC converters, which are not yet mature in the industry imposing challenges to the practical implementation of these systems. Besides, technical requirements and standard interfaces must be defined so that different HVDC converters from different vendors can operate harmonically on their DC side, electrically interacting and exchanging information.

- In an HVDC grid, the onshore HVDC stations are typically the ones responsible for regulating the voltages and power flow across the grid, which require these stations to operate in a droop mode to achieve a stable system. This is a similar operation to the primary frequency control in AC grids. However, differently from the frequency in an AC grid, which is a global parameter, voltage is a local parameter that varies according to voltage drops across the transmission system. This fact imposes some technical challenges for the control of the HVDC grid.

- Besides, undesired small-signal interactions can occur between the HVDC converters that are electrically interacting on their DC sides.

- To extend the wind energy availability in a DC OEH in case of the failure of one pole of an HVDC bipole, normally open backup couplers can be connected between the two poles of the converter on the AC grid offshore. Control and stability challenges may appear, related to the synchronization of the two offshore AC grids initially decoupled, when the coupler is closed to interconnect the two poles of the HVDC converter. Other option would be to shut down and restart both OWFs with the burden of temporary loss of generation for the OWF connected to the healthy pole of the bipole. This could be undesired especially if two different OWF developers are connected to each pole of the bipole.

- In an AC grid, frequency is the parameter that reflects the balance between generation and demand, whereas in a DC grid, it is the voltage that reflects this balance. The frequency dynamics in traditional AC grids are relatively slow (when considering for example rotor angle stability) since they are related to the considerably large amount of energy stored in the heavy rotating masses of the synchronous machines. The voltage dynamics in a DC grid are considerably faster as they are basically related to the relatively low capacitive energy stored in the cables of the network. For this reason, DC reactors are required, in combination with extremely fast DCCBs, to contain these fast dynamics in the HVDC grid during faults. However, big reactors can lead to control and stability challenges in the DC grid that must be studied and avoided.

- As a DC hub starts to expand, eventually it will become a highly meshed HVDC grid. Some of the offshore nodes can be located far away, electrically speaking, from the onshore HVDC stations that are responsible for regulating the DC voltages across the HVDC grid. These can be seen as “weak” nodes where the local voltage is highly sensitive to power injection variations. To preserve the local and global voltage stability of the HVDC grid, wind power curtailment or smoothening might be needed, which will require some control coordination between the HVDC station and the OWF connected to it.

- Finally, another challenge of a DC OEH, composed of HVDC converters in a bipole configuration, is the limitation of the neutral current, which is a consequence of power imbalances between the positive and negative poles of the bipole. If the HVDC bipole operates with its two poles decoupled from each other on the offshore AC side, then power imbalance will naturally occur between the two poles since each of them are connected to a different OWF, with random power generation. This power imbalance can eventually lead to overcurrent in the neutral circuit of the HVDC grid.

# 6. DC OEH PROTECTION DESIGN WITH TEMPORARY BLOCKING OF HVDC CONVERTERS

## 6.1. INTRODUCTION

This study investigates the impact of the HVDC converter operation during DC faults on the design and sizing of protection systems and it provides a comparison to a reference base case. The innovative contribution of this study is the assumption that the modular multilevel converter (MMC) temporary blocking feature (TBF) is available, in case of DC faults, and the impact of this feature is assessed for protection system design of DCCBs and DCRs. In [13] system behavior during DC faults is classified into three categories: Continuous operation (CO), temporary stop (TS) and permanent stop (PS). Normally, converter blocking is considered as a PS so to keep the system in CO it means that MMCs are not allowed to block during DC short circuit faults. This involves high design constraints on DC grid protection equipment and the controllability of the DC grid as outlined in [14]. The implementation of this newly proposed functionality, which consists in allowing the converters to block and deblock in a short timeframe after a fault in the DC grid, would be classified as a TS in the system. The expected timeframe is limited by the definitions of PS in different EU countries and surrounding onshore AC system constraints so it can be expected to be something around 100ms. The combination of the permission of TS in case of DC faults along with MMCs with the TBF implemented could significantly relax the DC grid protection design constraints. Since the focus of this work is on the DC protection system design, how the MMC TBF affects the offshore AC side controllability is out of the scope of the study.

The design of DCCBs and DCRs is carried out considering fault neutralization and fault suppression, which last around 20 ms. Moreover, in [15], it is shown that the primary protection sequence is responsible for DCCB and DCR design for typical fault identification algorithm times. Therefore, the timeframe considered relevant for the primary DC protection sequence studies is up to 20ms. To demonstrate the impact of this functionality in the studies performed, it is enough to allow the converter to block after a fault. The exact timeframe of this functionality, its implementation of deblocking and the behavior of the AC side during the event are considered out of the scope of this work. In the scope of the study, TBF is limited to the MMCs that interface OWFs to the MTDC grid.

This work's significance lies in revealing the advantages of this innovative converter operation approach, notably concerning the sizing of DCRs and the current breaking capability (CBC) of DCCBs, considering different DCCB operating times – 2ms, 5ms and 8ms. The primary finding is that enabling temporary MMC blocking significantly affects the dimensions of protection system components.

## 6.2. USE CASES AND METHODOLOGY

This study proposes an approach to size DCRs and to define DCCB CBC to be implemented in a multi-terminal DC grid use case defined and published by Energinet [8] (see Figure 53). The research methodology employs an electromagnetic transient (EMT) simulation tool to replicate critical primary sequence faults. The modelled bipolar system with a DMR operates at 525 kV voltage level and all converters are rated 1GW per pole. In the system modelling for the subsequent studies presented, the following assumptions were made to generalize the study and make it protection-specific based [1]: The HVDC converters are MMC half-bridge (HB) converters, offshore converters connected to the windfarms (WF), named MMC-WF, are in power control mode and the onshore converters, named MMC-OS, connected to areas A, B, C and D are in DC voltage-droop control mode. Two use cases are considered, the “Simple Radial”, which corresponds to the entire system shown in Figure 53 excluding the parts inside the green boxes, and the “Extended Radial”, which corresponds to the entire system shown in Figure 53 including the parts inside the green boxes.

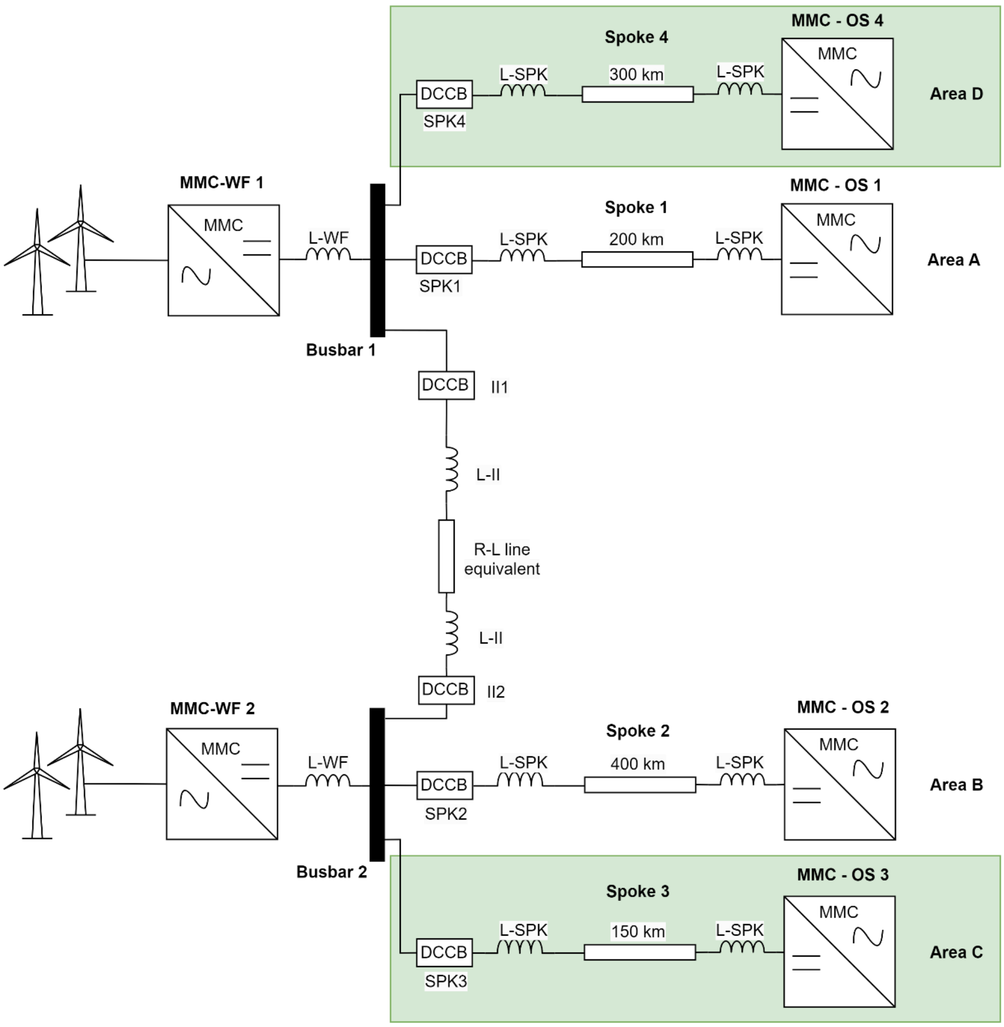


*Figure 53: Use cases – “Simple Radial” with indicated expansion in green for “Extended Radial”.*

The following power flow conditions are considered worst-case scenarios for protection system studies: In the case of the “Simple Radial” use case, MMCs WF1 and WF2 inject 1GW each into the system and MMCs OS1 and OS2 export 1GW to their respective areas. In the case of the “Extended Radial” use case, MMCs WF1, WF2 and OS4 inject 1GW each into the system and MMCs OS1, OS2 and OS3 export 1GW to their respective areas. The cables are represented through wide-band models based on the data available from [1], [16] for a bipolar cable with a DMR. The naming convention is taken from [1] referring to the long cables that connect buses to onshore areas as “spokes” and the connection between different buses (hubs) as “internal interconnectors” (IIs). It is assumed that both MMCs WF are in close vicinity (for example within an energy island) so the short II connecting the two respective busbars, placed a few hundred meters apart from each other, is represented by an R-L equivalent to avoid excessively-small time steps in the EMT simulations. DCRs are grouped into three sets based on their positions in the system, i.e., L-II (in an II), L-WF (in front of a MMC-WF) and L-SPK (in spokes). All DCRs of the same set are assumed to be of the same size in the subsequent studies.

### 6.2.1. PROTECTION SYSTEM SIZING METHODOLOGY WITH BLOCKING TABLES

Onshore AC grid constraints serve as pivotal guidelines for protection design. A framework centered on loss of active power is established to define which MMCs are allowed to block after a DC short circuit fault. MMC blocking tables based on [13], derived from fault probability analysis and AC system constraints, serve as boundary conditions for protection system design.

Based on the studies performed in [16], the MMC blocking overcurrent threshold is set to 3 pu of rated DC side current at MMC terminals for all simulations.

The faults used for the protection system sizing are busbar-to-ground faults on “Busbar 2” and pole-to-ground faults on the II and “Spoke 2”. For the spoke fault, a travelling wave generator (TWG) [15], [16] was implemented in the EMTP simulation environment to facilitate the simulations of faults with different distances to ensure the worst-case representation of fault current increase. Protection relay time ($T_{relay}$) is assumed to be 0.5 ms after fault inception to the terminals of converter stations [17]. Fault neutralization time ($T_N$) is then defined by adding $T_{relay}$ to DCCB operating time ($T_{op}$) as per [17]. The default $T_{op}$ is set to 5 ms.

Onshore AC system constraints, faults and their probabilities, and the MMC blocking tables for the case without temporary blocking have been defined in the framework of [1] as shown in Table 14. Taking the same assumptions, Table 14 is revised for the case where TBF is allowed, and the changes are underlined in Table 14. If the cells in the table are not split and not underlined, it accounts for both cases.

*Table 14: MMC blocking table for the case without temporary blocking and <u>underlined</u> for the case with temporary blocking.*

<table>
<tr><th></th><th>Busbar fault</th><th colspan="2">Line fault II</th><th colspan="2">Line fault spoke</th></tr>
<tr><td>Connected MMC WF</td><td>Allowed</td><td>Not Allowed</td><td><u>Allowed</u></td><td>Not Allowed</td><td><u>Allowed</u></td></tr>
<tr><td>Adjacent MMC WF</td><td>Not allowed</td><td>Not Allowed</td><td><u>Allowed</u></td><td colspan="2">Not Allowed</td></tr>
<tr><td>MMC spoke</td><td>Allowed</td><td colspan="2">Not Allowed</td><td colspan="2">Allowed</td></tr>
<tr><td>Adjacent MMC spoke</td><td>Not Allowed</td><td colspan="2">Not Allowed</td><td colspan="2">Not Allowed</td></tr>
</table>

These tables serve as firm guidelines during and after fault events and they are the main criteria for sizing of protection components. To show the impact of the TBF of the MMC-WF, the system is first designed without the TBF and then redesigned considering the TBF as described in Table 14. To design the DCRs, an iterative optimization process based on EMT simulations is carried out as illustrated in Figure 54. Initially, the value of 50 mH is adopted for all the DCRs in the system. Then the iterative process starts, which essentially consists in simulating the different fault types while increasing their corresponding DCR values in 50-mH steps until the criteria shown in Table 14 are met, i.e., only the stations that are allowed to block are blocked. The value of a DCR correspondent to a given fault case is optimized through the iterative process by fixing the other DCR values.

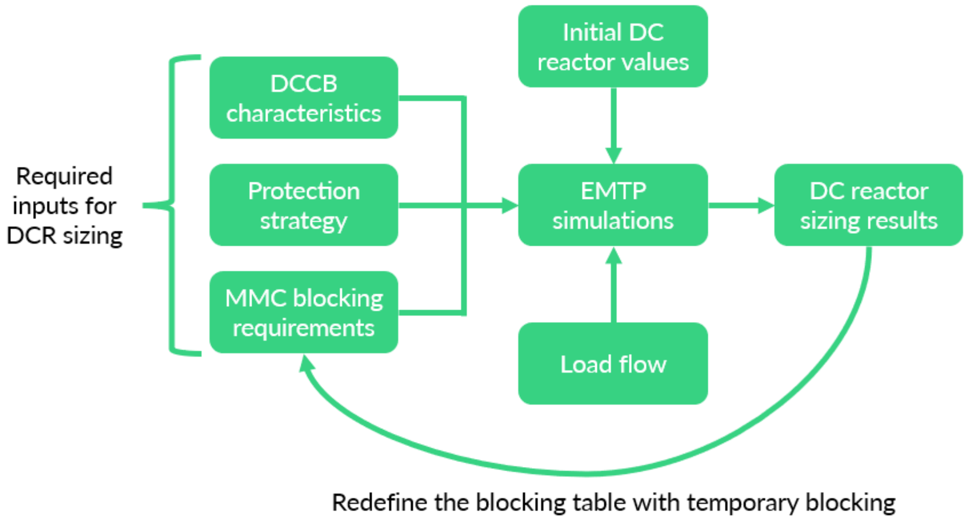


*Figure 54: Protection system dimensioning approach [13].*

### 6.2.2. AC SYSTEM REPRESENTATION AND PROSPECTIVE FAULT CURRENT

Before performing larger studies on the complete systems presented in Figure 53, a simplified scheme was developed to study the influence of AC system representation on the prospective fault current on the DC side, especially after converter blocking. Two options were used for the representation of the AC side, Thevenin sources as an AC system equivalent or an aggregated EMTP model of a wind farm [18]. Thevenin sources were set to represent a weak AC transmission grid with a short circuit level of 10GVA and R/L ratio of 31 and a strong AC transmission grid with a short circuit level of 40GVA and R/L ratio of 31.  The WF model used comes from the EMTP library model [18]. The wind turbine based on a full-converter technology ensures that the fault current contribution during an offshore AC fault, as well as an HVDC fault, is kept at a maximum value of 1.2 per unit (pu). The simulated system is shown in Figure 55. The fault applied to the system is a pole-to-ground fault at the end of a 400 km cable using the TWG. The DC source on the right-hand side provides the voltage reference to the MMC in steady state, before the fault, and it is disconnected at the instant of the fault.

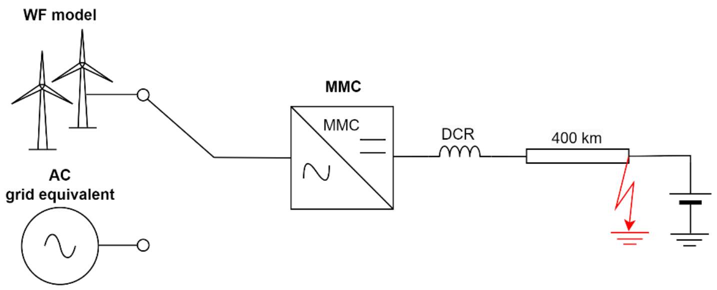


*Figure 55: Simulation scheme for comparing different AC system representations.*

The simulations of all three AC system variants were performed for the spoke DCR ranging from 100 mH to 900 mH with a 200mH step. To analyze trends and reach conclusions, it is enough to observe the results corresponding to the two extremes of the simulated range as shown in Figure 56. The curves with all the values of the spoke DCR are shown in Figure 57. The behavior observed in Figure 56 can be divided into two intervals – before and after converter blocking. Before MMC blocking, the increase of the DC fault current is rather independent of the AC grid representation. The rate of current rise depends mainly on the size of the DCR. After MMC blocking, the AC grid representation has a large impact on the fault current behavior due to the AC side current infeed to the DC side. The effect of the previously mentioned WTG current limit can be observed for the WF case, with the current decreasing after the blocking. In the case of the strong and weak AC grids, the current continues to rise following a similar trend but with different magnitudes of current [19].

The DC reactor and its size have a significant impact on the fault current rise and on the current contribution from the AC system after blocking. For both intervals, before and after the blocking, increasing the size of the DCR slows down the rate of current rise, smooths out the curve and decreases the magnitude of the current. In the first interval, reducing the current-rise rate would allow the DCCB to react to the fault before the converter blocking. For the 100-mH DCR, blocking occurs at around 3ms while with 900 mH it occurs close to 10ms, which means that slower DCCBs could be adopted for the 900-mH case. After the MMC blocking, with a higher DCR, the current magnitude is significantly lower, and the fluctuations are much less pronounced. Even though the rate of current rise is slower for the bigger DCR, the rate of current decrease is also considerably slower than for the lower DCR as can be noticed in the WF curve case, after the converter blocking.

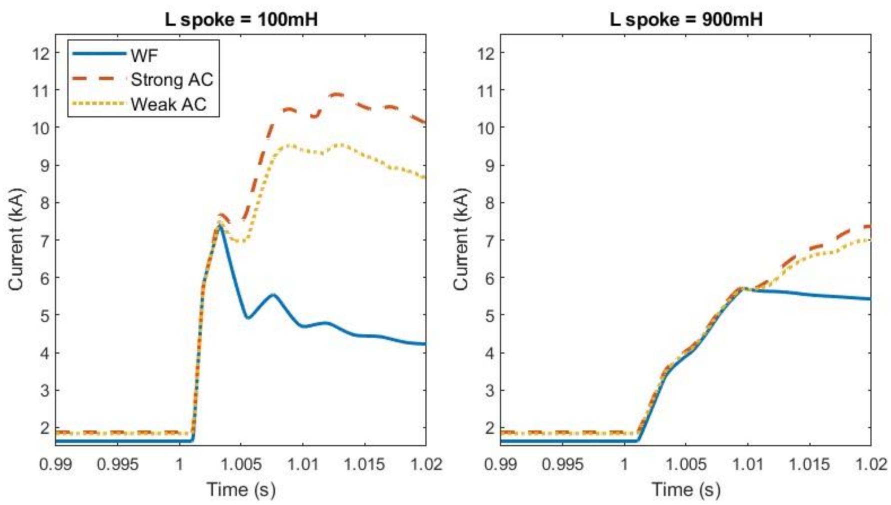


*Figure 56: Prospective current at the MMC output.*

Since the AC side representation mostly affects the DC current behavior after the MMC blocking, then the importance of the accuracy of the AC side representation is only marginal when the TBF is disregarded. On the other hand, Figure 56 demonstrates the importance of a correct AC side modelling for the TBF studies since, in this case, DCRs and DCCBs will be designed considering the fault current behavior after the MMC blocking.

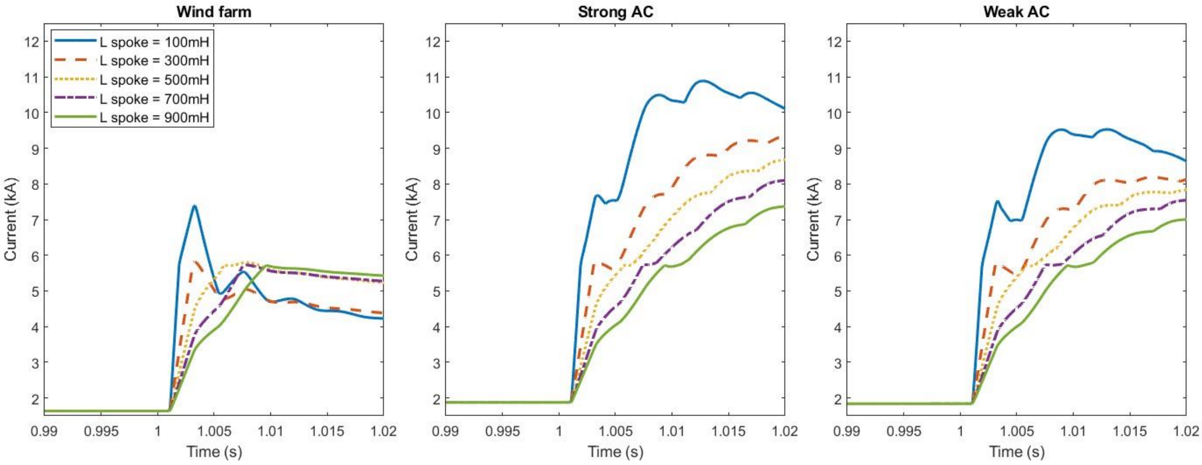


*Figure 57: Sensitivity analysis of the spoke DCR value for different AC system representations.*

## 6.3. PROTECTION SYSTEM COMPONENT SIZING COMPARISON

In this section, protection system components (DCRs and CBC of DCCBs) are designed for the use cases presented in Figure 53. It is important to note that for each case presented in this section, the sizing process is repeated from the beginning resulting in different DCR and DCCB ratings based on the specific set of parameters for that case. In all the cases, the DCRs were increased by 50 mH step in each iteration. This means that for a given case in the simulations, DCR size is increased by 50mH until the set criteria are respected.

### 6.3.1. DIFFERENT AC SYSTEM REPRESENTATIONS FOR SIMPLE RADIAL CONFIGURATION

As presented in section 6.2.2., the representation of the AC system connected to converters which are allowed to temporarily block can have a significant impact on DC fault current due to infeed currents from the AC side after blocking. In this section, the impact of TBF on the protection system component sizing is presented for different AC side representations. The different AC grid representations are varied only for the two offshore HVDC stations (MMC-WF 1 and MMC-WF 2) and, thus, the naming convention MMC-WF is kept even if the connected AC side representation is not a wind farm, and the power flow is kept the same. The DCCB $T_{op}$ is set to 5 ms with $T_{relay}$ of 0.5 ms. MMC-WF blocking follows Table 14. The outcomes of the sizing exercises are DCR sizing and DCCB CBC for each case.

The outcome of the sizing process is presented in Figure 58 and Table 15. At the outset, it is important to highlight the ramifications of allowing temporary blocking based on Table 14 and the results presented in this section. Both for a busbar fault and a spoke fault, the TBF of connected converters is allowed but the blocking of the adjacent MMC, connected via the II, needs to be avoided. After a fault and MMC blocking, a stronger AC grid connected to the MMC means a higher infeed current (see Figure 56) which will support DC voltage across the offshore hub. Consequently, DC voltage support will yield fewer current contributions via the II. Less current via the II will produce a lower fault current increase of adjacent converters contributing to avoiding their blocking. Throughout this section, currents and voltages are plotted to further analyze this behavior. The previous explanation exemplifies why a detailed representation of the AC system is important for the TBF analysis.

The system with WF connected to the MMC-WF needs a larger spoke DCR, larger windfarm DCR and smaller II DCR compared to Thevenin source representation, and it will require a lower DCCB CBC and surge arrester (SA) energy rating. On the other hand, when comparing weak and strong AC systems, the trend is different. A stronger system requires less inductance in series with the MMC-WF and on the spoke but requires more inductance on the II.

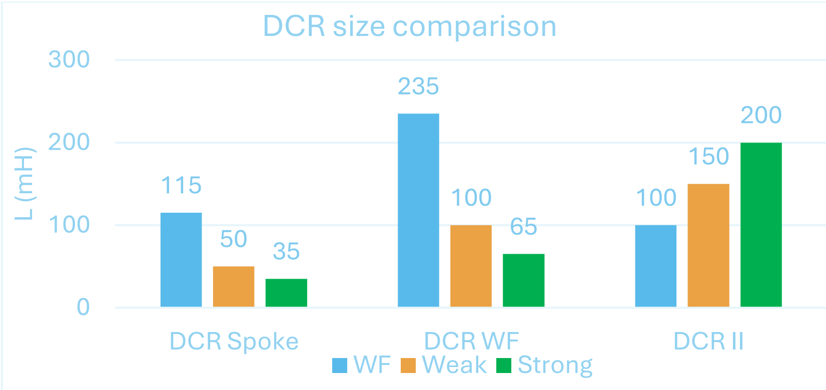


*Figure 58: DCR size comparison for different AC system representations.*

Overall, comparing the sizing outcomes in Table 15, the strong AC system case will require the lowest average of DCRs installed, the weak AC case will require only 5% more while the WF case will require the most DCRs installed, 60% more than the strong AC case (considering a total of four DCRs L-SPK, two DCRs L-WF and two DCRs L-II). This further emphasizes the importance of correctly representing the WFs in the simulations for protection system component sizing when a temporary blocking feature is considered.

*Table 15: DCCB current breaking capability, SA energy and DCR sum for different AC system representations.*

| (Top = 5ms) | Icbc w/ temp blocking | SA Energy w/ temp blocking | DCR sum | Averaged DCR value |
|---|---|---|---|---|
| WF | 13 kA | 27 MJ | 1130 mH | 141 mH |
| Weak | 15 kA | 39 MJ | 700 mH | 88 mH |
| Strong | 20.4 kA | 41 MJ | 670 mH | 84 mH |

To further demonstrate the difference in the system behavior between different AC side representations, currents, and voltages at MMC-WF1 and MMC-WF2 outputs were plotted in Figure 59 along with the DCCB current of faulted spoke. The behavior of the current through DCCB Spoke 2 and at the MMC-WF 2 terminals, after the fault, can be divided into intervals, i.e., before blocking, between blocking and DCCB opening (at $T_N = 5.5$ ms), and after $T_N$. Before blocking, the slope of the current rise is governed by the DCR size which in turn defines the moment when the converter blocks. After the fault, MMC-WF 2 blocks after 0.6 ms for a strong AC system, 0.9 ms for a weak AC system and 2.4 ms for a WF representation. Between blocking and DCCB opening, the system behavior is governed by the DCR size and the AC side representation which produces current infeed from the AC side of the converter and will require different DCCB CBCs. As stated before, the stronger AC system will support the voltage better than a weaker one which translates to higher fault currents on the DC side. After DCCB is opened at 5.5 ms, the MMC WF2 current is extinguished to zero since the deblocking functionality was disregarded in this study.

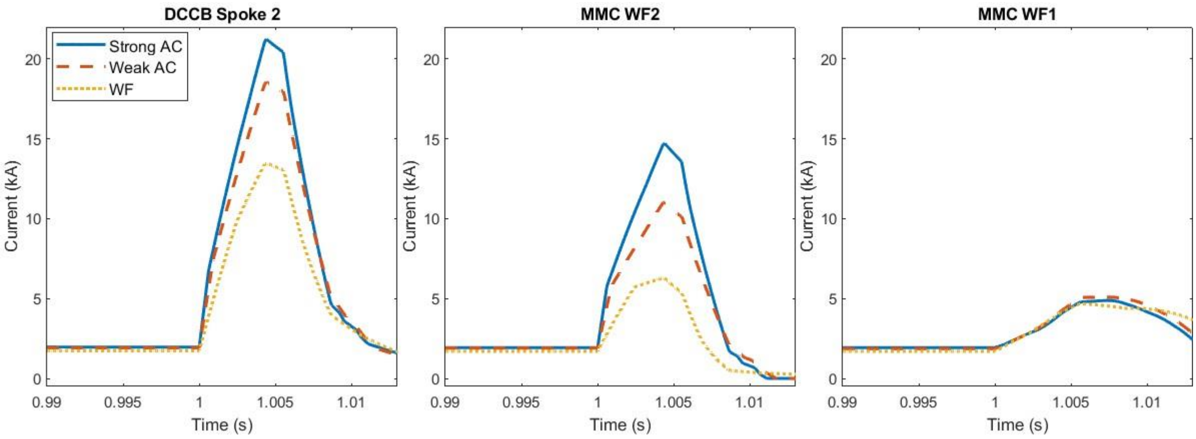


*Figure 59: DCCB current for different AC side representations for a pole-to-ground spoke-2 fault.*

By looking at the voltage behavior at the terminal of MMC-WF 2, it is possible to notice that strong and weak systems follow the same trend with a marginal difference in magnitude. The magnitude of the voltage drop of all three AC system representations can be related to the transient interruption voltage (TIV) produced by the DCCB and the characteristic of the surge arrester used. The combination of TIV, DCR size and the AC side representation will result in a different initial voltage drop behavior which is then followed by converter blocking directly related to DCR size for each case. Even if the blocking happens at different instances for each case, the voltage drops are almost the same for all three AC system representations.

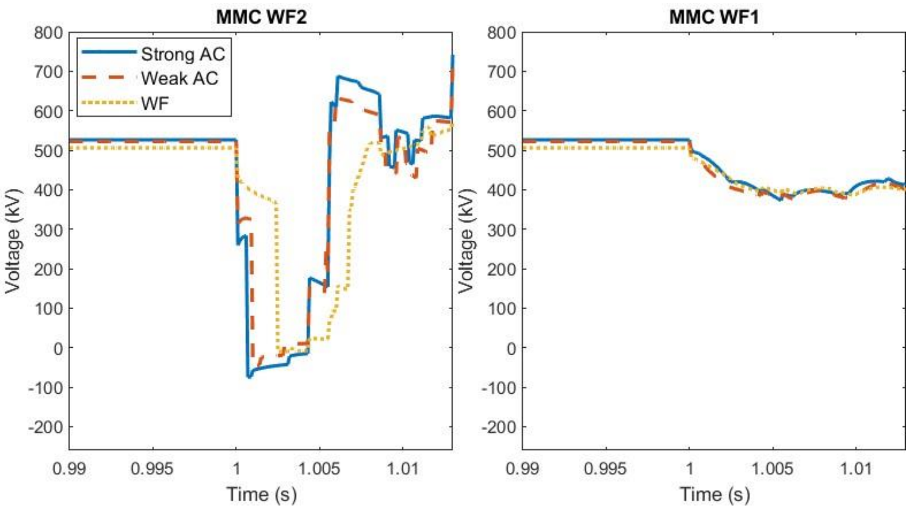


*Figure 60: Voltage measurements at MMC WF1 and MMC WF2 output and Busbar 2 for a pole-to-ground spoke-2 fault.*

Voltage and current behavior at MMC-WF 1 follow similar trends for all three system representations and the converter doesn't block. This can be attributed to two things. i.e., first, the voltage drop of MMC-WF 2 after the blocking is almost the same and will lead to a comparable response of the remote devices (MMC-WF 1). Moving from WF to a weak and strong AC system, the sizing of DCR-WF and DCR-spoke decreases but the sizing constraint of DCR -II increases since MMC-WF2 is allowed to block and MMC-WF1 is not allowed for certain faults in Table 14. This will directly affect the electrical separation of the two buses (hubs) and the response of the systems.

Having the system sized for the WF representation and taking it as a reference, it will require the lowest DCCB CBS and SA energy absorption while the weak and the strong AC system representation will require respectively 15% and 57% higher CBC and 44% and 51% higher SA energy absorption. On the other hand, the averaged DCR value necessary will be the highest for the WF representation and 38% and 40% lower for weak and strong AC systems respectively.

### 6.3.2. DIFFERENT DCCB OPERATING TIMES FOR SIMPLE RADIAL

To further generalize the study, different DCCB $T_{op}$ values (2 ms, 5 ms and 8ms) were considered which correspond to the possible operating times of different technologies from different DCCB manufacturers. Different DCCB implementations and operating times can be taken for the PROMOTioN project reports [20], [21]. DCCBs can be sorted in two main groups based on the mechanism of current breaking - mechanical or hybrid DCCBs. Starting from the fastest to the slowest, VSC Assisted Resonant Current (VARC) breakers are a subgroup of mechanical breakers, notable implementation is done by Scibreak [22] (now under Mitsubishi [23]) which can neutralize the current under 2ms. They are followed by hybrid breakers, for example by ABB (now Hitachi) [20], which operate in 2-5ms range and in the end general mechanical breakers, for example by Mitsubishi [23], which operate in the range between 5-8ms. Using these operating times, the protection system components are once again sized for all three operating times for both cases – with and without TBF of MMC-WF2. As the primary goal of this use case is to evacuate the power from WFs to different connected areas, WF models are used on the AC side of MMC-WFs.

DCR sizes as the outcome of the sizing process are shown in Figure 61. Solid-colored columns represent the sizing without the TBF, and patterned columns represent the sizing with the TBF. For the case without the TBF enabled, the higher the operating time, the higher the DCR sizing necessary. This is because DCRs limit the rate of current rise enough to respect the converter blocking constraints (see Table 14) while the DCCB opens to clear the fault. If the MMC-WF is allowed to block, DCR sizes to respect the blocking criteria are significantly lower in comparison to the case where the MMC-WF is not allowed to block. As observed in Subsection 6.2.2, by having the correct representation of the WF, the fault current will decrease after the converter blocking, leading to a lower CBC requirement for longer DCCB operating times and this can be seen in Figure 62. In the case without TBF, the main constraint is to avoid the blocking of the closest converter and hence to design DCR-SPK and DCR-WF accordingly. With the TBF, the constraint of DCR-II sizing is increased since one converter is allowed to block and the adjacent one is not. Taking the example of a pole-to-ground fault on spoke 2, MMC-WF 2 will be allowed to block while MMC-WF1 will not, and this will be reflected in the overall system sizing outcome as in Figure 61. Figure 62 shows the current progression at MMC-WF1 and MMC-WF2 terminals. MMC-WF2 blocks while MMC-WF1 stays below the blocking threshold (equal to 3 pu or 5.7 kA) in all three cases presented in the curve.

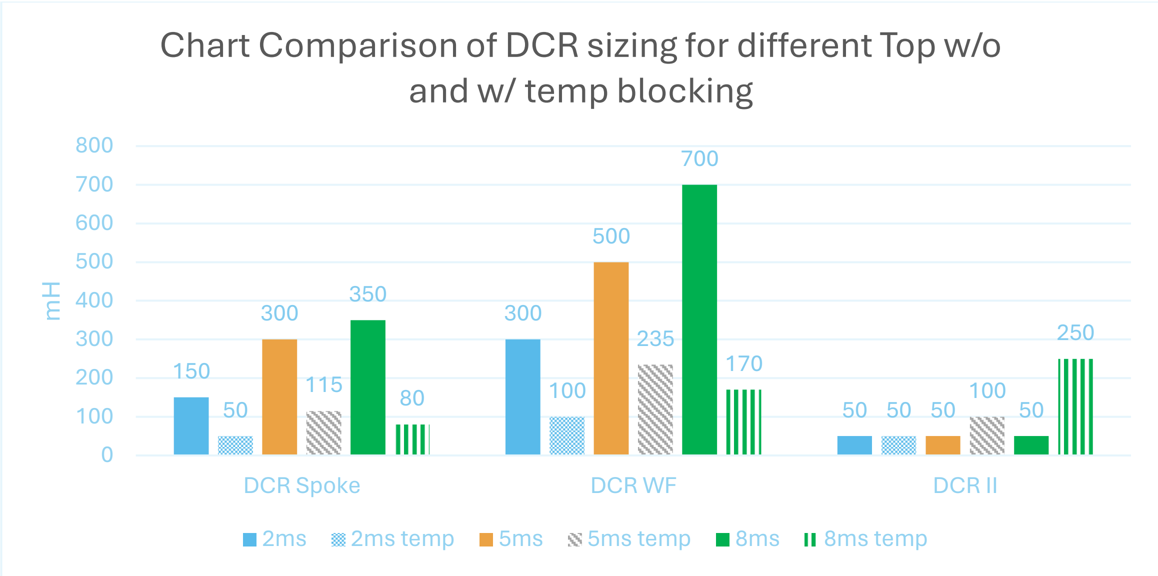


*Figure 61: DCR size comparison for different DCCB operating times and temporary blocking functionality.*

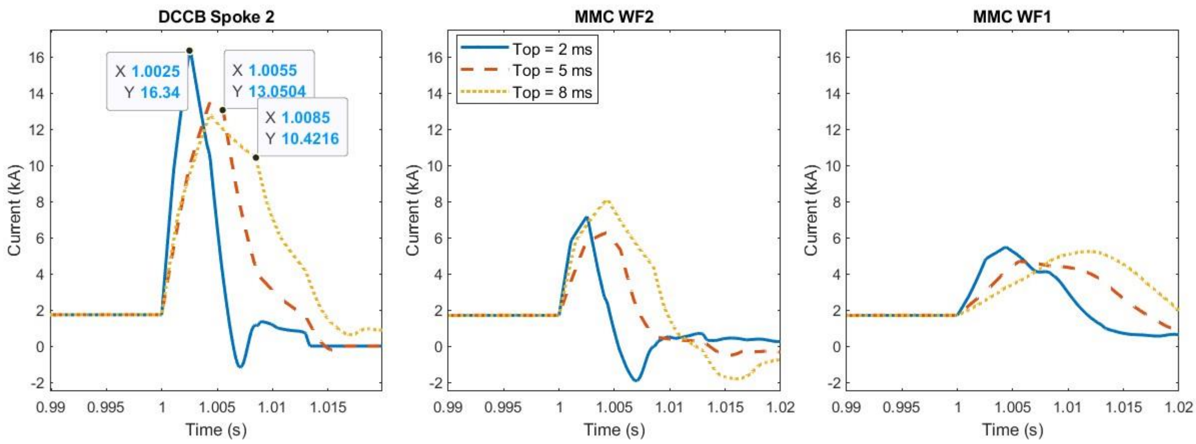


*Figure 62: DCCB current and current at outputs of MMC WF1 and MMC WF2 with temporary blocking feature*

*for a pole-to-ground spoke 2-fault.*

Figure 63 compares the necessary DCCB CBC and SA energy absorption. It is important to note that the DCCB CBC, since all DCCBs in the system are assumed to be the same, is determined by taking the highest value of current through a DCCB at $T_N$ considering all faults. This means that different faults produce the highest current at $T_N$, for the different cases presented, and govern the necessary CBC. Detailed values are listed and the determining faults for DCCB CBCs are bolded in Table 16.

Table 16: Current through DCCBs use to clear the faults listed in the table measured at $T_N$ with bolded DCCB CBC dimensioning values for each case simulated.

| Fault → | | Spoke 2 fault | Internal interconnector fault | | Busbar 2 fault | |
|---|---|---|---|---|---|---|
| DCCB operated → | | DCCB SPK 2 | DCCB II Bus 1 | DCCB II Bus 2 | DCCB II Bus 2 | DCCB SPK Bus 2 |
| Top = 2ms | w/o TBF | **9.4 kA** | 7.2 kA | 7.2 kA | 5.6 kA | 4.9 kA |
| | w/ TBF | **16.3 kA** | 11.4 kA | 11.4 kA | 7.8 kA | 10.5 kA |
| Top = 5ms | w/o TBF | 7.3 kA | **9.3 kA** | **9.3 kA** | 7.9kA | 5 kA |
| | w/ TBF | **13 kA** | 11 kA | 11 kA | 8.1 kA | 9 kA |
| Top = 8ms | w/o TBF | 8.8 kA | **10.3 kA** | **10.3 kA** | 9.3 kA | 5.3 kA |
| | w/ TBF | **10.4 kA** | 9.8 kA | 9.8 kA | 6 kA | 6.4 kA |

Without the TBF, the DCCB CBC needed is relatively similar for all three DCCB operating times considered while the SA energy absorption requirements increase two-fold from 27MJ, for 2ms DCCB, to 53 MJ, for 8ms DCCB. With temporary blocking, as previously mentioned, DCCBs will operate after the converter has blocked so the later the opening, the smaller the DCCB CBC needed. The SA energy absorption requirements are nearly the same between all operating times and this conclusion was obtained by simply measuring the energy values in each case. When TBF is considered, SA energy absorption requirements are 19% higher for 2ms, 21% lower for 5ms and 38% lower for 8ms in relation to the cases where the TBF is disabled. With the TBF enabled, the DCCB CBC needed is 75% higher for 2ms, 40% higher for 5ms and 1% higher for 8ms in relation to the cases where the TBF is disabled. All these values are within the CBC limitations of different technologies proposed by DCCB manufacturers.

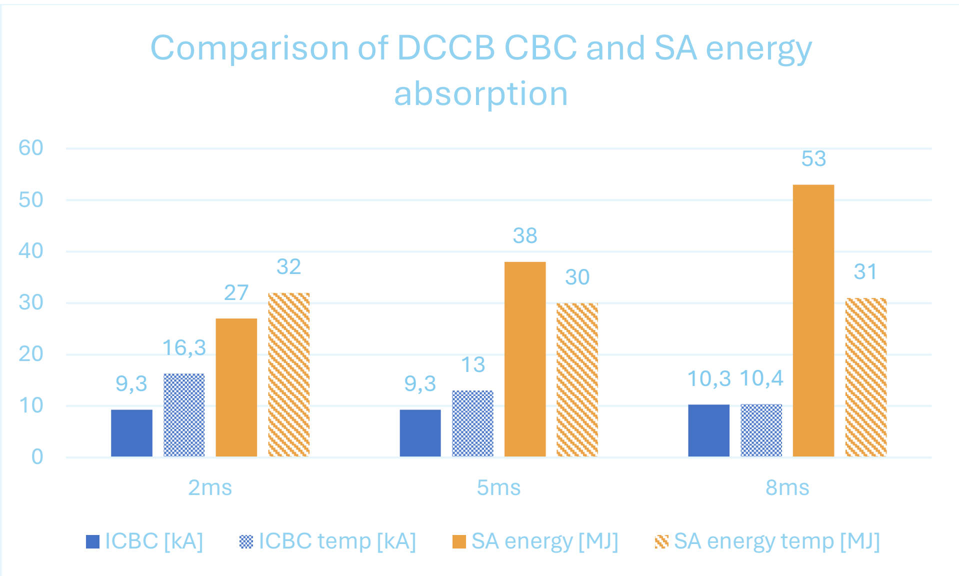


Figure 63: DCCB CBC and surge arrester energy absorption requirements

Table 17 summarizes the findings of this section and presents the difference of the overall sum of DCRs necessary in the system to respect the sizing criteria. The total DCR savings are significant when the TBF is enabled in comparison to when the functionality is disabled - averaged DCR is 61% smaller for 2ms, 51% smaller for 5ms and 60% smaller for 8ms with only a 4-mH difference between 5ms and 8ms. Large DCRs in the MTDC grid could negatively impact its control and stability. With the possibility of implementing TBF, the DCRs could be considerably reduced benefiting the system performance.

*Table 17: Summary of the protection system sizing process.*

| | DCR sum w/o TBF | Averaged DCR w/o TBF | DCR sum w/ TBF | Averaged DCR w/ TBF |
|---|---|---|---|---|
| Top = 2ms | 1300 mH | 163 mH | 500 mH | 63 mH |
| Top = 5ms | 2300 mH | 288 mH | 1130 mH | 141 mH |
| Top = 8ms | 2900 mH | 363 mH | 1160 mH | 145 mH |

### 6.3.3. EXPANSION FROM SIMPLE RADIAL TO EXTENDED RADIAL

This section presents the DCR design requirements considering the hypothetical planned expansion of the system from simple radial to extended radial (highlighted in green in Figure 53) with and without the TBF. As in previous sections, protection system components are sized for each case and then the outcomes are compared.

Figure 64 presents the DCR sizes resulting from this exercise. Simple radial cases are presented in solid columns and extended radial cases are presented in patterned columns. Without the TBF, with the expansion of the system, there is almost no change in the values of DCR required as the DCR-WF and DCR-II are the same while the DCR-spoke after the expansion is 50 mH smaller. When the TBF is enabled, larger DCRs are required for the "Extended Radial" case, for all three types of DCRs, in comparison to the "Simple Radial" case. As in the previous section, with the TBF enabled, the DCR-spoke and the DCR-WF sizes decrease while the constraints on the DCR-II are increased, and a larger DCR-II is necessary when comparing with the case without the TBF.

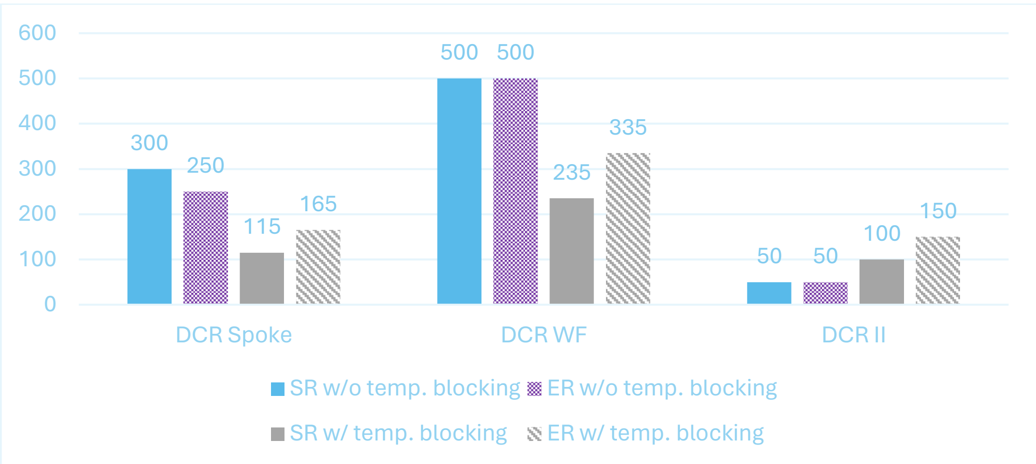


*Figure 64: DCR size comparison for both use cases with and without temporary blocking functionality.*

From  Figure 65 and Table 18, it can be seen that the extended radial will always require higher current breaking capability and SA energy absorption in comparison to the simple radial. On the other hand, for the extended radial use case, comparing the cases without and with TBF, there is only a marginal difference between DCCB CBC and SA energy absorption requirements.

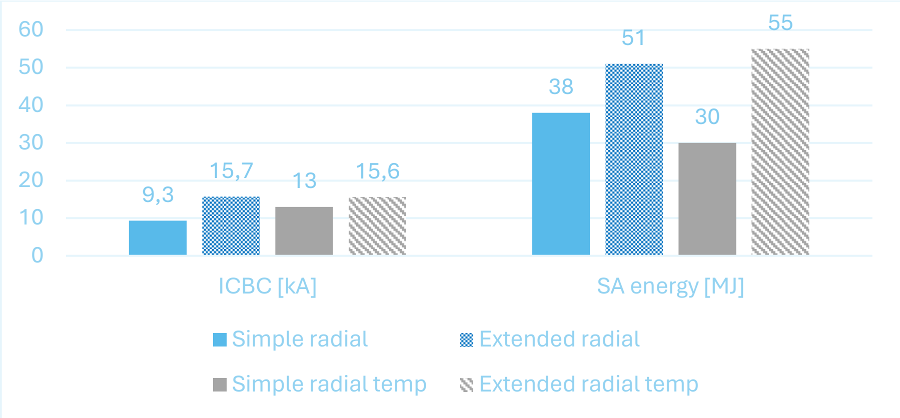


*Figure 65: DCCB CBC and surge arrester energy absorption requirements.*

By analyzing the values in Table 18 (where the DCR values are averaged based on the total number of DCR installed in the system since extended radial will have two more DCRs on each spoke [four more in total]), DCR requirements can be compared. If the expansion is made without the TBF implemented, averaged DCR value required after the expansion will be 10% lower. If the extension is made with the TBF, averaged DCR value required after the expansion will be 35% higher. Conversely, by comparing the values of the simple radial and extended radial, for the cases with and without TBF, it can be noticed that the averaged DCR values required are significantly lower in both cases when the TBF is implemented in comparison to the case the TBF is disabled. For the simple radial case, it is 51% lower and 26% lower for the extended radial case.

*Table 18: Summary of the protection system sizing process.*

| | DCR sum w/o TBF | Averaged DCR w/o TBF | DCR sum w/ TBF | Averaged DCR w/ TBF |
|---|---|---|---|---|
| Simple radial | 2300 mH | 288 mH | 1130 mH | 141 mH |
| Extended radial | 3100 mH | 258 mH | 2290 mH | 191 mH |

To summarize, in principle, when expanding the system from simple radial to extended radial, similar DCRs can be used if the TBF is not implemented. If the TBF is implemented, the expansion must be foreseen, in the initial planning phase, so that the adequate and larger DCRs are installed from the beginning since the DCR requirements for the extended radial case are larger than the ones for the simple radial. In both cases, DCCB CBC and SA rating should also be sized for the expansion in the initial phase since their performance requirements will be higher for the expanded case. Table 19 summarizes all the results presented in this section.

Table 19: Summary of all the results showing the sizing difference for all the simulated cases in relation to the reference case 'ref'.

| Top = 5ms | | Icbc | | SA Energy | | Averaged DCR | |
|---|---|---|---|---|---|---|---|
| WF | w/ TBF | 13 kA | ref | 27 MJ | ref | 141 mH | Ref |
| Weak | w/ TBF | 15 kA | +15% | 39 MJ | +44% | 88 mH | -38% |
| Strong | w/ TBF | 20.4 kA | +57% | 41 MJ | +52% | 84 mH | -40% |
| | | Icbc | | SA Energy | | Averaged DCR | |
| Top = 5ms | w/o TBF | 9.3 kA | ref | 38 MJ | ref | 288 mH | ref |
| | w/ TBF | 13 kA | +29% | 30 MJ | -21% | 141 mH | -51% |
| Top = 2ms | w/o TBF | 9.3 kA | +0% | 27 MJ | -29% | 163 mH | -43% |
| | w/ TBF | 16.3 kA | +75% | 32 MJ | -16% | 63 mH | -78% |
| Top = 8ms | w/o TBF | 10.3 kA | +11% | 53 MJ | +40% | 363 mH | +26% |
| | w/ TBF | 10.4 kA | 12% | 31 MJ | -18% | 145 mH | -50% |
| Top = 5ms | | Icbc | | SA Energy | | Averaged DCR | |
| Simple radial | w/o TBF | 9.3 kA | ref | 38 MJ | ref | 288 mH | ref |
| | w/ TBF | 13 kA | +40% | 30 MJ | -21% | 141 mH | -51% |
| Extended radial | w/o TBF | 15.7 kA | +69% | 51 MJ | +34% | 258 mH | -10% |
| | w/ TBF | 15.6 kA | +68% | 55 MJ | +45% | 191 mH | -34% |

# 7. CONCLUSIONS

The purpose of Task 2.1 was to carry out a feasibility assessment of the different OEH topologies aiming at identifying the preferred one to be used in next tasks of the project. However, the study performed in this report, along with the literature review carried out, suggests that each hub solution has its own merits and advantages depending on different circumstances, in particular the expected main mode of operation of the OEH.

The AC hub shows clear advantages when the main purpose of the hub is the export of wind power, and the capacity of the connected spokes does not exceed the capacity of the locally connected OWFs. It both, provides a higher availability of wind power, and comes with a significantly lower cost for this type of configuration. If the spoke capacity exceeds the capacity of the OWFs and the purpose of the hub is therefore shifted towards operation in interconnector mode (for the power exchange between different onshore AC areas), the DC hub solution is beneficial. It features a higher availability of the interconnectors and a lower cost if two additional spokes are considered. While the hybrid hub has the highest initial investment cost, it offers the highest flexibility as it allows to conveniently adjust its operating mode to improve either wind or interconnection availability. It was also highlighted in this report the fact that a DC hub can be adapted to become a type of hybrid solution by coupling the individual poles of the converter bipole system on their offshore AC sides. This coupling can increase the wind power availability to a certain extent but still cannot achieve the same performance as the AC solution. Moreover, it is important to emphasize that the cost of the DC hub topology is highly dependent on the component cost and size of DC protection (DCCBs and DCRs). It is expected that these devices will become cheaper and more compact with time, as their technologies mature in the industry, potentially shifting the overall cost favour towards the DC hub solution in a long-term scenario.

It is therefore recommended that none of the solutions are ruled out at this stage. Once again, all of them have advantages, as well as control and stability challenges, as discussed in this report. The different challenges of the different topologies shall be explored in studies to be carried out at later stages of this project, allowing for a wider range of possibilities from an academic perspective. However, focus should be put on the DC and hybrid solutions that, through their DC interfaces, allow integration to an interconnected offshore HVDC grid, which is probably the future of power systems, especially interconnecting offshore wind and hydrogen production to onshore systems.

When it comes to the OEH DC protection design considering the HVDC converter's TBF, the study revealed the inter-dependability of this functionality and the protection system components sizing based on all the hypotheses stated. The conclusions can serve as a guideline beyond this generalized study, i.e., to different use cases.

In the DC protection design study, it was shown that the modelling of the HVDC converter's AC-side system considerably affects its current infeed profile, especially after the converter blocking. The influence of the AC side representation on the protection design was analyzed for the "Simple Radial" case with the TBF enabled. It was demonstrated that the proper AC side representation can have considerable effect on the DCR sizing as well as on the definition of the DCCB CBC and the SA energy values. Besides, in the DC protection design investigation, the advantages of having the TBF available became evident. By having this functionality, a significant reduction in the DCR sizes can be obtained at the price of higher requirements for the DCCB CBC, however still being within the range of the current solutions offered by manufacturers. The overall comparative results are graphically shown in Figure 66.

Finally, the expansion of the system from simple radial to extended radial was investigated. It was shown that the expansion of the system needs to be tackled from the initial planning phase, especially if the TBF is considered, to properly design the components since the DCR requirements for the extended case are higher than for the original case. As a general conclusion, HVDC systems with the TBF implemented present several benefits for the protection system sizing, which were presented throughout this report. As mentioned in the report, the oversizing of DCRs can present challenges not only from an economic perspective but also from a control and stability perspective of the HVDC grid.

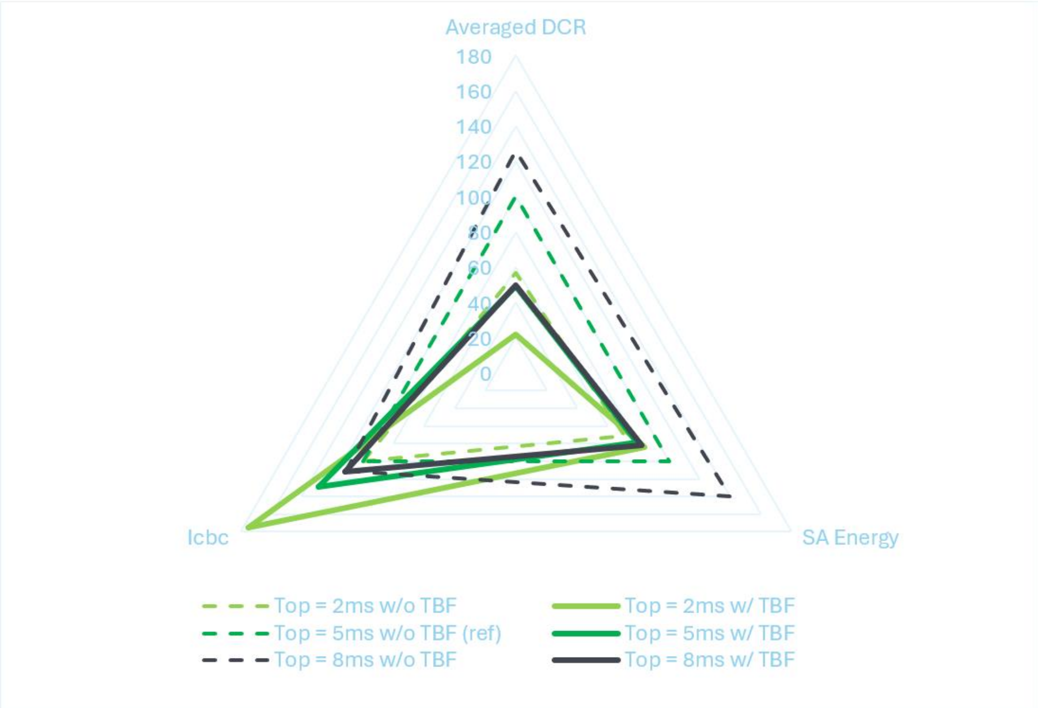


*Figure 66: Summary of results for different DCCB $T_{op}$ for cases with and without TBF.*

# 8. REFERENCES

[1] NSWPH-Consortium, "NSWPH Validation Technical Requirements – SoW A Final Feasibility Report," 2022.

[2] DNV-GL, "Screening of possible hub concepts to integrate offshore wind capacity in the North Sea," Danish Energy Agency, 2022.

[3] TenneT, ""The 2GW Program"," [Online]. Available: https://www.tennet.eu/about-tennet/innovations/2gw-program.

[4] TenneT, "T01 - 2 GW HVDC Grid Design and Reliability & Availability," 2019.

[5] Energinet, "ENERGY ISLAND BORNHOLM: HVDC converters and technical interface," [Online]. Available: https://ens.dk/sites/ens.dk/files/Vindenergi/powerpoint_from_market_dialogue_-_energinet.pdf.

[6] TenneT, "T09 - Control & Protection design 66 kV".

[7] Tennet, "T11 - J-tubes & Number of bays".

[8] Energinet, "Offshore Energy Hubs - High Level System Description and Requirements," 2023.

[9] A. Antonio-Ferreira and O. Gomis-Bellmunt, "Modular multilevel converter losses model for HVDC applications," *Electric Power Systems Research,* vol. 146, p. 80–94, 2017.

[10] L. Yang, Y. Li, Z. Li, P. Wang, S. Xu and R. Gou, "A simplified analytical calculation model of average power loss for modular multilevel converter," *IEEE Transactions on Industrial Electronics,* vol. 66, no. 3, p. 2313–2322, 2019.

[11] National-Grid-UK, "National Grid's Strategy Paper to address Transmission Licence Special Condition 2K: Electricity Transmission Losses," 2019. [Online]. Available: https://www.nationalgrid.com/electricity-transmission/document/132276/download.

[12] ABB, "XLPE Submarine Cable Systems: Attachment to XLPE Land Cable Systems - User´s Guide," 2010. [Online]. Available: https://new.abb.com/docs/default-source/ewea-doc/xlpe-submarine-cable-systems-2gm5007.pdf. [Accessed 08 12 2023].

[13] A. Zama and et.al., "North Sea Wind Power Hub Feasibility Study: Methodology for Protection Design (part II)," in *International Conference on Renewable Energies and Smart Technologies (REST)*, Tirana, Albania, 2022.

[14] CENELEC, "HVDC Grid Systems and connected Converter Stations - Guideline and Parameter Lists for Functional Specifications - Part 1: Guidelines," WG06, CENELEC/TC 8X, 2018.

[15] P. Torwelle and et.al., "North Sea Wind Power Hub pre-FEED study: DC Protection Functional Requirements and Parameter Ranges for HVDC Building Blocks," in *" B4 International SC Meeting and Colloquium*, Vienna, Austria, 2023.

[16] NSWPH-Consortium, "NSWPH MT HVDC Functional Requirements".

[17] CIGRE-WG-A3/B4.34, "Technical requirements and specifications of state-of-the-art HVDC switching equipment," CIGRE Technical Brochure 683, 2017.

[18] "Simulation models for wind parks with variable speed wind turbines in EMTP," EMTP documentation, 2017.

[19] P. Torwelle, A. Bertinato, B. Raison, T. Dung-Le and M. Petit, "Fault current calculation in MTDC grids considering MMC blocking," *Electric Power Systems Research,* vol. 207, 2022.

[20] "Deliverable 6.1 Develop system level model for hybrid DCCB," PROMOTioN Workpackage 6, 2016.

[21] "Deliverable 6.2 Develop system level model for mechanical DCCB," PROMOTioN Workpackage 6, 2016.

[22] Scibreak, "Our Technology — The VARC Circuit Breaker" https://scibreak.com/technology/vsc-varc/".

[23] "Mitsubishi Electric Acquires Scibreak," [Online]. Available: https://scibreak.com/posts/mitsubishi-electric-acquires-dc-circuit-breaker-developer-scibreak/.